Enhanced Antibiofouling of Reverse Osmosis Membranes by Surface Modifications

HAMED KARKHANECHI

(Degree)
博士（学術）

(Date of Degree)
2014-03-25

(Date of Publication)
2016-03-25

(Resource Type)
doctoral thesis

(Report Number)
甲第6078号

(URL)
https://hdl.handle.net/20.500.14094/D1006078

Doctoral Dissertation

Enhanced Antibiofouling of Reverse Osmosis Membranes

by Surface Modifications

表面修飾による逆浸透膜の耐バイオファウリング性の向上

January, 2014

Graduate School of Engineering
Kobe University

Hamed Karkhanechi

Acknowledgment

First and foremost, I would like to express my deep and sincere gratitude to my supervisor Professor Hideto Matsuyama of the Department of Chemical Science and Engineering, Kobe University, for accepting me to complete my PhD studies as a member of his accomplished research group, and I extend my deepest thanks to him for all of the opportunities he has presented me. His gracious attention and excellent supervision during my studies helped me in building confidence while handling the project with great skill and dedication. I hope to someday become as warm-hearted teacher and advisor as he has been to me.

I am deeply thankful to Professor Ryosuke Takagi for his kind support throughout this work. I am grateful to him for always welcoming me and offering his help me with a warm smile. I have learned many valuable points about membrane science, and life, during our numerous long discussions. I do not doubt that this work could not have been accomplished without him as a constant source of guidance and support in all steps.

I owe sincere gratitude to Prof. Satoru Nishiyama and Prof. Atsunori Mori of Kobe University for their kindness during the reviewing and examining of this thesis and giving constructive comments to improve upon it. I would also like to extend my sincere thanks to Dr. Tatsuo Maruyama, Dr. Yoshikage Ohmukai, Dr. Eiji Kamio, Dr. Toru Ishigami, Dr. Saeid Rajabzadeh, Dr. Daisuke Saeki, Dr. Isao Sawada, Dr. Yuriko Kakihana, Dr. Fachrul Razi, Dr. Sri Muliyati, for their friendship and ongoing kind support during my studies at

Kobe University. I am also thankful to the Japanese Ministry of Education for the generous sponsorship without which my work would have been impossible.

I wish to also thank the members of Prof. Matsuyama's laboratory. It was a pleasure for me to meet each of them, and their kindness helped me during these years on occasions too numerous to mention, but I want to thank all of them for always being good colleagues and friends.

Last but not least, no words can express the gratitude I owe my parents, who raised me with love and supported me in all my pursuits with wholehearted encouragement and prayer for my success. I am thankful for my sisters who have faithfully supported me in my life as well. And to my sweet daughter, Fatemeh, with whom I wish I could have spent more time and been more available for during studies, who nonetheless has kindly supported me continuously without complaint to the sacrifice. On many nights I recall coming up to find she stayed up to await my return and wish me well. And most of all to my lovely, supportive, encouraging, and very patient wife, Mahboobeh, for all her efforts and support during the tough times of our student life in Japan. Without her generosity and contributions, my graduate studies would have been impossible, as the support they have given me has kept me grounded and focused. Thank you all most sincerely; I dedicate this thesis work to all those who have made it possible.

Hamed Karkhanechi

Graduate School of Science and Technology

Kobe University, 2014

Table of Content

Chapter 1-General Introduction

Chapter 4- Biofouling resistance of reverse osmosis membrane modified with polydopamine

Chapter 1

General introduction

1.1. Membrane technology

1.1.1. Water scarcity

Water is one of the most precious materials in the world for beings and industries. Although water covers 71% of the Earth's surface, 97% of the water is found in seas and only 3% of the water is freshwater as shown in Fig 1.1 [1, 2]. It can be seen that 98.8% of fresh water, that includes icecaps (68.7%) and groundwater (30.1%), is not easily accessible. Furthermore, even the small amount of the fresh water existing in rivers, lakes and etc. (i.e. 0.003% of Earth's water) is being polluted by human activities [2, 3]

Safe fresh water is essential to human-beings and other beings even though it provides no energy or no organic nutrients. The United Nations (UN) suggests that each person needs 20-50 liters of safe freshwater a day to ensure their basic needs for drinking, cooking and cleaning. It is reported that 2.6 billion people lived under unacceptable sanitary conditions in 2002 [4]. According to this report, every 20 seconds, a child dies as a result of poor sanitation. That's 1.5 million people preventable deaths a year. It is estimated that around 3.5 billion people will be facing water-based vulnerability by 2025 [4, 5]. Thus, the 21st century is called the “water century” [6].

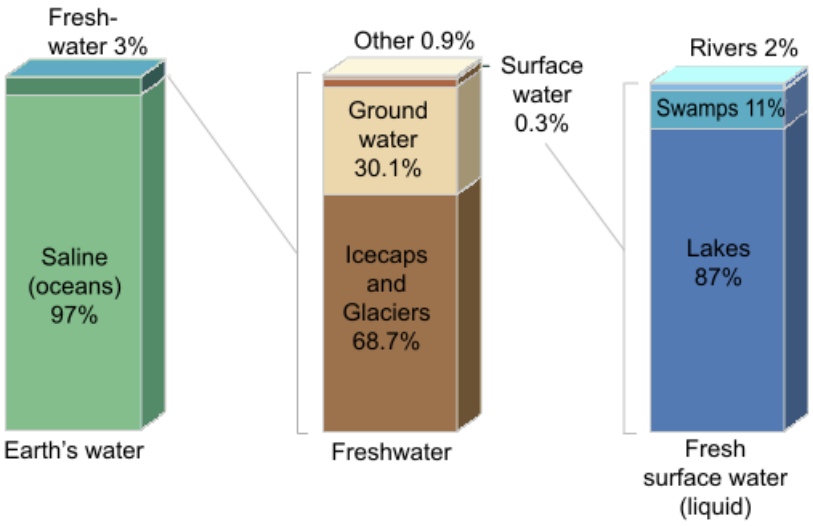

Fig. 1.1. Distribution of Earth's water [2]

The uneven distribution of freshwater shown in Fig 1.1 and large population living in arid areas exacerbates water shortage problem. Hydrologists typically evaluate a water scarcity by looking at the population-water relation. The area, where annual water resources decline to below 1,700 m^3 per person, is experiencing a water stress. If the annual water resources drop below 1,000 m^3 per person, the population faces water scarcity, and below 500 m^3 "absolute scarcity" [7]. Figure 1.2 shows freshwater availability (m^3 per person per year).

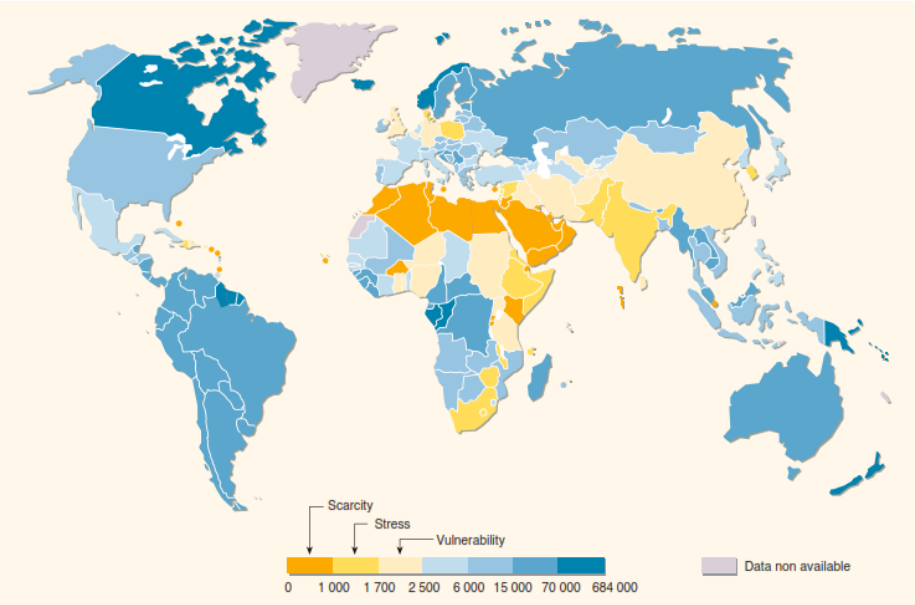

Fig. 1.2. Freshwater availability (m^3 per person per year, 2007) [7]

It is noteworthy that a low water stress does not automatically suggest easy access to water, which is a paradox that a large group of the global population currently face. Whereas water stress is a function of the availability of water resources, the concept of water scarcity is also affected by accessibility. This is called economic water scarcity. In economic scarcity, accessibility is not limited by water resource availability, but by human, institutional and financial constraints over distribution of the resource to different user groups. Thus, the water shortage problem is caused by economic water scarcity, not by water resource availability in some areas.

Considering the water stress index and economic water scarcity, if potential water resources such as seawater and produced water from oil and natural gas processing are economically purified, it could be possible to overcome the water shortage problem.

1.1.2. Water purification technology

There are many water purification technologies. However, none of these technologies can completely purify water alone [8, 9]. Thus, a well-designed water purification system uses a combination of purification technologies to achieve desired water quality. These technologies include activated carbon filters for removal of organic compounds and chlorine, ultraviolet radiation and chlorine treatment for sterilization of microorganisms such as bacteria and viruses, distillation for removal of nonvolatile contaminants, and deionization (or ion exchange) for desalination.

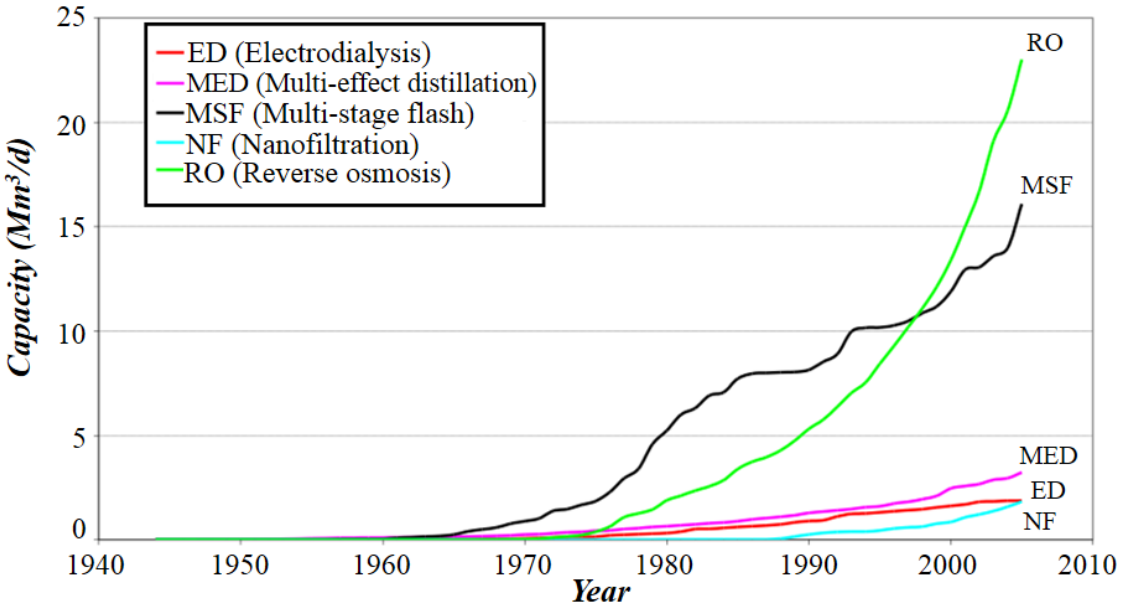

Fig 1.3. Global desalination capacity trends [10].

As shown in Fig. 1.1, the main source of water on the Earth is ocean. Thus, the seawater desalination would be a main strategy to fix the water shortage problem. Generally a distillation and membrane technology are the major technologies. Recently, the membrane technology has overtaken the thermal technologies such as Multi Stage

Flash (MSF), because the distillation is highly energy consuming process. As it was shown in Fig. 1.3, more than half of the global desalination capacity belongs to the membrane technology including reverse osmosis (RO), nanofiltration (NF) and electrodialysis (ED). The membrane process is more economic than the distillation. Thus, membrane processes are attractive to water purification based on economic point of view and their versatility (*i.e.*, membranes can remove nearly all water contaminants); especially RO membrane technology has attracted growing attention in seawater desalination.

1.1.3. Water purification with membrane process

1.1.3.1. Historical Development of Membranes

A membrane is a layer of material which serves as a selective barrier between two phases and is impermeable to specific particles, molecules, or substances when exposed to the action of a driving force. Some components are allowed to pass through the membrane into a permeate stream, whereas others are retained and accumulate in the retentate stream [11, 12].

Historical studies of membrane phenomena can be traced to the eighteenth century. J. Abbe Nollet discovered the phenomenon of 'osmosis' to describe a permeation of water through a diaphragm in 1748. The first publication on osmosis was: J.A. Nollet, Lecons de physique experimental, Hippolyta-Louis Guerin and Louis-François Dilator, Paris, 1748 [13, 14]. The membrane process was introduced as new methods of separation process since the early of 1930s. However, the breakthrough of the

membrane process was considered as one of technically important separation processes in the early 1960s. Since that time, the membranes processes have been used successfully in a wide variety of large-scale industrial applications such food industry, manufacture of dairy products, waste water treatment, drinking water production and automotive industry for the recovery of electro-painting baths. The numbers of such application is still growing [12, 15, 16]. Figures 1.4 and 1.5 are pictures of the first membrane plant and recent membrane plant.

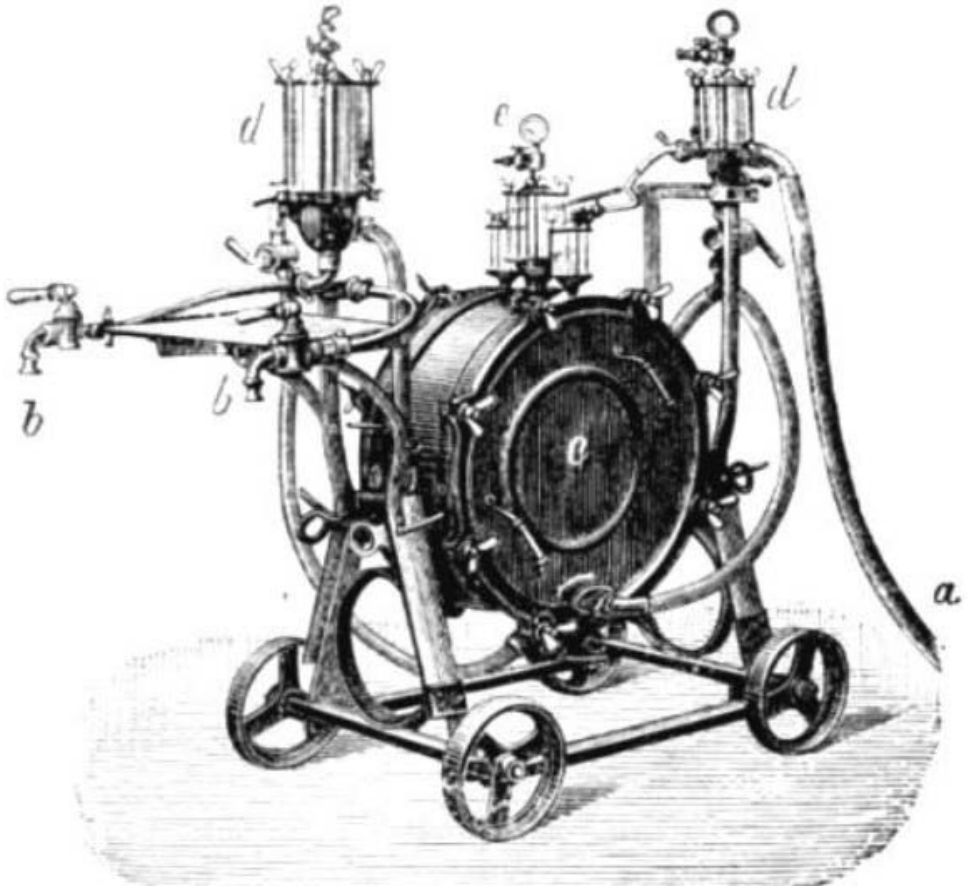

Fig. 1.4. First membrane plant [14]

Fig. 1.5. Recent high-pressure RO module unit [6]

1.1.3.2. Overview of membrane in a separation process

Membrane technology as a new tool in the field of separation process has been progressed along a development of synthetic materials which are used to fabricate various membranes. Therefore, the membrane technology is an emerging technology and because of its versatile aspects, it is used in a large number of separation processes. Some advantages of membrane technology that make it competitive to conventional techniques can be summarized as follow [12, 15-19]:

- ✓ Separation can be carried out continuously;
- ✓ Low energy consumption;
- ✓ Separation can be carried out under mild conditions;

- ✓ Easy to Scale-up;
- ✓ Membrane properties are variable and can be adjusted;
- ✓ Small footprint and greater flexibility in system design;
- ✓ Less capital investment;
- ✓ Produces high quality product;
- ✓ Environmentally friendly;
- ✓ Membrane processes can easily be combined with other separation process (hybrid processing);

Membranes can be classified from several points of view. The first classification is by nature, i.e. biological or synthetic membranes. Synthetic membranes can be subdivided into organic (polymeric or liquid) and inorganic (ceramic, metal) membranes. Figure 1.6 shows a categrization of synthetic membranes according to their geometry, bulk structure, production method, separation regime and applications. As shown in Fig. 1.7, symmetric membranes have a uniform structure throughout the entire membrane thickness, wheras asymmetric membranes have a gradiant in structure. The separation properties of symmetric membranes are detrmined by their entire structure. On the other hand, the separation properties of assymetric membrane are mostly detrmeined by the densest region in the membrane. This layer is usually called as an active layer [12, 13, 15, 16, 20]. RO membranes treated in this thesis are categrized in assymetric membrane.

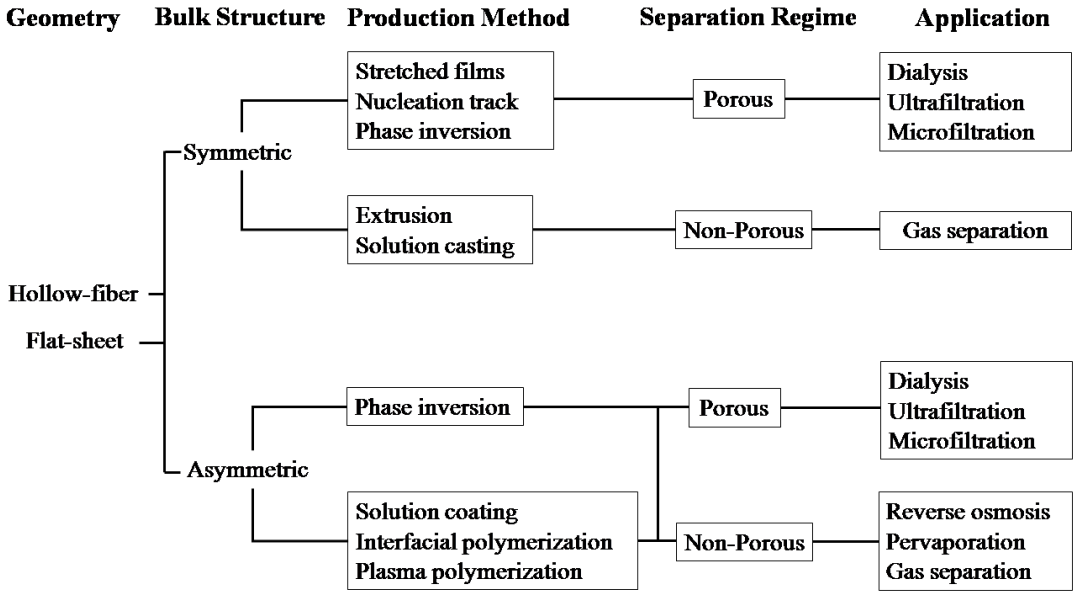

Fig. 1.6. Classification scheme of synthetic membranes based on their geometry, bulk structure, production method, separation regime, and application [15].

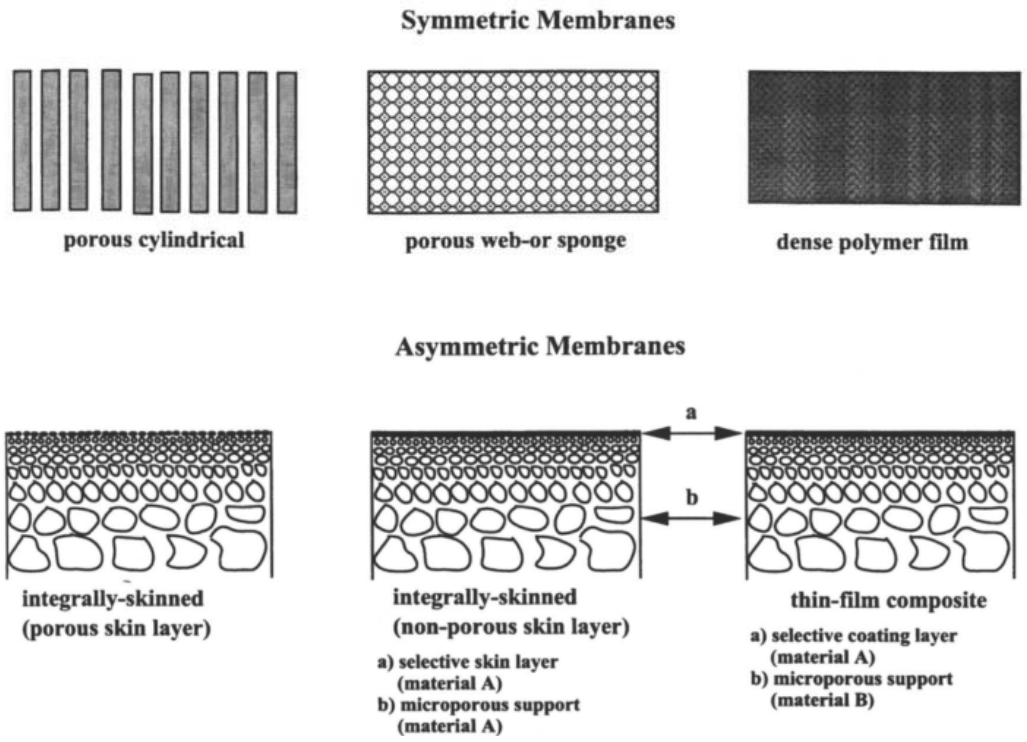

Fig. 1.7. Schematic representation of symmetric and asymmetric membrane structure [15]

1.1.3.3. Principle of membrane separation process

There are many kinds of membrane processes based on different separation fundamentals or mechanisms. The broad size range from particles to molecules can be covered with membrane process. The membrane, as heart of every membrane process, can be considered as a permselective barrier or an interface between two phases which transport one component more easily than others. Figure 1.8 shows a schematic representation of membrane separation. The phase 1 is usually considered as the feed or upstream side while phase 2 is considered permeate or downstream side. Transport through the membrane takes place under the driving force such as gradient in concentration, pressure, temperature or electrical potential of the individual components across the membrane [12, 13].

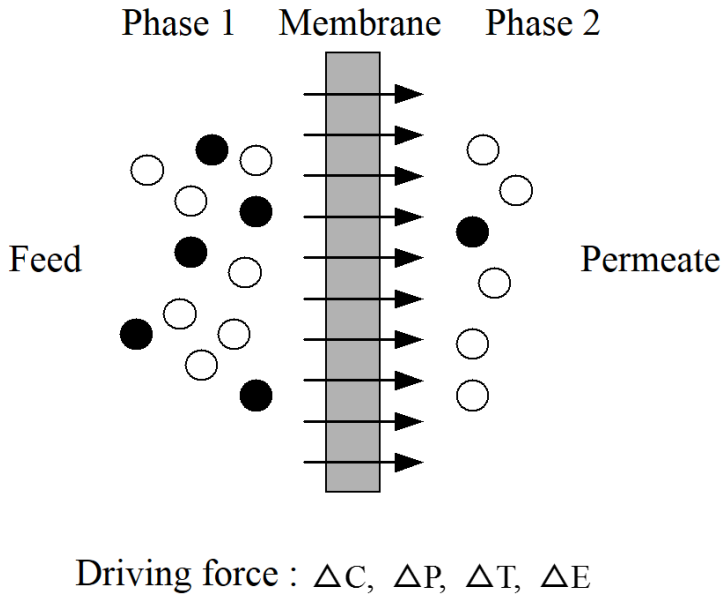

Fig. 1.8. Schematic representation of a two-phase system separated by a membrane [12]. ΔC indicates a concentration gradient, ΔP a pressure gradient, ΔT a temperature gradient and ΔE an electrical potential gradient.

The driving force depends on the type of the membrane separation. The concentration gardient (ΔC) is used in a dialysis [13]. The pressure gradient (ΔP) is used as a driving force in microfiltration (MF), ultrafiltration (UF), nanofiltration (NF) and RO processes. The temperature gradient (ΔT) is used in a membrane distillation process [12, 13]. The electrical potential gradient (ΔE) is used in an electrodialysis (ED) process [19]. Among these driving forces, the pressure gradient (ΔP) is the most widely used driving force in membrane processes.

1.1.3.4. Membrane processes driven by ΔP

MF membranes have pore in the range of 0.1 to 10 μm and are used in separation of particulates and colloidal matters. They are often applied to separate bacteria or cell (all of which usually have a hydrodynamic diameter in between 0.1 μm and 5 μm) in food and pharmaceutical industries, as well as drinking water treatment. Wastewater treatment, in which particulates and colloidal matters are the primary contaminants, can also be accomplished using MF membranes. MF membranes are typically fabricated from polymers such as polyethylene (PE), polypropylene (PP), poly(tetrafluoroethylene) (PTFE), and poly(vinylidene fluoride) (PVDF) [9, 13, 16, 21].

UF membranes are commonly used to purify liquid streams containing macromolecules (e.g., proteins and polysaccharides) and particles with effective diameters ranging from 1 nm to 100 nm. They have enormous potential to treat wastewater streams containing small colloidal particles and organic matters, such as end-product wastewater in latex emulsion processing plants, poultry farms,

metalworking facilities, food and beverage processing plants, textile plants, and sewage waters. UF membranes are typically fabricated from hydrophobic polymers such as polysulfone, polyethersulfone (PES), and PVDF, although polyacrylonitrile and other somewhat more hydrophilic polymers are also used to prepare UF membranes [9, 13, 16]

NF membranes are often used to purify water containing divalent ions or dissolved organic solutes with molecular weights around 100 [13, 22, 23]. NF membranes have small permanent pores that are approximately one order larger than atomic dimensions, but are still much smaller than UF membrane pores. Initially, NF membrane was called as "loose RO" before they were named as NF. They have higher flux than RO membranes and can, therefore, be used at lower operating pressures. However, they have lower rejection of small ions, such as sodium and chloride, than RO membranes. The market of RO and NF membranes is dominated by interfacial polymerized polyamide membranes, because traditional cellulose acetate membranes are much more prone to biological attack and are not as competitive with respect to water flux or salt rejection [9, 13, 16].

MF and UF membranes are similar in that they are both porous membranes in which particles are rejected based on their size relative to the membrane's pore size. In RO membranes, the "pore" size is on the order of 0.1 nm. Therefore, these membranes are sometimes considered to be nonporous. In most cases, RO membranes are designed to allow only water to pass through these dense layers while prevent the passage of solutes (such as salt ions). RO process requires a high pressure on the high concentration side of the membrane, usually 2–17 bar for fresh and brackish water. The

applied pressure for seawater is about 40–70 bar, because an osmotic pressure of seawater is around 24 bar that must be overcome by applied pressure. Other applications for RO include producing ultrapure water for the electronics and pharmaceutical industries and wastewater treatment [6, 9, 16, 20].

As mentioned above, the particle size that can be separated depends on the membranes. Figure 1.9 illustrates a graphic description of the size-sieving capabilities of each membrane category.

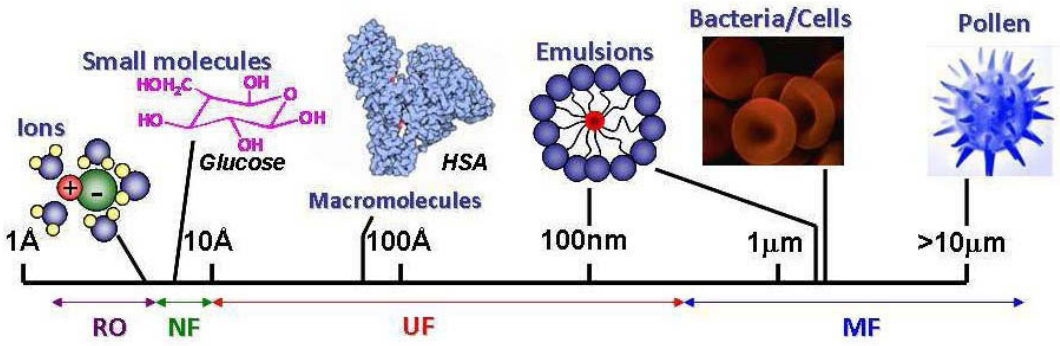

Fig. 1.9. The relative size of different solutes removed by each class of membrane. Human serum albumin is abbreviated as HSA [9].

The target of this study is the modification of RO membrane to improve the antibiofouling properties. Thus, the principle and development trend of this membrane was discussed as below.

1.1.3.5. Reverse osmosis membrane

1.1.3.5.1. Principle of Reverse Osmosis

When a membrane is placed between pure water and aqueous sodium chloride

solution, water flows from the chamber filled with pure water to that filled with the sodium chloride solution, whereas sodium chloride solution does not flow (Fig. 1.10 (a)). As water flows into the sodium chloride solution chamber, the water level of this chamber increases until the flow of pure water stops (Fig. 1.10 (b)) at the steady state. The difference between the water level of the sodium chloride chamber and that of pure water chamber at the steady state is called "osmotic pressure" converted to hydrostatic pressure. When a pressure higher than the osmotic pressure is applied to the sodium chloride chamber, the flow of pure water is reversed; the water flow from the sodium chloride chamber to pure water chamber occurs. There is no flow of sodium chloride through the membrane (Fig. 1.10 (c)). As a result, pure water can be obtained from the sodium chloride solution. The above separation process is called "reverse osmosis" process [20, 24].

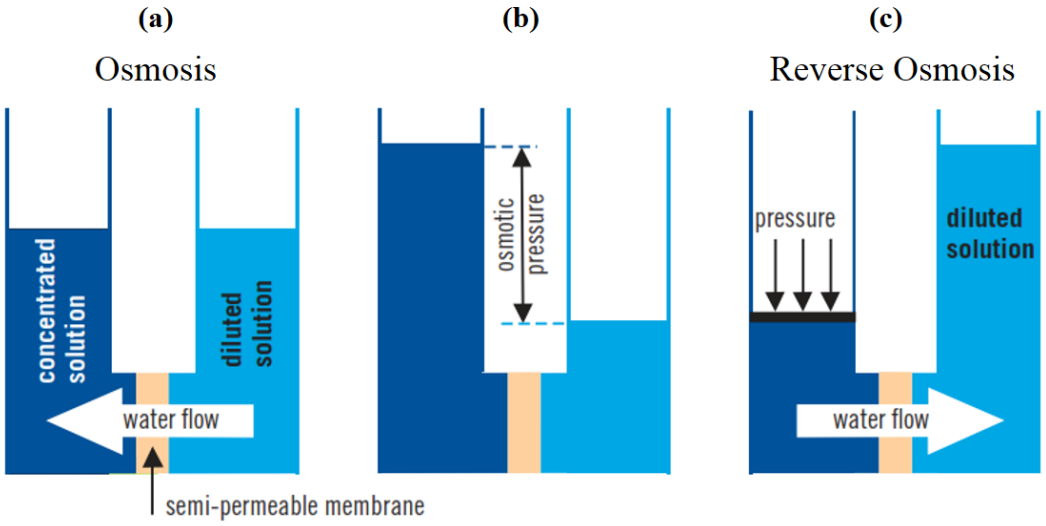

Fig. 1.10. Principle of osmosis and reverse osmosis [24]

1.1.3.5.2. Development of reverse osmosis membranes

Anisotropic cellulose acetate membranes were the industry standard through the 1960s to the middle of 1970s until Cadotte developed the interfacial polymerization method to produce composite membranes. These kinds of composite membranes had extremely high salt rejections, combined with good water fluxes. Fluid Systems introduced the first commercial composite membrane fabricated by interfacial polymerization in 1975 [13]. Figure 1.11 shows a summary of some of the milestones in the development of the reverse osmosis membranes.

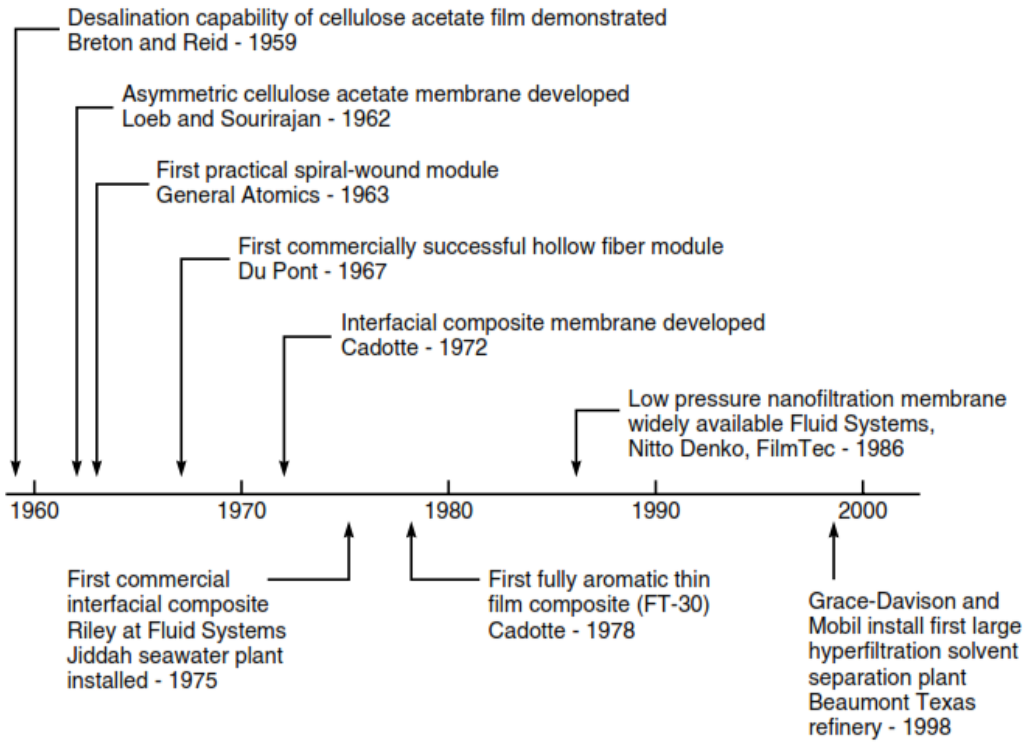

Fig. 1.11. Milestones in the development of reverse osmosis membranes [13]

Figure 1.12 shows the progress of low-pressure membrane performance trends in RO membrane on brackish water desalination from the 1970s to the 1990s, including

industrial water treatment such as ultrapure water production. In the 1970s, much effort was devoted to developing high-performance membrane materials and improving the membrane performance. As a result, the performance was improved with a new developed material of cross-linked aromatic polyamide and with developing membrane morphology and fabrication technology. The cross-linked fully aromatic polyamide composite membrane developed in 1987 has four or five times larger water flux and five times higher product water quality than those of the CA membrane (Kurihara et al., 1987). Since 1987, membrane performance has been drastically developed.[6].

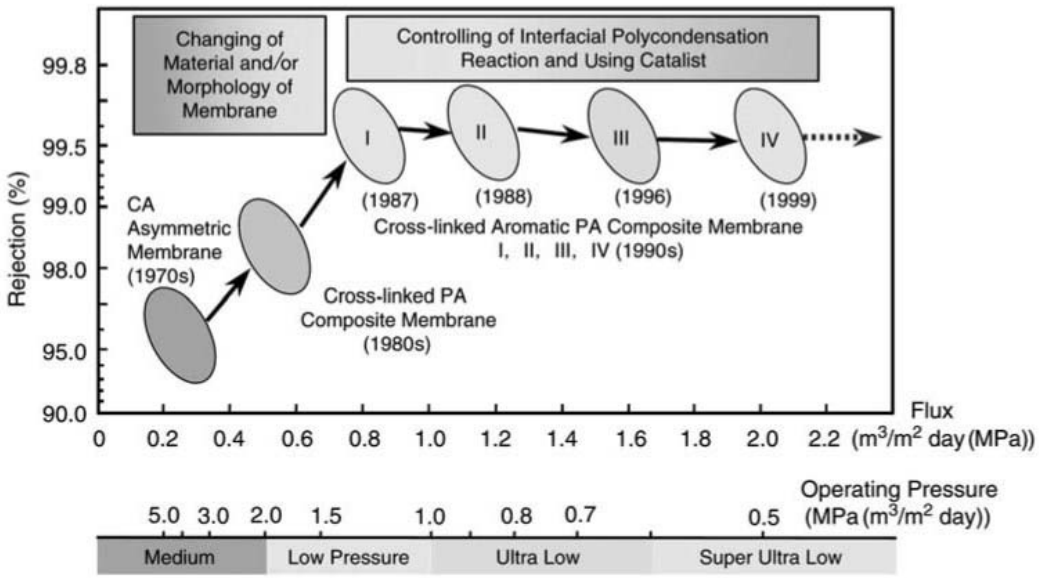

Fig. 1.12. Performance trends in RO membrane for brackish water desalination [6]

Figure 1.13 shows the progress of RO membranes for seawater desalination. It is very important to increase the water recovery ratio on seawater desalination systems to achieve further cost reduction. Most seawater RO desalination systems used today are limited to approximately 40% conversion of the feed water (salt concentration 3.5%),

since most of commercially available RO membrane do not allow for high-pressure operation of more than around 7.0 MPa [6].

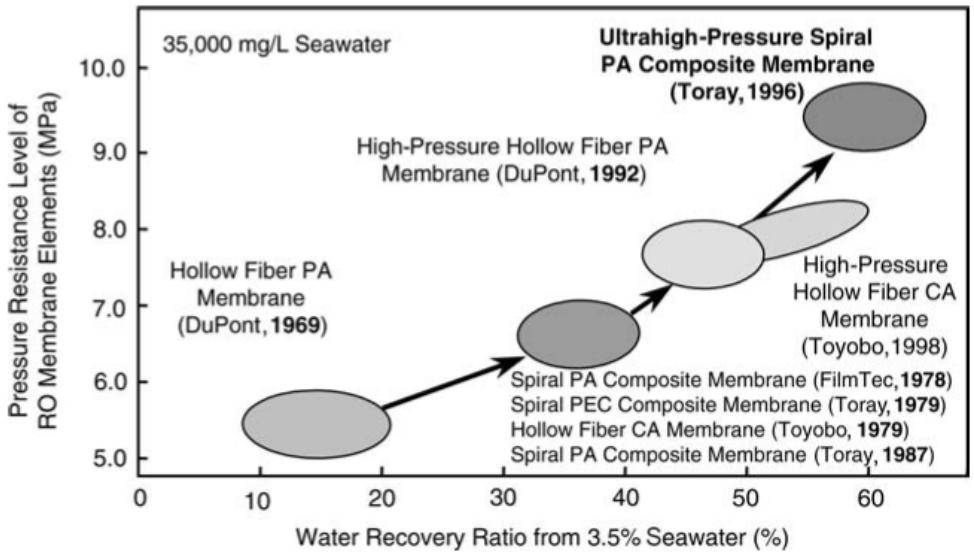

Fig. 1.13. Performance trends in RO membranes for seawater desalination [6]. PA: Polyamide; CA: Cellulose Acetate; PEC: Polyether Composite

As it was shown in Fig 1.3, the global installed capacity of desalination technology is growing fast. According to the international desalination association (IDA) report (2009-2010), more than 14,754 desalination plants have installed in worldwide with a capacity higher than 63.1 million m^3/day and about 40% of these plants have a capacity higher than 50,000 m^3/day [25]. It is noteworthy that more than 61% of the global desalination capacity (i.e. 38.5 million m^3/day) belongs to RO membrane technology [13, 25]. Thus, the RO membrane is the main technology of desalination in the world. Table 1.1 presents a list of the largest seawater reverse osmosis (SWRO) desalination plants built from 1996 to 2005. The total capacity of these facilities is approximately 1.5 million m^3/day.

Table 1.1. Large SWRO Plants Constructed from 1996 to 2005[a]

Plant Name/Location	Capacity (m^3/day)	In Operation Since
Ashkelon/Israel	325,000	2005
Tuas/Singapore	136,000	2005
Cartagena–Mauricia/Spain	65,000	2004
Fujairah/UAE	170,000	2003
Tampa Bay/United States	95,000	2003
Alikante/Spain	50,000	2003
Carboneras–Almeria/Spain	120,000	2003
Point Lisas/Trinidad	110,000	2002
Larnaca/Cyprus	54,000	2001
Al Jubail III/Saudi Arabia	91,000	2000
Muricia/Spain	65,000	1999
Bay of Palma/Palma de Mallorca	63,000	1998
Dhekelia/Cyprus	40,000	1997
Marbella–Mallaga/Spain	55,000	1997
Okinawa/Japan	40,000	1996

[a] This table includes only seawater RO desalination plants with a capacity of 40,000m3/day or higher.

Today, seawater desalination is mostly used to produce fresh drinking water for human consumption and crop irrigation. Industrial applications of desalinated seawater are typically limited to a low-salinity power plant boiler water, process water for oil refineries, chemical manufacturing plants, commercial fishing installations, canneries and other food industries [6].

As discussed above, a recent advances in membrane technology have made this technology a main process for water purification. In addition, in particular, RO process is major process for the seawater desalination compared to the evaporation desalting processes such as multi-stage flash and multi effect distillation that consume nearly 10 times more energy than RO processes [9]. However, the fouling is a serious problem in RO process as well as other membrane process, because the fouling declines the membrane performance. This thesis focuses primarily on biofouling of commercial RO

membrane and different strategies to improve the antibiofouling properties.

1.2. Membrane fouling

1.2.1. Fouling phenomena

The membrane can be considered the heart of a desalination plant where the cost of membrane unit is about 20–25% of the total capital cost [26]. Consequently, it is very important to understand parameters which affect not only membrane performance and durability, but also fouling, because the fouling is a major obstacle in water purification. Fouling is the deposition of feed components that are called foulants, in the pores of membrane (internal fouling) or on its surface (external fouling). Fouling leads to a change in membrane transport characteristics, such as flux and rejection. Fouling reduces the membrane flux either temporarily or permanently during separation process at constant pressure condition. Thus, membrane fouling deteriorates membrane performance, increases operating cost and ultimately shortens membrane life [27, 28]. Figure 1.14 shows the influence of protein fouling on permeance vs. time in a PVDF MF membrane in cross-flow protein (bovine serum albumin) solution filtration. After only 10 hours of operation, the membrane's permeance has been reduced by three orders of magnitude [9].

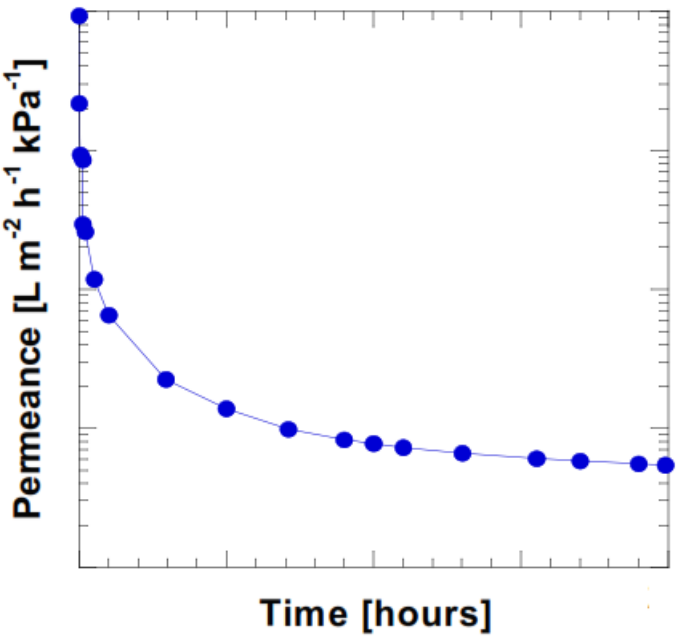

Fig. 1.14. The effect of fouling on water permeance tendency vs. filtration time in a PVDF MF membrane (0.2 μm nominal pore size) in cross-flow protein filtration of BSA solution (1 g/L).

Generally, membrane fouling is caused by the interaction between the membrane surface and the foulants. The foulants not only physically interact with the membrane surface but also degrade chemically the membrane surface [29-31]. Foulants are substances in many different forms. Normally, foulants can be classified into the following four categories [32]:

- Particulates: inorganic or organic particles/colloids (e.g. Silica) act as foulants which can physically cover the membrane surface and block the pores, or hinder transport to the surface by the development of a cake layer;
- Inorganic: dissolved components (e.g. iron, manganese and silica) which tend to precipitate onto the membrane surface due to pH change or due to oxidation (e.g.

iron or manganese oxides). Coagulant/flocculant residuals may also be present as inorganic foulants; the membrane fouling caused by this kind of foulants is called as inorganic fouling or scaling.

- Organic: dissolved components and colloids (e.g. humic and fulvic acids, hydrophilic and hydrophobic materials and proteins) which would attach to the membrane surface by adsorption; the result of organic foulants adsorption would be organic fouling.
- Micro-biological organisms: the microbiological category covers vegetative matter such as algae, and microorganisms such as bacteria which can adhere to the membranes and cause biofouling (biofilm formation).

In another categorization, the fouling was classified into three generic forms by depending on its mechanism [21, 27, 32].

(a) Pore narrowing: when particle size is much smaller than the pore size, particles can be adsorbed onto the surface or inside the pores of the membrane and make pore narrowing or constriction.

(b) Pore plugging: when particle size is almost the same with membrane pore size, particles can block the pores and make the pore plugging.

(c) Cake layer formation: when the particle size is larger than pore size, particles cannot pass through the membrane and precipitate on the membrane surface to form the gel/cake layer. Cake layer is usually formed by the deposition or aggregation of colloid, micro particles, microorganism, proteins, et al. As a result of the formation of cake layer, the water permeability decreases due to increasing of the permeation resistance. These three types of fouling mechanisms are schematically shown in Fig. 1.15.

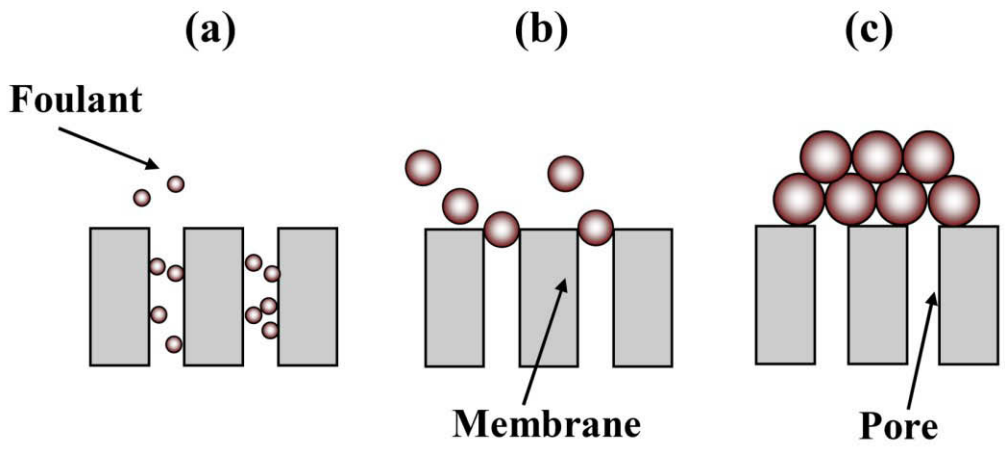

Fig. 1.15. Illustration of particle fouling mechanisms a) Incomplete pore blockage, pore narrowing, ($d_{particle} < d_{pore}$), b) Complete pore blockage or Pore plugging ($d_p \geq d_{pore}$), and c) Cake layer formation ($d_{particle} >> d_{pore}$)

Figure 1.16 shows a typical image taken during a fouling experiment with the feed flow from left to right and the permeate exits from the top right. The deposited cake is observed on the active filtration area as a dark layer on channel surface.

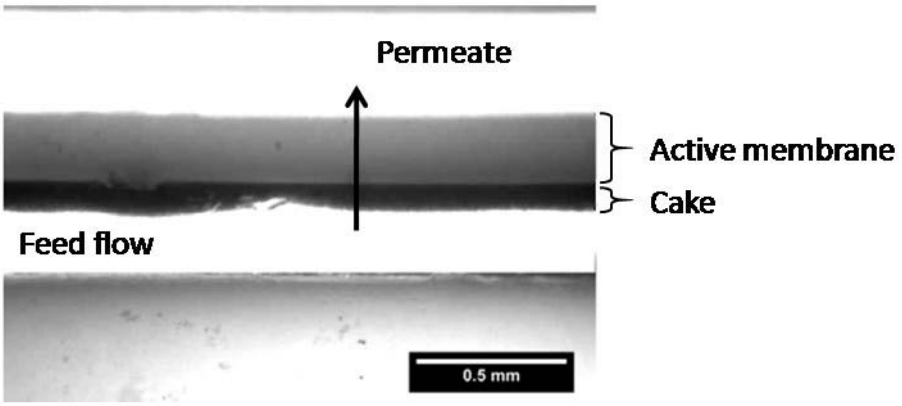

Fig. 1.16. Typical image of fouling experiment after 8 hour (feed from left to right, permeate from top channel), inset image after thresholding [21].

Foulants described above cause the fouling mainly in RO membrane processes

[33]. The inorganic and organic fouling were briefly discussed in below; because they were not the aims of this study. In this study, I particularly focused in membrane biofouling and effective strategies to improve antibiofouling properties.

1.2.2. Inorganic/Organic fouling (Parameters affecting membrane fouling)

Scale formation at the membrane surface is serious problem and resulting from the increased concentration of one or more species beyond their solubility limits and their ultimate precipitation onto the membranes. The term 'membrane scaling' (i.e. "Inorganic fouling") is commonly used when the precipitate forms a hard scale on the surface of the membrane. Scaling usually refers to the formation of deposition layer of salts such as $CaCO_3$, $CaSO_4$, silica, and calcium phosphate [34]. Figure 1.17 illustrates schematically both bulk and surface crystallization. When the bulk phase becomes supersaturated, both mechanisms of crystallization simultaneously proceed [35]. Figure 1.18 shows the SEM image of a forward osmosis (FO) membrane surface that scaled by silica.

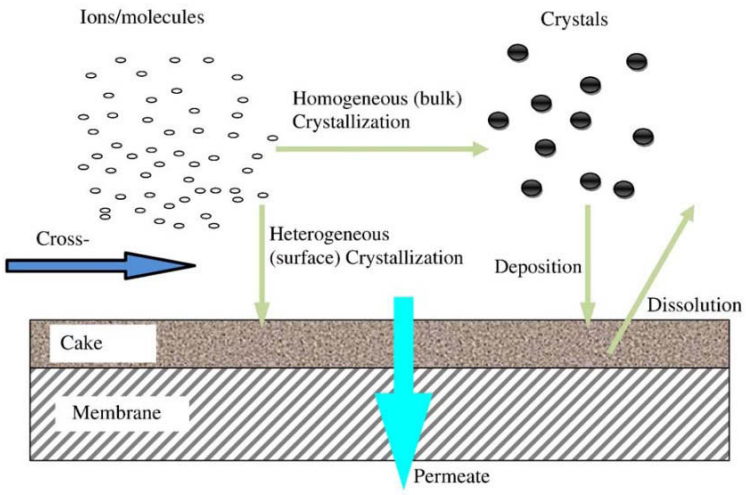

Fig. 1.17. Schematic representation of inorganic scaling mechanism [35].

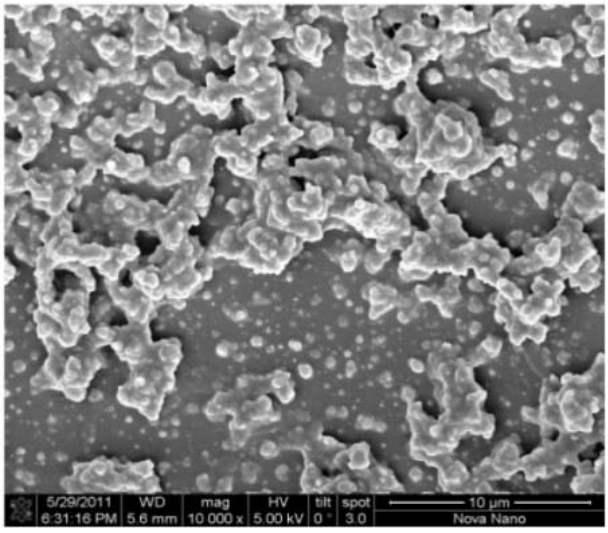

Fig. 1.18. Inorganic fouling (silica scaling) on the active layer of the FO membrane [36].

The previous studies showed that membrane fouling due to inorganic salts is dependent on membrane properties (e.g. porosity, roughness, etc.) on the crystallization of inorganic salts. It is well known that polished surface has fewer crystal at the end of crystallization experiment compared to a rough surface. The primary cause of inorganic scaling is super saturation. When the solubility of a salt is exceeded, the salt precipitates and forms scale. Other effective parameters are module geometry and membrane materials, feed solution characteristics and operating conditions (e.g. shear rate and operating pressure) [32, 35].

A membrane can also be fouled by dissolved organic compounds. Dissolved organic matter is everywhere in surface water and sewage, which can be classified into three different categories according to their origins as follows:

a) Refractory natural organic matter (NOM) derived from drinking water source.

b) Synthetic organic compounds added by consumers and disinfection byproducts

generated during disinfection processes of water and wastewater treatment.

c) Soluble microbial products formed during the biological treatment processes due to decomposition of organic compounds [37].

In drinking water treatment by low pressure membranes (MF/UF), natural organic matter has been identified as a major foulant of polymeric membranes in drinking water applications. Moreover, as the major component of dissolved organic matter are soluble microbial products, they can affect both kinetic activity and flocculating properties of activated sludge during biological wastewater treatment [32].

The interaction between membrane and the materials in the feed solution affect membrane fouling. Such interactions depend on the foulant materials, membrane properties, operation conditions, membrane module structure and so on as shown below.

a) Factors of feed solution side; the properties of the feed solution such as pH, viscosity, temperature, the ionic strength and etc. [38, 39].

b) Factors of the membrane side; the nature membrane properties such as hydrophilicity, charge density and roughness of membrane surface. As it is well known, the hydrophilic materials have a less tendency to be fouled as compared to hydrophobic material. The other factors are membrane surface charge and surface roughness. These factors should be also considered as a significant factor that affects membrane fouling. Since the most of foulants have negative charge, the antifouling properties are improved by increasing negative surface charge. Also, antifouling potential of membrane is enhanced by improving of surface smoothness [40-44].

c) Factor of process conditions; the operation conditions, such as the operation pressure and temperature, flow velocity, type of pump, pipe design and so on.

The above mentioned factors and suggested methods are just some examples because membrane fouling is very complicated and each separation process needs own specific treatment.

1.2.3. Biofilm and Biofouling

One of the most serious operational problem in a membrane application is biofouling. Biofilm formation is the accumulation of microorganisms (e.g. bacteria, algae and fungi) and extracellular compounds (Extracellular Polymeric Substances (EPS)) on a surface due to deposition and/or growth. Biofouling is the extent of biofilm formation causing unacceptable (operational) problems. In this context "unacceptable" means that operational parameters are undesirability changed. For example applied pressure is increased or water flux and salt rejection are declined [24, 28, 45]. In addition, biofouling causes the secondary pollution of the purified water by cell and their product metabolism, membrane biodegradation and finally caused a membrane failure [46, 47]. Biofilm typically develop in a series of five stages as below [48, 49]. Figure 1.19 shows schematically the biofilm formation in different stages.

I. A conditioning film comprised of proteins and other organic matter is formed on the surface.
II. Bacteria are brought close to the surface by fluid flow.
III. Bacteria adhere to the conditioned surface.
IV. The microorganisms grow and divide, colonizing the surface and producing extracellular matrix polymers.
V. Detachment to the planktonic state to colonize other locales.

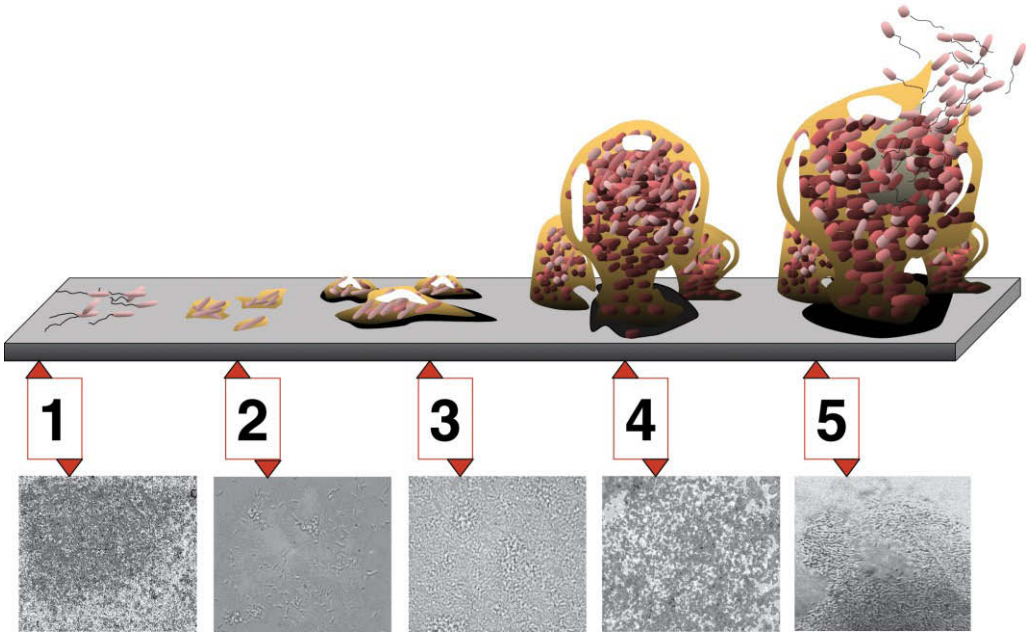

Fig. 1.19. Illustration of biofilm formation in five stages, Stage 1, initial attachment; stage 2, irreversible attachment; stage 3, maturation I; stage 4, maturation II; stage 5, dispersion. Each stage of development in the diagram is paired with a photomicrograph of a developing *P. aeruginosa* biofilm [48].

Figure 1.20 shows a picure of membrane module before and after biofouling. It can be seen that an irrivesible biofilm cover the membrane surface.

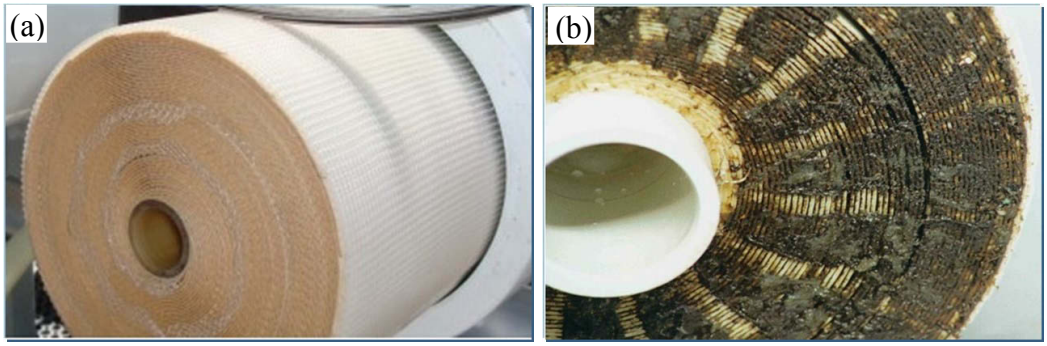

Fig. 1.20. A membrane module (a) before biofouling and (b) after biofilm formation

As already mentioned the conquest of biofouling is very important challenge in membrane process. Many research gropus are studying on this subject and numerous

papers are published every year. Since the first peer reviewed paper on membrane biofouling was puplished in 1982, the number of published papers has been steadily increased year by year as shown Fig. 1.21.

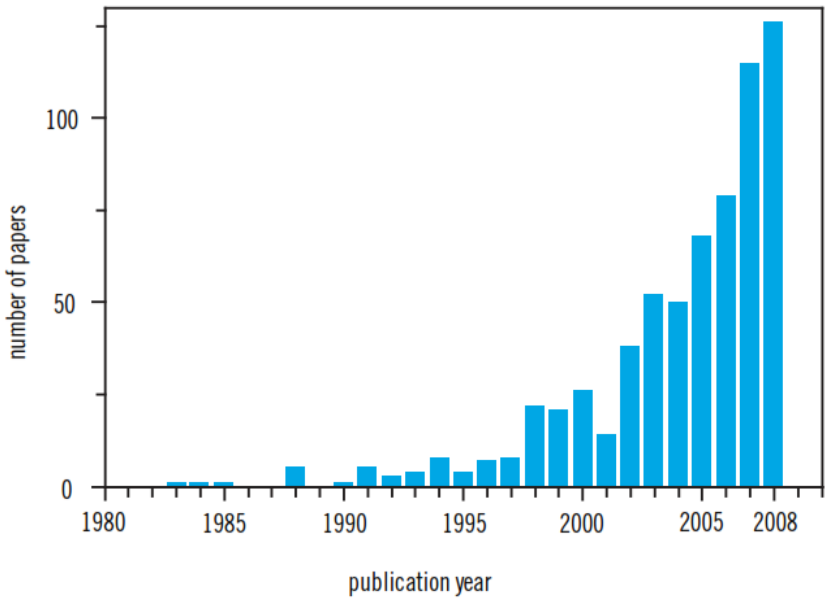

Fig. 1.21. Increasing in peer reviewed publications on membrane biofouling in the period 1982-2008 [24].

1.3. Improvement of antibiofouling properties

1.3.1. Detection, monitoring and evaluation techniques of membrane biofouling

Nowadays, numerous methods and apparatus have assisted the study about the membrane fouling. These apparatuses include scanning electron microscopy (SEM), transmission electron microscopy (TEM), atomic force microscopy (AFM), attenuated total reflection Fourier transform infrared spectrometry (ATR-FTIR), confocal laser scanning microscopy (CLSM) and so on. Generally, membrane biofilm formation can be detected by direct or indirect methods [45, 46, 50-52].

- **Direct methode:**

(a) Microscopy inspection of exposed membrane surface, for expample with CLSM apparatus, it is posible to observe the bacteria and distingush between alive and dead bacteria adhered on the membrane surface (Refer to section 2.2.3.5.2 of Chapter 2). Figure 1.22 shows outer surface of PES hollow fiber membrane observed by CLSM after 1 week immersion in bacteria suspension (1–5 × 10^7 cfu/ml). In addition, membrane surface observation by SEM is another proper method to investigate biofim formation. Figure 1.23 shows outer surface of PES hollow fiber membrane observed by SEM;

(b) biochemical/microbiological characterization of material that scraped from membranes surfaces (e.g., heterotrophic plate count determination).

- **Indirect method:**

(a) Measuring the parametres releted to membrane performance could indirectly imply the biofilm formation. For example a decline of water flux, increase in module differential pressure and solute transport resistance or decrease in salt rejection could be attributed to biofilm formation.

(b) An extremmely greater number of bacteria in the brine flow (retentate flow) than that in the feed water implies biofilm growth and cell detachment.

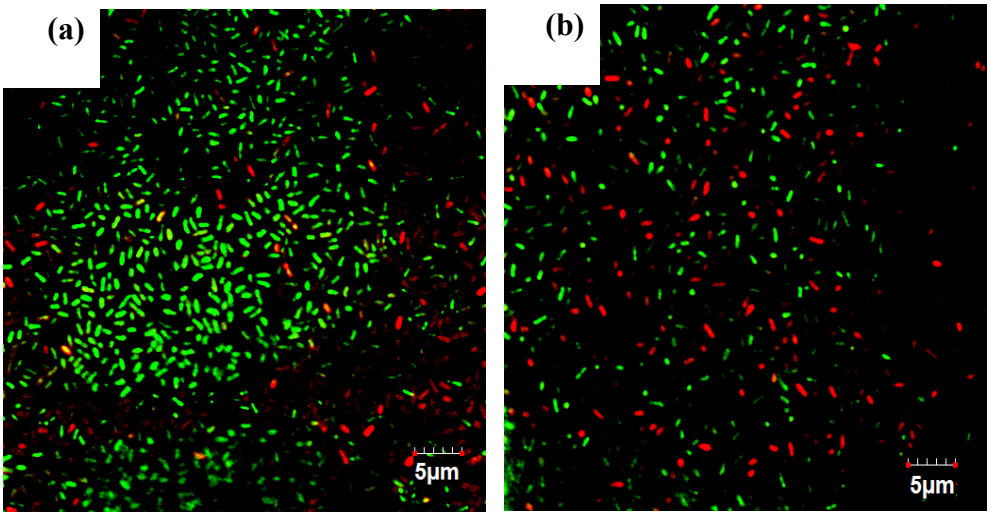

Fig. 1.22. CLSM images of membrane outer surfaces of PES hollow fiber membrane after 1 week of immersion in 10^7 cfu/ml of *P. putida* in 40 ml of Vogel-Banner Minimal Medium (VBMM) (a) Unmodified of PES hollow fiber membrane, (b) PES modified by grafting of a quaternary ammonium [52]. Black background is membrane surface and green points are alive bacteria and red points are dead bacteria.

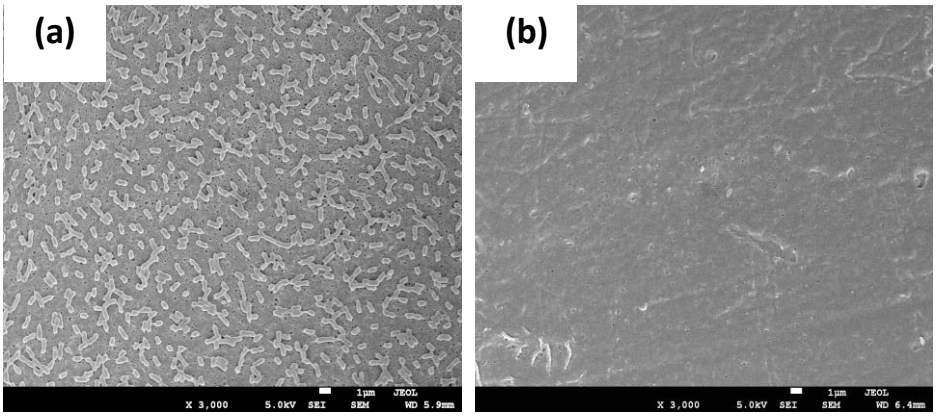

Fig. 1.23. SEM images of the membrane outer surfaces after adhesion test. Membranes were immersed into 10^7 cfu/ml of *P. putida* suspension for 1 week, (a) Unmodified PES membrane, (b) Polyzwitterion modified PES [51]. The adhered bacteria on the unmodified membrane surface are clear.

To evaluate the biofouling resistance, measuring of antibacterial property is a common method. The antibacterial properties, including biocide leaching and contact killing abilities, are usullay evluated by a shake flask test using *E. coli* as a model gram-negative bacterium. The procedure of this test is described in section 2.2.3.5.1 of Chapter 2 in ditail.

1.3.2. Strategies to improve antibiofouling properties

Biofouling is too complicated to present a common method to prevent it. However, existing methods can be classified into four general catgories as shown below:

A. Selection and optimization of effective feed water treatment.
B. Optimization of system operating pressure.
C. Selection of the most appropriate membrane.
D. Optimization of effective membrane cleaning

Manipulating membrane surface properties, feed water characteristic, operation conditions and effective cleaning systems can directly lead to optimize systems with minimized fouling (Fig. 1.24) [34].

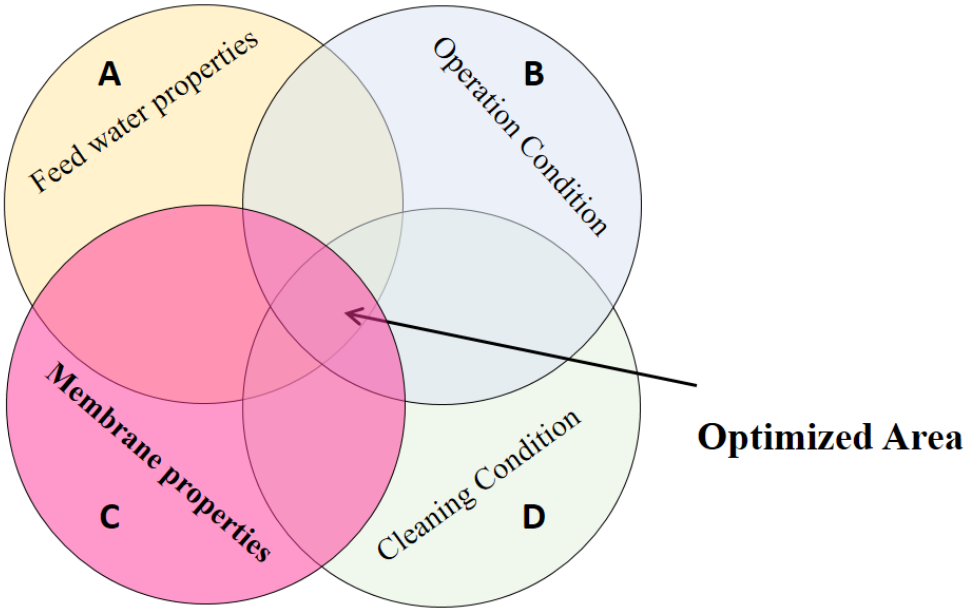

Fig. 1.24. Venn diagram of factors influencing operational membrane processes

It is noteworthy that biofouling problem in polyamide based NF and RO is exacerbated, because polyamide membranes cannot disinfected with chlorine treatment or backwashing [53]. From the membrane surface design point of view, there are two general strategies to control biofouling in the membrane filtration systems. These strategies are usually based on two important properties. The first one is based on antiadhesion property and the second one is based on the antimicrobial properties. The second strategy is divided into two approaches, improving contact killing and biocide leaching (release killing). Contact killing is based on direct contact between the biocide and the bacteria cell, while for release killing, ions are released from the biocide material and come into contact with, and kill bacteria. Most of studies on antibiofouling improvement have been based on these strategies [46, 54-56]. Figure 1.25 shows a schematic of the chief approaches to prevent biofouling.

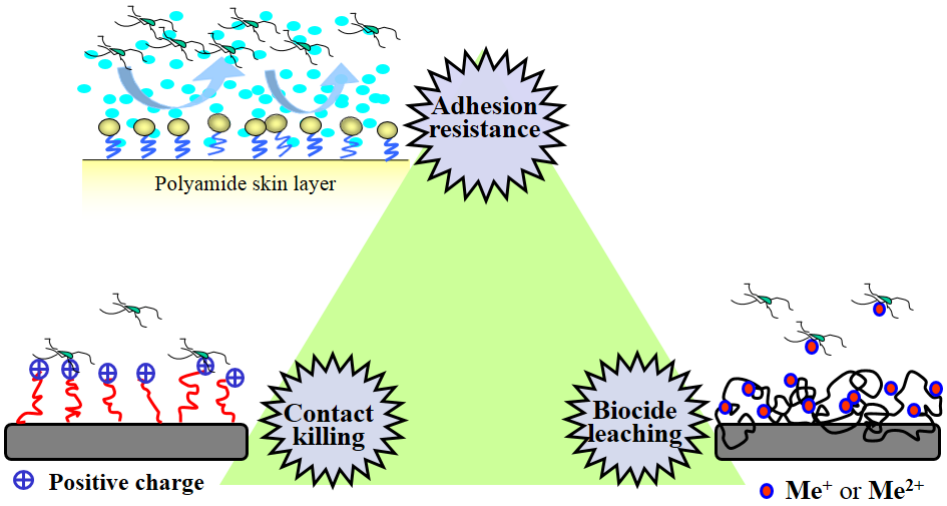

Fig. 1.25. The main approaches for controlling biofouling

The antiadhesion property increases the adhesion resistance of the surface against the bacteria attachment. This approach has focused to enhance antiadhesion property by the improvement of hydrophilicity and smoothness, and also by the increase of negative charge density of membrane surface. Thus, versatile surface modification methods such as blending, grafting and coating have being used to improve antiadhesion property [31, 42-44, 54].

The antibacterial properties improve the bacteria lysis. The contact killing is based on direct contact of bacteria with the biocide. In this approach, the membrane surface is functionalized with antibiotic groups. They include antimicrobial peptides, which are usually compounds that present positive charges. The presented positive charges can theoretically penetrate the cell membrane that disrupts the bacteria cell membrane integrity and induces cell lysis. Some kinds of these compounds are quaternary ammonium salts, guanidine polymers, phosphonium salts, and chitosan [52, 55, 56]. On the other hand, the biocide leaching (release killing) depends upon the release of

ions from the biocide materials, which then come into contact with and kill bacteria. This is one of the oldest method that has been employed since ancient times to disinfect drinking water using silver or copper [57, 58].

1.3.2.1. Materials possessing antimicrobial property

Antibacterial agents including organic and inorganic compounds are commonly used to improve the antibiofouling properties of membranes. Among the inorganic antibacterial agents, nano-sized particles of silver, gold and copper are well known as very good biocides which exhibit strong biocidal effect on as many as 16 types of bacteria including *Escherichia coli (E. coli)* and *Pseudomonas putida (P. putida)* [59]. The contact between biocide and bacteria can be improved by using nanoparticle size of antibacterial agents due to extremely large specific surface area. In addition, to immobilize and increase the durability of biocide leaching, biocide materials (e.g. silver nanoparticles) can be embedded in polyelectrolyte multilayers (PEMs) [56, 60]. In this case, metallic silver slowly releases bacteria toxic silver ions and/or interact directly with cell membranes in nanoparticle form.

Another type of inorganic antibacterial agents are metal oxides such as TiO_2, CuO, NiO, ZnO and so on. These are also effective antibacterial agents under UV irradiation. For these particles, the antibacterial mechanisms are believed to be due to the strong photo-oxidization property of the active oxygen species generated by these metal oxides particles under UV irradiation [61]. Metal hydroxides, including $Ca(OH)_2$ and $Mg(OH)_2$, also show antibacterial property due to direct contact with bacteria or changing the solution pH to alkaline condition [61, 62].

Organic antibacterial agents are also employed to improve the antibacterial property of membrane. However, their applications are limited because of low heat resistance and short life time. Organic material such as quaternary ammonium salts (QAS), guanidine polymers, quaternary phosphonium salt (QPS), and chitosan possess high antimicrobial property. Their cationic charges are able to interact with bacteria that attempt to adhere to the surface. It is considered that these positive charges penetrate the cell membrane that disrupts the cell membrane integrity and induces cell lysis by contact killing mechanism [52, 63, 64].

1.3.2.2. Membrane modification

As shown in Fig. 1.25, an increasing in adhesion resistance is one of the chief strategies to improve the antibiofouling properties. On the other hand, this improvement is primarily dependent on the membrane properties such as hydrophilicity, roughness and surface charge density. To achieve this aim, membrane modification methods such as blending, coating, grafting and so on, is the general approach especially for available commercial membranes. In this section, these methods are briefly discussed.

1.3.2.2.1. Blending

Blending is a process in which two (or more) polymers are physically mixed to obtain the required properties. The blending of hydrophobic polymers with hydrophilic polymers such as poly(vinylpyrrolidone) (PVP) has been widely applied to increase the hydrophilicity of membrane surfaces and produce antifouling properties [65]. Polymer blending is used to produce antifouling membranes during the membrane fabrication.

Surface treatment by graft polymerization or polymer coating adds more steps to the membrane preparation, which means it is not suitable for industrial large scale production. By contrast, in the polymer blending method, hydrophilic polymers are included in the doping solution, and the surface can be modified at the same time as the membrane fabrication. The problem with this method is that the blended hydrophilic polymers like polyethylene glycol (PEG) leak during the membrane preparation process [66, 67]. However, blend polymer membranes based on polyethersulfone (PES) have been successfully prepared in combination with PVP, cellulose acetate, cellulose acetate phthalate, soybean phosphatidylcholine and etc. [68, 69].

1.3.2.2.2. Coating

Coating is the most popular method to improve antifouling and/or antibiofouling potential of membrane surface. In this method, the coating material(s) covalently or non-covalently attached on the substrate and forms a thin layer. Some of the general coating methods are as follows:

Self-assembled alternating multilayers of cationic and anionic polyelectrolytes that is also called Layer-by-Layer (LbL) method is versatile approach to assemble nanometer-scale multilayers on solid surfaces to modify the membrane surface. The LbL is adsorption of oppositely charged species from aqueous media onto solid surface. Antifouling potential of membrane surface was improved by LbL adsorption due to the increase the hydrophilicity and negative surface charge density [70-72]. In addition, LbL is a promising method to immobilize particles such as silver nanoparticles on the membrane surface [60] .

Polydopamine (PDA) coating is also a surface modification method that formed tight layer on the surface by strong covalent and non-covalent interactions with substrate. [73]. The surface modification with PDA is reported for several kinds of membranes such as microfiltration (MF) [74], ultrafiltration (UF) and RO membranes [74-76]. It is well known that PDA is a super hydrophilic material that improves the hydrophilicity of hydrophobic surfaces such as polyethylene (PE), poly (vinyl fluoride) (PVDF) and polytetrafluoroethylene (PTFE) [77-80]. Thus, a sufficient improvement of antifouling property is expectable due to the increase of surface hydrophilicity and surface charge density. Furthermore, PDA coating is reported as pretreatment to coat another layer like heparin [80] or immobilize silver particles on the membrane surface [81].

1.3.2.2.3. Grafting

Grafting techniques to produce antifouling surfaces have been extensively studied. Both "grafting to" and "grafting form" using hydrophilic polymers are used to generate dense brush structure. There are several common techniques which usually to initiate grafting such as: (I) chemical, (II) photochemical and/or via high-energy radiation, (III) the use of a plasma, and (IV) enzymatic. The choice for a specific grafting technique depends on the chemical structure of the membrane and the desired characteristics after surface modification [82, 83]. One emerging strategy for creating bacteria-resistant surfaces involves the exploitation of hydrophilic polymers or polymer segments that are capable of strong hydrogen-bonding interactions with water. For example, poly(ethylene glycol) (PEG) immobilized or grafted onto surfaces forms a highly

hydrated layer that significantly curtails adsorption of protein and adhesion of platelets, bacteria and tissue cells attributable to PEG's strong affinity for water molecules. [84, 85].

There are some other modification methods include chemical modification (e.g. hydrophilization treatment, chemical coupling and plasma polymerization or plasma-induced polymerization), composite, UV photochemical irradiation induced graft polymerization. However, these methods are not the scope of this study. So, the detail of them was not mentioned here.

1.4. Aim and overview of this thesis

I described above the water shortage problem and the important role of membrane technology and in particular RO membrane to deal with this problem. The motivation of this project is the study about biofouling problem as major obstacle of RO membrane process. I focused on different methods to improve the antibiofouling properties of a commercial RO membrane. The overview of thesis chapters is described as follow:

This thesis was divided into 6 parts. The **Chapter 1** introduced the background of this study as well as the purpose of this study.

In **Chapter 2**, the RO membrane active layer was modified by a deposition of polyelectrolyte multilayers (PEMs) embedded with silver nanoparticles to improve antibiofouling properties. The modified membrane was further coated with an amphiphilic polyzwitterion, 2-methacryloyloxyethyl phosphorylcholine (MPC) copolymer with 2-aminoethyl methacrylate (AEMA). Thus, the modified surface layer

consisted of PEMs embedded with silver nanoparticles and polyzwitterion as a top layer. Embedding of silver nanoparticles and polyzwitterion coating were confirmed TEM and X-ray photoelectron spectroscopy (XPS). The effectiveness of biocide release from the modified membranes was evaluated with *P. putida* and *E. coli* and the anti-adhesion property was studied using *P. putida*. The silver nanoparticles embedded within PEMs showed biocidal property due to released silver ions and polyzwitterion at the top layer showed high antiadhesion properties because of the high hydrophilicity of surface. Thus, the membrane modified by PEMs embedded with silver nanoparticles and polyzwitterion as a top layer showed a high antibiofouling properties, attributed to the combined effect of biocide release and adhesion resistance.

In **Chapter 3**, the RO membrane was modified by adsorption of copper hydroxide ($Cu(OH)_2$) particles to improve antibiofouling properties of the membrane. The adsorption of $Cu(OH)_2$ particles was confirmed by SEM and energy dispersive spectroscopy. The proportion of adsorbed $Cu(OH)_2$ particles was measured by flame atomic absorption spectrophotometry. The antibacterial properties of the modified membranes were evaluated by a shake flask test with *E. coli* and the antiadhesion properties were evaluated by an immersion test using *P. putida*. The $Cu(OH)_2$ modified membranes showed good antibacterial activity compared with the unmodified membranes. The antibacterial activity was attributed to release of Cu^{2+}ions from $Cu(OH)_2$ particles adsorbed to the membrane. The antiadhesion properties of the membrane were improved by $Cu(OH)_2$ modification. This is attributed to an increase of the hydrophilicity and negative charge density of the membrane surface. The membrane

modified with $Cu(OH)_2$ particles showed high antibiofouling performance, attributed to a combination of antibacterial and antiadhesion effects.

In **Chapter 4**, I attempted to modify the RO membrane with Polydopamine (PDA) to improve an antibiofouling potential. The deposition of PDA was confirmed by XPS, FTIR and so on. The improvement of antibiofouling property was confirmed by the cross-flow filtration of bacteria (*P.putida*) suspension. In addition, the high antiadhesion property of the PDA modified membrane was confirmed by the SEM surface images after 20 hours filtration of bacteria suspension. Furthermore, it was shown that the PDA modified membrane had a bactericidal property by a shake flask test with *E. coli*. From the shake flask tests in the different pH solutions, it was concluded that the antibiofouling property of PDA modified membrane was attributed to the bactericidal property of protonated amine groups of PDA deposited on the membrane surface.

In **Chapter 5**, I attempted to use the PDA coating as a precursor layer to enhance durability and antibiofouling potential of polyzwitterion (PZ) immobilized membrane. The deposition of PDA and PZ was confirmed by X-ray photoelectron spectroscopy. The hydrophilicity was not clearly increased by surface modification. Moreover, the membrane surface charge density changed from negative to neutral by PZ immobilization. Nevertheless, the improvement of antibiofouling properties was confirmed by cross-flow filtration of a bacterial (*P. putida*) suspension. The high antiadhesion property of the modified membranes with PDA coating and/or PZ immobilization was confirmed by scanning electron microscope surface images after

1200 minutes filtration of the bacterial suspension. Moreover, the PDA coating as precursor layer was confirmed to increase the stability of PZ immobilized layer on the membrane surface by the filtration of bacterial suspension after one month immersion into 2 M NaCl aqueous solution.

Chapter 6 summarized the conclusions of this dissertation.

Refrences

[1]T. Oki, S. Kanae, Global hydrological cycles and world water resources, Science, 313 (2006) 1077-1081.
[2]P.H. Gleick, Water in Crisis: A Guide to the World's Freshwater Resources, Oxford University Press, (1993) .
[3]A. Fenwick, Waterborne infectious diseases - Could they be consigned to history?, Science, 313 (2006) 1077-1081.
[4]Drinking Water, Sanitation & Hygiene, UN Water Organization, http://www.unwater.org/statistics_san.html.
[5]R.F. Service, Desalination freshens up, Science, 313, (2006) 1088-1090.
[6]Norman N. Li, Anthony G. Fane, W. S. Winston Ho, T. Matsuura, Advanced Membrane Technology and Applications, John Wiley & Sons, Inc. , Hoboken, New Jersey(2008) .
[7]Managing Water under Uncertainty and Risk, The United Nations World Water Development Report 4, Volume 1(2012) .
[8]J. Mallevialle, P. E. Odendaal, M. R. Wiesner, The Emergence of Membranes in Water and Wastewater Treatment, in Water Treatment: Membrane Processes, McGraw Hill Co., New York, NY. 1.1-1.10.(1996)
[9]B.D. McCloskey, Novel Surface Modifications and Materials for Fouling Resistant Water Purification Membranes, Ph.D. Thesis, University of Texas at Austin(2009) .
[10]B. Alspach, SWRO Trends in the USA, Australia, and Beyond, KAUST International Symposium, Shanghai ,China(2010) .
[11]Andrew L. Zydney, Leos J. Zeman, Microfiltration and ultrafiltration: principles and applications, New York: CRC,1996.
[12]M. Mulder, Basic Principles of Membrane Technology, Kluwer Academic publishers, the Netherlands(1996) .
[13]R.W. Baker, Membrane Technology and Applications, 2nd ed., John Wiley & Sons Ltd, England, (2004) .
[14]A.B. KOŁTUNIEWICZ, The History and State of Art in Membrane Technologies, WROCLAW Uni. OF Tech., Chemistry Dept. Institute of Chem. Eng.(2005) ,.

[15]I. Pinnau, B. D. Freeman, Editors, Membrane Formation and Modification, American Chemical Society, 744, Washington, DC (1999) 1-20.
[16]S. P. Nunes, K.-V. Pienemann, Membrane Technology in the Chemical Industry, Wiley-VCH Verlag GmbH, (2001) .
[17]G. Srikanth, Membrane separation processes: technology and business opportunities, Water Conditioning and Purification Magazine International(2008), 50.
[18]S. Madaeni, The application of membrane technology for water disinfection, Water Research, 33 (1999) 301-308.
[19]S. Mulyati, Modeling of Electrodialysis Process and Improvement of Anion Exchange Membrane Performance by Surface Modification with Polyelectrolyte Ph.D. Thesis, Graduate School of Science and Technology, Kobe University, Japan.(2013)
[20]T .Matsuura, Synthetic Membranes and Membrane Separation Processes, CRC Press.(1994) ,
[21]I. Ngene, Real time visual characterization of membrane fouling and cleaning, PhD Thesis, University of Twente, The Netherlands, (2010) .
[22]R.J. Petersen, Composite reverse osmosis and nanofiltration membranes, Journal of Membrane Science, 83 (1993) 81-150.
[23]N. Hilal, H. Al-Zoubi, N.A. Darwish, A.W. Mohamma, M. Abu Arabi, A comprehensive review of nanofiltration membranes:Treatment, pretreatment, modelling, and atomic force microscopy, Desalination, 170 (2004) 281-308.
[24]H. Vrouwenvelder, Biofouling of spiral wound membrane systems, PhD thesis Delft University of Technology, Delft , The Netherlands, (2009) .
[25]IDA Desalination Yearbook 2009-2010 The International Desalination Association.
[26]P. Dydo, M. Turek, J. Ciba, K. Wandachowicz, J. Misztal, The nucleation kinetic aspects of gypsum nanofiltration membrane scaling, Desalination, 164 (2004) 41-52.
[27]A. G. Fane, W. Xi, W. Rong, Membrane filtration processes and fouling, Interface Science in Drinking Water Treatment, (Editor: G. Newcombe and D. Dixon), Elsevier (2006) pp.109-115.
[28]T.R. Bott, Industrial Biofouling, Elsevier, (2011) .
[29]W. Yuan, A.L. Zydney, Humic acid fouling during microfiltration, Journal of Membrane Science, 157 (1999) 1-12.
[30]Y.-q. Wang, T. Wang, Y.-l. Su, F.-b. Peng, H. Wu, Z.-y. Jiang, Remarkable Reduction of Irreversible Fouling and Improvement of the Permeation Properties of Poly(ether sulfone) Ultrafiltration Membranes by Blending with Pluronic F127, Langmuir, 21 (2005) 11856-11862.
[31]D. Rana, T. Matsuura, Surface Modifications for Antifouling Membranes, Chemical Reviews, 110 (2010) 2448-2471.
[32]W. Guo, H.-H. Ngo, J. Li, A mini-review on membrane fouling, Bioresource Technology, 122 (2012) 27-34.
[33]G.-d. Kang, Y.-m. Cao, Development of antifouling reverse osmosis membranes for water treatment: A review, Water Research, 46 (2012) 584-600.
[34]A. Al-Amoudi, R.W. Lovitt, Fouling strategies and the cleaning system of NF membranes and factors affecting cleaning efficiency, Journal of Membrane Science, 303 (2007) 4-28.
[35]S. Shirazi, C.-J. Lin, D. Chen, Inorganic fouling of pressure-driven membrane processes — A critical review, Desalination, 250 (2010) 236.248-

[36]Gary Amy, Z. Li, Seawater Desalination by Osmotically Driven Membrane Process, Research Summry, (2009) .
[37]J.E. Drewes, P. Fox, Fate of natural organic matter (NOM) during groundwater recharge using reclaimed water, Water Science and Technology, 40 (1999) 241-248.
[38]N. Lee, G. Amy, J.-P. Croué, H. Buisson, Identification and understanding of fouling in low-pressure membrane (MF/UF) filtration by natural organic matter (NOM), Water Research, 38 (2004) 4511-4523.
[39]D. Jermann, W. Pronk, S .Meylan, M. Boller, Interplay of different NOM fouling mechanisms during ultrafiltration for drinking water production, Water Research, 41 (2007) 1713-1722.
[40]A. Weis, M.R. Bird, M. Nyström, C. Wright, The influence of morphology, hydrophobicity and charge upon the long-term performance of ultrafiltration membranes fouled with spent sulphite liquor, Desalination, 175 (2005) 73-85.
[41]Y. Kim, D. Rana, T. Matsuura, W.-J. Chung, K.C. Khulbe, Relationship between surface structure and separation performance of poly(ether sulfone) ultra-filtration membranes blended with surface modifying macromolecules, Separation and Purification Technology, 72 (2010) 123-132.
[42]Colin Hobbs, Seungkwan Hong, J. Taylor, Effect of surface roughness on fouling of RO and NF membranes during filtration of a high organic surficial groundwater, Aqua- Journal of Water Supply: Research and Technology, 55 (2006) 559.
[43]J.S. Louie, I. Pinnau, I. Ciobanu, K.P. Ishida, A. Ng, M. Reinhard, Effects of polyether–polyamide block copolymer coating on performance and fouling of reverse osmosis membranes, Journal of Membrane Science, 280 (2006) 762-770.
[44]W. Lee, C.H. Ahn, S. Hong, S. Kim, S. Lee, Y. Baek, J. Yoon, Evaluation of surface properties of reverse osmosis membranes on the initial biofouling stages under no filtration condition, Journal of Membrane Science, 351 (2010) 112-122.
[45]M. Al-Ahmad, F.A. Abdul Aleem, A. Mutiri, A. Ubaisy, Biofuoling in RO membrane systems Part 1: Fundamentals and control, Desalination, 132 (2010) 173-179.
[46]C.X. Liu, D.R. Zhang, Y. He, X.S. Zhao, R. Bai, Modification of membrane surface for anti-biofouling performance: Effect of anti-adhesion and anti-bacteria approaches, Journal of Membrane Science, 346 (2010) 121-130.
[47]V.M. Kochkodan ,N. Hilal, V.V. Goncharuk, L. Al-Khatib, T.I. Levadna, Effect of the surface modification of polymer membranes on their microbiological fouling, Colloid J, 68 (2006) 267-273.
[48]D. Monroe, Looking for Chinks in the Armor of Bacterial Biofilms, PLOS BIOLOGY, 5 (2007) 2458-2461.
[49]Steven Lane Percival, James Taggari Walker, P.R. Hunter, Microbiological Aspects of Biofilms and Drinking Water, CRC Press, (2000) .
[50]C.H. Worthley, K.T. Constantopoulos, M. Ginic-Markovic, R.J. Pillar, J.G. Matisons, S. Clarke, Surface modification of commercial cellulose acetate membranes using surface-initiated polymerization of 2-hydroxyethyl methacrylate to improve membrane surface biofouling resistance, Journal of Membrane Science, 385–386 (2011) 30-39.

[51]F. Razi, I .Sawada, Y. Ohmukai, T. Maruyama, H. Matsuyama, The improvement of antibiofouling efficiency of polyethersulfone membrane by functionalization with zwitterionic monomers, Journal of Membrane Science, 401–402 (2012) 292-299.
[52]F. Razi, I. Sawada, Y. Ohmukai, T. Maruyama, H. Matsuyama, Surface functionalization by grafting of (2-dimethylamino)ethyl methacrylate methyl chloride quaternary salt (DMAEMAq) onto hollow fiber polyethersulfone (PES) membranes for improvement of antibiofouling properties, Solvent Extr. Res. Dev, 19 (2012) 101-115.
[53]R. Bernstein, S. Belfer, V. Freger, Bacterial Attachment to RO Membranes Surface-Modified by Concentration-Polarization-Enhanced Graft Polymerization, Environmental Science & Technology, 45 (2011) 5973-5980.
[54]J. Mansouri, S. Harrisson, V. Chen, Strategies for controlling biofouling in membrane filtration systems: challenges and opportunities, Journal of Materials Chemistry, 20 (2010) 4567-4586.
[55]J.A. Lichter, K.J. Van Vliet, M.F. Rubner, Design of Antibacterial Surfaces and Interfaces: Polyelectrolyte Multilayers as a Multifunctional Platform, Macromolecules, 42 (2009) 8573-8586.
[56]Z. Li, D. Lee, X. Sheng, R.E. Cohen, M.F. Rubner, Two-Level Antibacterial Coating with Both Release-Killing and Contact-Killing Capabilities, Langmuir, 22 (2006) 9820-9823.
[57]C. Marambio-Jones, E.V. Hoek, A review of the antibacterial effects of silver nanomaterials and potential implications for human health and the environment, J Nanopart Res, 12 (2010) 1531-1551.
[58]Gadi Borkow, J. Gabbay, Copper, An Ancient Remedy Returning to Fight Microbial, Fungal and Viral Infections, Current Chemical Biology, 3 (2009) 272-278.
[59]V. Thomas, M.M. Yallapu, B. Sreedhar, S.K. Bajpai, A versatile strategy to fabricate hydrogel–silver nanocomposites and investigation of their antimicrobial activity, Journal of Colloid and Interface Science, 315 (2007) 389-395.
[60]X. Zan, Z. Su, Polyelectrolyte multilayer films containing silver as antibacterial coatings, Thin Solid Films, 518 (2010) 5478-5482.
[61]C. Dong, D. Song, J. Cairney, O.L. Maddan, G. He, Y. Deng, Antibacterial study of Mg(OH)2 nanoplatelets, Materials Research Bulletin, 46 (2011) 576-582.
[62]C. Dong, J. Cairney, Q. Sun, O. Maddan, G. He, Y. Deng, Investigation of Mg(OH)2 nanoparticles as an antibacterial agent, J Nanopart Res, 12 (2010) 2101-2109.
[63]N. Hilal, V. Kochkodan, L. Al-Khatib, T. Levadna, Surface modified polymeric membranes to reduce (bio)fouling: a microbiological study using E. coli, Desalination, 167.300-293 (2004)
[64]P. Majumdar, E. Lee, N. Gubbins, S.J. Stafslien, J. Daniels, C.J. Thorson, B.J. Chisholm, Synthesis and antimicrobial activity of quaternary ammonium-functionalized POSS (Q-POSS) and polysiloxane coatings containing Q-POSS, Polymer, 5 (2009) 0 .1133-1124
[65]J.F. Hester, P. Banerjee, A.M. Mayes, Preparation of Protein-Resistant Surfaces on Poly(vinylidene fluoride) Membranes via Surface Segregation, Macromolecules, 32 (1999) 1643-1650.
[66]A. Moriya, P. Shen, Y. Ohmukai, T. Maruyama ,H. Matsuyama, Reduction of fouling on poly(lactic acid) hollow fiber membranes by blending with poly(lactic acid)–

polyethylene glycol–poly(lactic acid) triblock copolymers, Journal of Membrane Science, 415–416 (2012) 712-717.
[67]P. Shen, A. Moriya, S .Rajabzadeh, T. Maruyama, H. Matsuyama, Improvement of the antifouling properties of poly (lactic acid) hollow fiber membranes with poly (lactic acid)–polyethylene glycol–poly (lactic acid) copolymers, Desalination, 325 (2013) 37-39.
[68]A. Rahimpour, S.S .Madaeni, Polyethersulfone (PES)/cellulose acetate phthalate (CAP) blend ultrafiltration membranes: Preparation, morphology, performance and antifouling properties, Journal of Membrane Science, 305 (2007) 299-312.
[69]F. Ran, S. Nie, W. Zhao, J. Li, B .Su, S. Sun, C. Zhao, Biocompatibility of modified polyethersulfone membranes by blending an amphiphilic triblock co-polymer of poly(vinyl pyrrolidone)–b-poly(methyl methacrylate)–b-poly(vinyl pyrrolidone), Acta Biomaterialia, 7 (2011) 3370-3381.
[70]S. Mulyati, R. Takagi, A. Fujii, Y. Ohmukai, T. Maruyama, H. Matsuyama, Improvement of the antifouling potential of an anion exchange membrane by surface modification with a polyelectrolyte for an electrodialysis process, Journal of Membrane Science, 417–418.143-137 (2012)
[71]S. Mulyati, R. Takagi, A. Fujii, Y. Ohmukai, H. Matsuyama, Simultaneous improvement of the monovalent anion selectivity and antifouling properties of an anion exchange membrane in an electrodialysis process, using polyelectrolyte multilayer deposition, Journal of Membrane Science, 431 (2013) 113-120.
[72]T. Ishigami, K. Amano, A. Fujii, Y. Ohmukai, E. Kamio, T. Maruyama, H. Matsuyama, Fouling reduction of reverse osmosis membrane by surface modification via layer-by-layer assembly, Separation and Purification Technology, 99 (2012) 1-7.
[73]H. Lee, S.M. Dellatore, W.M. Miller, P.B. Messersmith, Mussel-Inspired Surface Chemistry for Multifunctional Coatings, Science, 318 (2007) 426-430.
[74]B.D. McCloskey, H.B. Park, H. Ju, B.W. Rowe ,D.J. Miller, B.J. Chun, K. Kin, B.D. Freeman, Influence of polydopamine deposition conditions on pure water flux and foulant adhesion resistance of reverse osmosis, ultrafiltration, and microfiltration membranes, Polymer, 51 (2010) 3472-3485.
[75]S. Kasemset, A. Lee, D.J. Miller, B.D. Freeman, M.M. Sharma, Effect of polydopamine deposition conditions on fouling resistance, physical properties, and permeation properties of reverse osmosis membranes in oil/water separation, Journal of Membrane Science, 4.216-208 (2013) 426-25
[76]S. Azari, L. Zou, Using zwitterionic amino acid l-DOPA to modify the surface of thin film composite polyamide reverse osmosis membranes to increase their fouling resistance, Journal of Membrane Science, 401-402 (2012) 68-75.
[77]Z.-Y. Xi, Y.-Y. Xu, L.-P. Zhu, Y. Wang, B.-K. Zhu, A facile method of surface modification for hydrophobic polymer membranes based on the adhesive behavior of poly(DOPA) and poly(dopamine), Journal of Membrane Science, 327 (2009) 244-253.
[78]L.-P. Zhu, J.-H. Jiang, B.-K. Zhu, Y.-Y. Xu, Immobilization of bovine serum albumin onto porous polyethylene membranes using strongly attached polydopamine as a spacer, Colloids and Surfaces B: Biointerfaces, 86 (2011) 111-118.
[79]J.-H. Jiang, L.-P. Zhu, X.-L .Li, Y.-Y. Xu, B.-K. Zhu, Surface modification of PE porous membranes based on the strong adhesion of polydopamine and covalent immobilization of heparin, Journal of Membrane Science, 364 (2010) 194-202.

[80]L.-P. Zhu, J.-Z. Yu, Y.-Y. Xu, Z.-Y. Xi, B.-K .Zhu, Surface modification of PVDF porous membranes via poly(DOPA) coating and heparin immobilization, Colloids and Surfaces B: Biointerfaces, 69 (2009) 152-155.
[81]W. Wang, R. Li, M. Tian, L. Liu, H. Zou, X. Zhao, L. Zhang, Surface Silverized Meta-Aramid Fibers Prepared by Bio-inspired Poly(dopamine) Functionalization, ACS Applied Materials & Interfaces, 5 (2013) 2062-2069.
[82]K.C. Khulbe, C. Feng, T. Matsuura, The art of surface modification of synthetic polymeric membranes, Journal of Applied Polymer Science, 115 (2010) 855-895.
[83]M. Ulbricht, Advanced functional polymer membranes, Polymer, 47 (2006) 2217-2262.
[84]H. Ma, J. Hyun, P. Stiller, A. Chilkoti, "Non-Fouling" Oligo(ethylene glycol)-Functionalized Polymer Brushes Synthesized by Surface-Initiated Atom Transfer Radical Polymerization, Advanced Materials, 16 (2004) 338-341.
[85]Y.-L. Su, W. Cheng, C. Li, Z. Jiang, Preparation of antifouling ultrafiltration membranes with poly(ethylene glycol)-graft-polyacrylonitrile copolymers, Journal of Membrane Science, 329 (2009) 246-252.

Chapter 2

Improvement of antibiofouling performance of RO membranes through biocide release and adhesion resistance

2.1. Introduction

In the first chapter, I discussed that the water shortage problem is one of the most challenge in the world that caused to call 21st century the "water century". Conversely, 97% of Earth's water is saline, thus the desalination process is a main strategy to overcome water shortage problem. Among many methods, reverse osmosis (RO) membrane technology is one of the most popular water purification technologies, because of its properties such as the high salt rejection and permeation rates as well as their excellent chemical, thermal and mechanical stability [1]. However, fouling is a major problem in RO process as well as in other membrane processes. Membrane fouling negatively affects membrane performance by decreasing water permeability. As a result, the costs of membrane processes are increased by higher energy consumption and the frequent need for cleaning and maintenance [2-4].

Many studies have been carried out to prevent the fouling in RO processes and various methods have been suggested to control membrane fouling. Membrane fouling can be broadly categorized into inorganic fouling, organic fouling and biofouling [5].

Inorganic fouling is caused by the scale formation at the membrane surface [5] and organic fouling by the deposition of organic foulants (such as surfactants and proteins) on the membrane surface [5-9]. Biofouling is the undesired attachment of microorganism communities to a membrane surface. Bacteria adhered to the surface release extracellular polymeric substances (EPS) and consequently, a biofilm EPS matrix with embedded bacteria is formed [3, 10]. Membrane biofouling is a more serious problem than organic fouling, particularly in drinking water production and water treatment, because of the secondary pollutants generated as metabolic products of the bacteria that have attached and grown on the membrane surface [4, 11]. In addition, biofouling cannot be removed by chlorine treatment or backwashing [3], while inorganic fouling and organic fouling can be reversed [5].

Generally, the antibiofouling properties are improved through two main strategies (see Fig. 1.25). These strategies are usually based on two important properties. The first one is based on antimicrobial properties and the second one is based on the antiadhesion property. The first strategy is divided into two approaches, improving biocide leaching (release killing) and contact killing. Thus, these strategies totally include three approaches; biocide leaching, contact killing and antiadhesion [12].

In the first approach (biocide leaching), the cytotoxic compounds are released from biocide chemicals embedded into the surface, killing bacteria in the feed solution. Thus, the attachment of bacteria on the membrane surface is reduced. Silver (Ag) nanoparticles are a conventional biocide, used as a source in the biocide leaching approach. Sawada et al. improved the antibiofouling properties of a polyethersulfone

(PES) membrane by forming an acrylamide surface layer embedded with silver nanoparticles [2]. Other researchers also used Ag nanoparticle as a strong biocide leaching source in their studies [13-16].

In the second approach (contact killing), the surface is modified by antibacterial materials such as antimicrobial peptides and chemicals with quaternary ammonium groups [16-19]. Razi et al. improved the antibiofouling properties of a polyethersulfone (PES) hollow fiber membrane by grafting (2-dimethylamino) ethyl methacrylate methyl chloride quaternary salt (DMAEMAq) onto the membrane surface [17].

In the third approach (adhesion resistance), groups with the same electrostatic charge polarity as bacteria enhances the antiadhesion properties of the membrane surface through electrostatic repulsion between the bacteria and the membrane surface [20]. Zwitterionic monomers, such as methacryloyloxyethyl phosphorylcholine (MPC), are chemicals with cationic and anionic groups on their backbone structures and are electrically neutral. These zwitterionic monomers are biocompatible and are known for their high hydrophilicity [21-23]. Thus, grafting zwitterionic monomers onto a membrane surface is another method to improve adhesion resistance [3, 4]. Razi et al. improved antibiofouling properties of PES hollow fiber membranes by surface modification with zwitterionic monomers [4].

The combination of different properties is a promising technique for effective improvement of the antibiofouling performance of membranes. However, few studies have reported the effects of combining two different approaches [16, 20, 24]. Rubner et al. improved the bacteriocidal properties of a polystyrene surface through the

release of Ag ions and the contact killing properties of the surface through surface immobilization of a chemical with quaternary ammonium groups [16]. Bai et al. improved the antibacterial properties by incorporating Ag nanoparticles into a membrane surface (release killing) and by surface modification with heparin (antiadhesion effect) [20]. Zan et al. grafted the poly (L-lactic acid) (PLLA) surface with a poly(vinyl alchohol) (PVA) hydrogel loaded with silver nanoparticles. The film showed antibacterial property due to silver nanoparticles and cell adhesion resistance property due to high water content and soft nature of the PAV hydrogel [24].

In this chapter, I describe the attempt to improve the antibiofouling performance of a commercial RO membrane by imparting both release killing and adhesion resistance properties. The membrane surface is modified by a polyelectrolyte multilayers (PEMs) embedded with silver nanoparticles and polyzwitterion as a top layer. It is expected that silver nanoparticles provide a good release killing property as a biocide and polyzwitterion with amphiphilic structure at the top surface improves antiadhesion property of membrane.

2.2. Experimental

2.2.1. Materials

A commercial RO membrane (ES20, Nitto Denko, Osaka, Japan) was used as the base membrane. This is an ultra-low pressure RO membrane with an aromatic polyamide selective layer. The nominal value of rejection in company catalogue is 99.7% for 0.05% NaCl. Poly(allylamine hydrochloride) (PAH) (average molecular weight, M_W: 58,000) (Sigma-Aldrich, St. Louis, MO, USA) was used as a polycation

and poly(sodium 4-styrene sulfonate) (PSS) (average, M_W: 70,000) (Sigma-Aldrich) was used as a polyanion. A 2-methacryloyloxyethyl phosphorylcholine (MPC) copolymer with 2-aminoethyl methacrylate (AEMA) (MPC-co-AEMA, NOF Corporation, Tokyo, Japan) was used as the polyzwitterion. The molar ratio of MPC to AEMA was 90:10. The chemical structure of PAH, PSS and MPC-co-AEMA are illustrated in Fig. 2.1. Silver nitrate and sodium tetrahydroborate (Wako Pure Chemicals, Osaka, Japan) were used to incorporate silver nanoparticles. Sodium chloride, potassium chloride, KH_2PO_4 and Na_2HPO_4 (Wako Pure Chemicals) were used to prepare phosphate buffered saline (PBS). *Escherichia coli* (*E. coli*) (NBRC 3310) and *Pseudomonas putida* (*P. putida*) (NBRC100650) (Biological Resource Center at the National Institute of Technology and Evaluation, Shibuya, Japan) were used as bacteria. Difco nutrient broth (NB) (Becton, Dickinson and Company, Franklin Lakes, NJ, USA) was used as a nutrient in experiments. All chemicals were used without further purification. Milli-Q water (18.2 MΩ cm^{-1}, Millipore, Billerica, MA, USA) was used to prepare solutions and for rinsing.

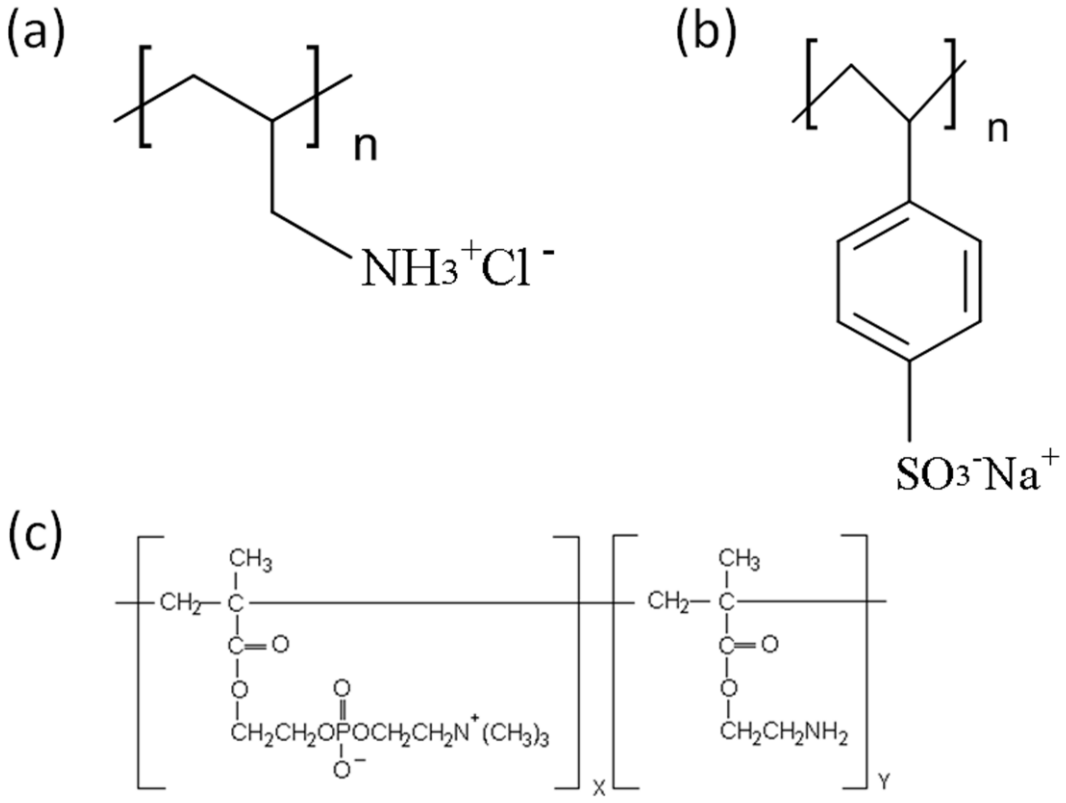

Fig. 2.1. Chemical structure of (a) PAH, (b) PSS and (c) MPC-co-AEMA (X: Y=90:10)

2.2.2. *Membrane Modification*

Polyelectrolyte solutions were prepared by dissolving 0.1 kg/m^3 of PAH or PSS with 1M NaCl as a supporting electrolyte in 10 mM Tris-HCl buffer (pH 7). The base RO membrane was placed in the membrane cell shown in Fig. 2.2 and PAH and PSS polyelectrolyte solutions were alternately passed through the membrane (30 min, flow rate 1×10^{-6} m^3/min, pressure 7.5 MPa) and PEMs were formed on the membrane surface. The membrane was rinsed for 30 min with Milli-Q water (flow rate 9.91×10^{-6} m^3/min) prior to applying each polyelectrolyte solution.

To load silver ions on the membrane surface after PSS deposition and rinsing, the top surface of the membrane was exposed to an $AgNO_3$ solution (0.1 M) for 30 min at room temperature and then lightly rinsed with Milli-Q. The membrane was then immersed in a freshly prepared aqueous solution of $NaBH_4$ (0.15 M) for 30 min and subsequently rinsed with about 900 ml of Milli-Q water for 90 min. When the PEMs-modified membrane was immersed in $AgNO_3$ solution, counterions (Na^+) within the top PSS layer were exchanged with silver ions and these were then reduced to silver particles by exposing them to $NaBH_4$ solution [25, 26].

Polyzwitterion solution was prepared by dissolving 0.1 kg/m^3 of MPC-co-AEMA with 0.5 M NaCl as a supporting electrolyte in 10 mM Tris buffer (pH 9.6) and was then deposited on the membrane surface as a top coat, similar to other polyelectrolyte solutions. Hereafter, abbreviations are used to denote the different samples. For example, to prepare a (PAH/PSS/Ag^0)$_2$PAH/PSS/MPC-co-AEMA membrane, at first two bilayers of (PAH/PSS with embedded Ag^0) were deposited onto the base membrane. Ag^0 denotes silver nanoparticles. After these treatment, the membrane was coated by 3 layers in order of PAH, PSS and MPC-co-AEMA.

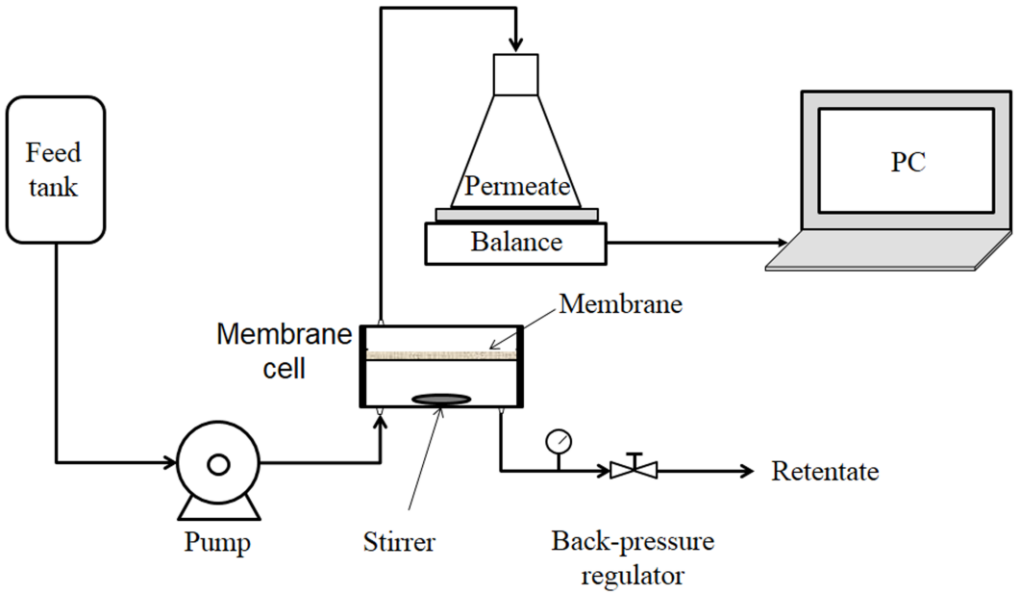

Fig. 2.2. Diagram of the cross-flow setup

2.2.3. Membrane Characterization

2.2.3.1. Morphology Observation

Surface morphologies of the unmodified and modified RO membranes were observed by a field scanning electron microscope (FE-SEM, JSF-7500F, JEOL Co. Ltd., Tokyo, Japan) with an accelerating voltage of 5 kV. The membrane samples were first dried on a freeze dryer (FDU-1200 EYELA, Tokyo Rikakikai Co. Ltd., Tokyo, Japan) overnight and then coated by Pt/Pd sputtering. Cross-sections of the modified membranes were observed to confirm the formation of silver nanoparticles with a transmission electron microscope (TEM, Tecnai G2, FEI Co., Tokyo, Japan) with an accelerating voltage of 120 kV. Samples were embedded in epoxy resin and sliced into 50 nm sections by an ultramicrotome (Reichert Ultracut S, Leica Co., Germany).

2.2.3.2. Surface chemical composition

The chemical composition of the modified membrane surface was analyzed with X-ray photoelectron spectroscopy (XPS) using a JPS-9010MC instrument (JEOL Co.). Measurements were conducted using AlKα as the X-ray source (1486.6 eV) at a power of 300 W (i.e. 10 kV potential and 30 mA emission current). Samples were mounted on an adhesive carbon sheet, stored in the sample chamber for ca. 12 h under vacuum (100 mPa) at ambient temperature for ageing and moisture removal. Calibration of the spectra was performed by taking the C 1s electron peak (Eb 284.6 eV) as an internal reference.

2.2.3.3. Membrane performance

The laboratory scale cross-flow membrane test unit shown in Fig. 2.2 was used to evaluate the performance of the RO membranes. The unit was composed of a membrane cell, pump (NPL-120, Nihon Seimitsu Kagaku Co., Tokyo, Japan) to control the flow rate of solutions and a back-pressure regulator to control applied pressure. An aqueous solution of 0.05 wt% sodium chloride was used as the feed solution. The effective membrane area was 7.5×10^{-4} m^2 with the diameter of 3.1×10^{-2} m. The volume of membrane cell for this setup was 1.6×10^{-5} m^3. The flow rate and applied pressure were 1.0×10^{-6} m^3/min and 0.75 MPa, respectively. The feed side of the membrane was stirred at 400 rpm by a magnetic stirrer. The water flux was obtained from the increase in weight of water permeate. The observed NaCl rejection was calculated from the NaCl concentration of the permeate and retentate flows using Eq. (1). The NaCl concentration

was determined using a conductance meter (CM-30R, DKK-TOA Corporation, Tokyo, Japan).

$$R_{obs} = (1 - \frac{2C^{p}_{NaCl}}{(C^{r}_{NaCl} + C^{f}_{NaCl})}) \times 100 \qquad (1)$$

where, C^{p}_{NaCl}, C^{r}_{NaCl} and C^{f}_{NaCl} indicate the NaCl concentrations in the permeate, retentate and feed, respectively.

2.2.3.4. Contact angle

Water and air contact angle measurements were performed to evaluate the hydrophilicity of the membrane surface by a contact angle meter (Drop Master 300, Kyowa Interface Science Co. Ltd., Niiza, Japan). For the water contact angle, 0.5 µl of water was dropped onto the membrane surface. For the air contact angle, an air bubble was injected onto the surface of the membrane immersed in a water chamber. Each contact angle was measured 10 times and the average value was obtained.

2.2.3.5. Antibacterial properties

2.2.3.5.1. Bactericidal property

The bactericidal properties of the unmodified and modified membranes were evaluated by a shake flask test using *P. putida* and *E. coli* as model gram-negative bacteria. The bacteria were cultured in NB media and placed in an incubator-shaker overnight. The incubation temperatures in all steps for *P. putida* and *E. coli* were 30°C and 37°C, respectively. The bacterial suspension was diluted in PBS to 1-5×10^{7} cfu/ml.

Three pieces of each sample membrane with a total weight of 10 ± 2 mg were immersed in 20 ml of PBS containing 200 µl of 1-5×10^7 cfu/ml of bacterial suspension. At the same time, 20 ml PBS containing 200 µl of bacteria suspension was prepared as a control. Bacteria suspensions with and without membranes were incubated and shaken for 8 hr at 30°C/37°C. After 8 hours, 1 ml of the bacteria suspension was added to 27 ml of NB/Agar solution. After solidification, NB/Agar plates were incubated for 2 days and the numbers of live bacteria counted for each plate. The bacteria killing ratio to the control sample (PBS buffer without membrane) was calculated using Eq. (2).

$$bacteria\ \ killing\ \ ratio\ \ (\%) = \left(\frac{N_B - N_S}{N_B} \right) \times 100 \qquad (2)$$

where N_B indicates the number of bacteria in control PBS buffer [cfu/ml] and N_S is the number of bacteria in PBS buffer containing a membrane [cfu/ml].

In addition to the procedure mentioned above, 3 pieces of $(PAH/PSS/Ag^0)_2$ and $(PAH/PSS/Ag^0)_2$PAH/PSS/MPC-co-AEMA membranes (total weight: 10±2 mg) were immersed in 20 ml of PBS solution (without bacteria) each and shaken in an incubator shaker at 200 rpm for 8 hr. The membranes were then removed and the resultant PBS solution was expected to contain Ag^+ ions released from the Ag nanoparticles embedded in PEMs on the membrane surface. 200 µl of *P. putida* or *E. coli* suspension (1-5×10^7 cfu/ml) was added to this solution and again incubated and shaken for 8 hr at 30°C/37°C and the bacteria killing ratios were calculated by Eq. (2). If this solution displayed a bactericidal property, this would arise from biocide release (release killing).

2.2.3.5.2. Antiadhesion properties

The antiadhesion properties of the modified membranes were evaluated by the static adhesion test. In this test, *P. putida* was used to prepare a bacterial suspension because *P. putida* can form a biofilm more easily than *E. coli.* If the *E. coli* was used in this experiment, the biofilm formation would be slow and unclear in comparison. So, we did this experiment with only *P.putida*. The unmodified and modified membranes were immersed into 40 ml of *P. putida* suspension (10^7 cfu/ml) in Vogel Banner Minimum Medium (VBMM) [4] and incubated at 30°C for 1 week. The membranes were then removed and rinsed 4 times with NaCl solution (0.85 wt%). The residual bacteria on each type of membrane were stained for 15 min by immersion in a staining solution. The staining solution was prepared by dissolving 1.5 µl of a cell-permeable green fluorescence dye (Syto 9) and 1.5 µl of a viable cell-impermeable red dye (propodium iodide (PI)) (Molecular Probes, OR, Life Technologies Corporation, Tokyo, Japan) in 1 ml of 0.85 wt% NaCl solution. The membranes were then rinsed thoroughly with NaCl solution (0.85 wt%) and immersed in 2.5% (v/v) glutaraldehyde solution at 4°C to fix the adhered bacteria. After 1 h, the amount of total bacteria on the membrane surface was observed using confocal laser scanning microscopy (CLSM, FV 1000 D, Olympus Co. Ltd., Tokyo, Japan).

2.3. Results and discussion

2.3.1. Morphology of modified membranes

Figure 2.3 shows a surface view of unmodified and $(PAH/PSS/Ag^0)_2PAH/PSS/$ MPC-co-AEMA membranes. The color of the modified membrane changed from white to brownish. This brownish color change is well known as evidence of embedded Ag nanoparticles [2]. This figure shows in macroscopic scale that the Ag nanoparticles are almost uniform distributed on the membrane surface.

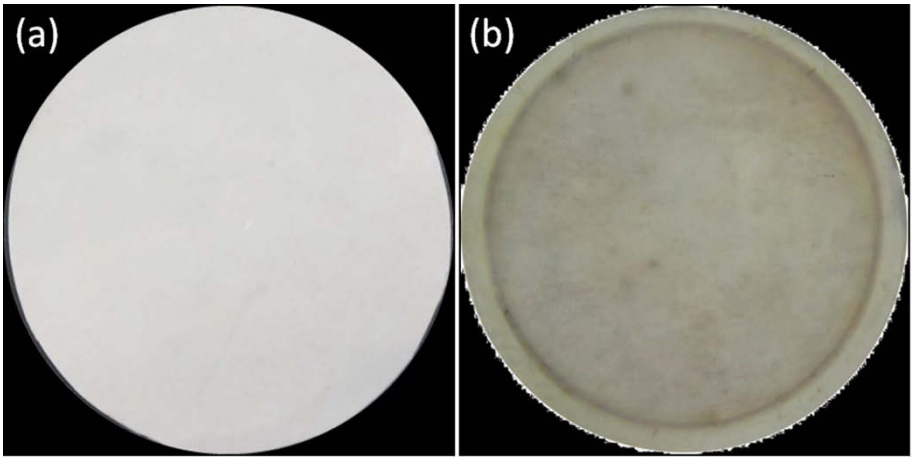

Fig. 2.3. Surface view of **(a)** unmodified membrane and **(b)** modified membrane

Figure 2.4 shows the outer surface of the unmodified membrane and a $(PAH/PSS/Ag^0)_2PAH/PSS/MPC$-co-AEMA membrane. The specific structure of the unmodified RO membrane showed a rough surface morphology. In contrast, it can be concluded that a thin layer was deposited by the polyelectrolyte multilayers deposition, as the rough surface morphology became smoother.

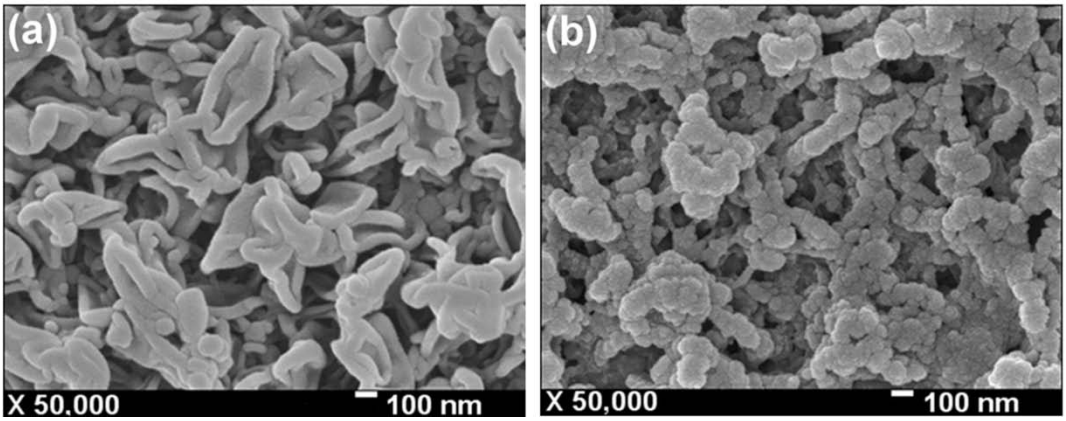

Fig. 2.4. FE-SEM images **(a)** unmodified membrane surface and **(b)** $(PAH/PSS/Ag^0)_2PAH/PSS/MPC\text{-}co\text{-}AEMA$ membrane surface.

Figure 2.5 shows TEM cross-sectional images, at two magnifications, of the same membrane as that shown in Fig. 2.4 (b). These images confirm that polyelectrolyte multilayers were deposited over the entire surface. As shown in Fig. 2.5, silver nanoparticles (black points) were distributed almost uniformly and the size of these particles ranged within the nm scale. This figure thus confirms that silver nanoparticles were embedded into the PEMs.

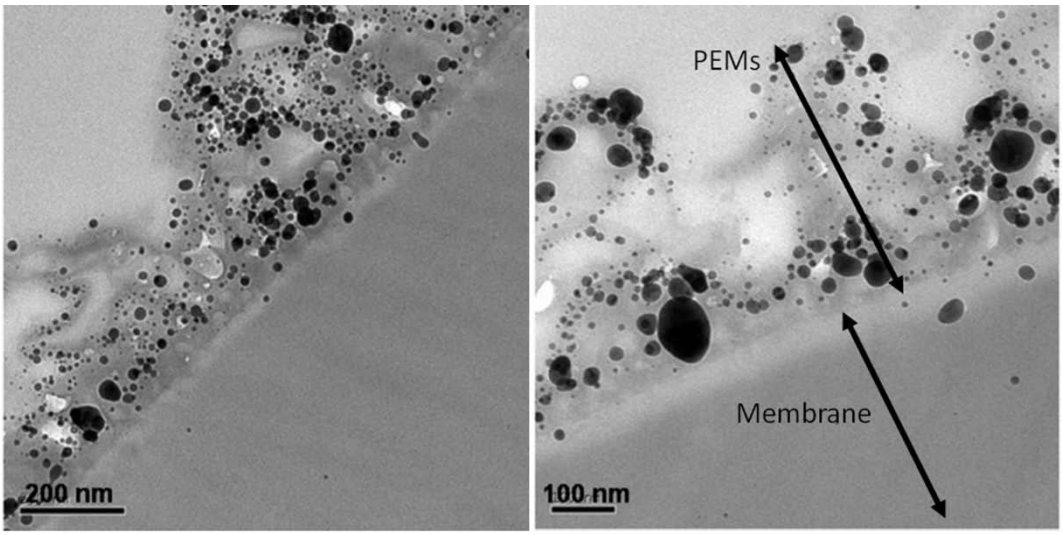

Fig. 2.5. Cross-sectional TEM images of $(PAH/PSS/Ag^0)_2PAH/PSS/MPC$-co-AEMA membrane. Black points in these images represent silver nanoparticles.

2.3.2. Chemical components

The unmodified membrane and the deposited layers on the modified membranes were characterized by XPS analysis. Figure 2.6 shows the XPS spectra of the unmodified and modified membranes.

In Fig. 2.6, a clear sulfur (S) peak was observed at 168 eV in the modified membranes (lines b and c), which could be attributed to the polymeric structure of PSS (Fig. 2.1), while this element was not detected in the unmodified membrane (line a). This sulfur peak therefore confirmed the deposition of a PSS layer on the membrane surface. For membranes modified with MPC-co-AEMA (line c), a phosphorus peak at 134.5 eV was detected. This peak implies the successful deposition of polyzwitterion onto the membrane surface.

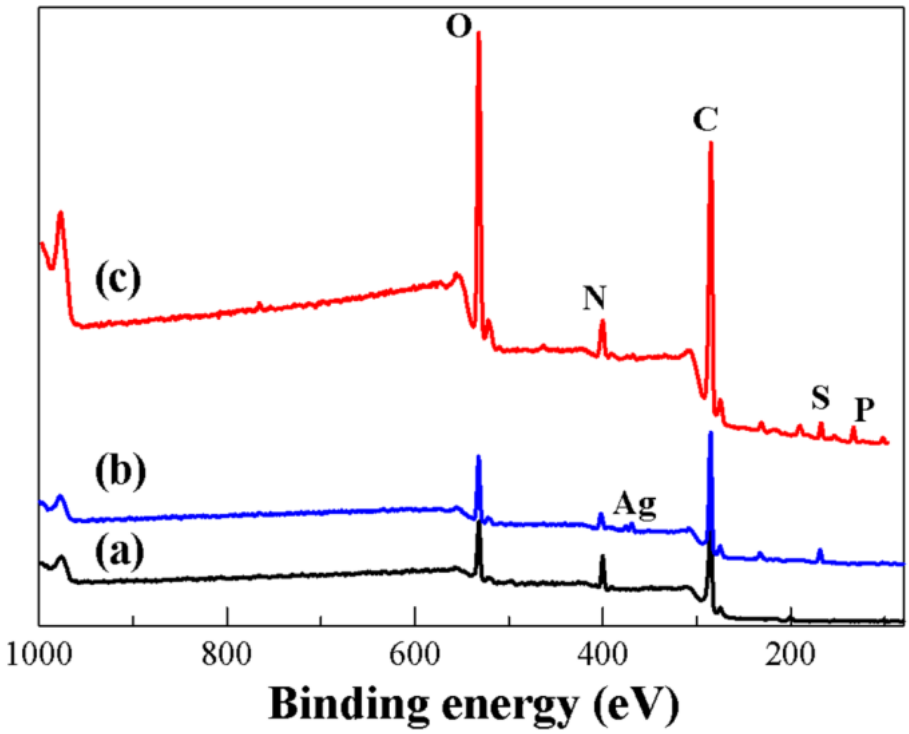

Fig. 2.6. Ag, S, N and P peaks of **(a)** unmodified membrane, **(b)** $(PAH/PSS/Ag^0)_2PAH/PSS$, **(c)** $(PAH/PSS/Ag^0)_2PAH/PSS/MPC\text{-}co\text{-}AEMA$

Figure 2.7 shows high-resolution XPS spectra for Ag 3d and N 1s components. As shown in Fig. 2.7 (A), the modified membranes (lines b and c) exhibited peaks at 374.5 and 368.5 eV, attributed to Ag $3d_{3/2}$ and $3d_{5/2}$ cores, respectively. These peaks indicate that Ag particles were incorporated into the PEMs. In Fig. 2.7(B), a single strong band at 400 eV was assigned to the amide N from the unmodified membrane structure. A band at 402 eV was assigned to quaternary nitrogen [2, 3] and this band became stronger when membrane was modified by PAH and/or MPC-co-AEMA layers. The increase in the 402 eV peak indicates the successful deposition of PAH and polyzwitterion onto the membrane surface.

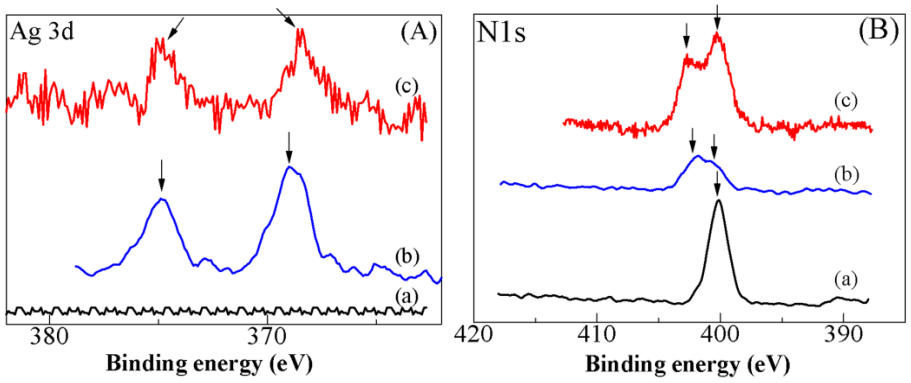

Fig. 2.7. Ag 3d and N1s peaks of **(a)** unmodified membrane, **(b)** $(PAH/PSS/Ag^0)_2PAH/PSS$, **(c)** $(PAH/PSS/Ag^0)_2PAH/PSS/MPC\text{-}co\text{-}AEMA$

The composition ratios for the unmodified and modified membranes are presented in Table 2.1. The C:O and C:N ratios for the unmodified membrane were 4.4 and 6.4, in agreement with the typical composition of aromatic polyamide membranes [3, 27]. The percentage of quaternary nitrogen was increased from 1.5 in the unmodified membrane to 71.3 and 38.4 for $(PAH/PSS/Ag^0)_2PAH/PSS$ and $(PAH/PSS/Ag^0)_2PAH/PSS/MPC\text{-}co\text{-}AEMA$ membranes, respectively. Considering quaternary nitrogen in the PAH and MPC structures, in addition to the increase in the 402 eV peak in Fig. 2.7 (B), it was concluded that the PAH layer and polyzwitterion were successfully deposited by the PEMs method. For the modified membranes coated with MPC-co-AEMA as a top coat, the C:O ratio decreased from 4.4 in unmodified membrane to 2.5 because of the additional oxygen content in the MPC-co-AEMA structure (See Fig. 2.1). Thus, PEMs deposition and silver particle incorporation onto the membrane surface were also confirmed by XPS analysis.

Table 2.1. Chemical composition (in atomic percent) of the unmodified and modified membranes, measured by high-resolution XPS

Membrane	C1s	N1s	O1s	S2p	Ag3d	P2p	C: O	C:N	N, of total N	
									400 eV	402 eV
Unmodified RO (ES20)	72.2	11.3	16.5	0	0	0	4.4	6.4	98.5	1.5
$(PAH/PSS/Ag^0)_2PAH/PSS$	72.6	5.4	16.7	4.6	0.8	0	4.4	13.4	28.7	71.3
$(PAH/PSS/Ag^0)_2PAH/PSS/$ MPC-co-AEMA	64.9	5.4	25.7	1.71	0.15	2.18	2.5	12.1	61.6	38.4

2.3.3. Hydrophilicity

Water contact angles of the unmodified membrane and the $(PAH/PSS/Ag^0)_2PAH/PSS/MPC$-co-AEMA membrane were 40±3° and 31±5°, respectively; and the air contact angles were 145±3° and 151±1°, respectively. This means that hydrophilicity was significantly increased by PEMs modification. It indicates that the free water content in the polyzwitterion layer was increased. It is well known that the antibiofouling and anti-organic fouling properties of membranes can be improved by increasing the free water content of the membrane surface [4, 25, 28, 29].

2.3.4. *Bactericidal properties*

The bacteria killing ratios measured by the shake flask test are summarized in Table 2.2. $(PAH/PSS/Ag^0)_2$ and $(PAH/PSS/Ag^0)_2PAH/PSS/MPC$-co-AEMA membranes showed high bactericidal properties towards both *P. putida* and *E. coli* because of the

Ag nanoparticles embedded within the PEMs. Thus, the killing properties for these modified membranes were confirmed. On the other hand, the unmodified membrane and a membrane without PEMs modification that was simply exposed to $AgNO_3$ and $NaBH_4$ (i.e. unmodified membrane+Ag^0) showed no antibacterial property towards *E. coli*, while the unmodified membrane+Ag^0 showed weak antibacterial property towards *P. putida*. When the membrane surface without PEMs was exposed to $AgNO_3$ and $NaBH_4$, a small amount of silver nanoparticles could be physisorbed onto the membrane surface. This small amount of Ag^0 was sufficient to partially kill *P. putida* but was ineffective against *E.coli* because it is more resistant against silver ions than *P. putida* [30]. Also, PAH/PSS layers alone did not provide antibacterial properties. Thus, it is clear that PEMs are necessary to form Ag nanoparticles on the membrane surface.

Table 2.2. Antibacterial properties measured by the shaking flask test

Sample	*P. putida*			*E.coli*		
	Total Bacteria Killing Ratio	**Release Killing Ratio**	**Contact Killing Ratio***	**Total Bacteria Killing Ratio**	**Release Killing Ratio**	**Contact Killing Ratio***
Unmodified membrane	0	0	0	0	0	0
Unmodified membrane+ Ag^0	62	62	0	0	0	0
$(PAH/PSS)_2$	0	0	0	0	0	0
$(PAH/PSS/Ag^0)_2$PAH/PSS	100	100	0	99.9	90.0	9.9
$(PAH/PSS/Ag^0)_2$ PAH/PSS/ MPC-co-AEMA	100	100	0	99.9	88.7	11.2

* The contact killing ratio was estimated from the difference between total and release killing ratios.

The obtained bacteria release killing ratios of $(PAH/PSS/Ag^0)_2$ and $(PAH/PSS/Ag^0)_2$PAH/PSS/MPC-co-AEMA membranes towards *E. coli* were 90.0 and

88.7%, respectively, and for *P. putida* were 100%. Therefore, it was concluded that the dominant mechanism for bacteria killing properties observed in these modified membranes was biocide release killing.

2.3.5. Antiadhesion resistance

To evaluate the antiadhesion property of the unmodified and modified membranes against bacteria, an immersion test was carried out. The membrane surface was observed by CLSM after one week of immersion in a bacterial suspension. *P. putida* was selected for this test because it can easily form a biofilm. The observations are shown in Fig. 2.8. In these images, the black background is the membrane surface and the green points are stained viable bacteria.

It was found that the number of bacteria adsorbed onto the surface of the $(PAH/PSS/Ag^0)_2$ PAH/PSS membrane was significantly decreased (Fig. 2.8 (b)) compared with the unmodified membrane (Fig. 2.8 (a)). This was probably due to electrostatic repulsion between the bacteria and the membrane surface. The top surface of this modified membrane has a negative charge (ζ-potential = -12 mV) from the terminal layer of PSS [29] and *P. putida* also has a negative charge (ζ-potential = -33 mV) [31]. In addition, the number of bacteria in the bacterial suspension was decreased by Ag ion release, as shown in Table 2.2. The total killing activity of this membrane was 100% in the shake flask test. However, some bacteria remained viable on the membrane surface during the immersion test. During the shake flask test, flasks contained only PBS buffer and no carbon source was available as a nutrient for bacterial

growth. Thus, bacteria were killed by silver ions but could not grow or increase their numbers. On the other hand, VBMM was used as the nutritious media in the immersion test. In this case, bacterial growth and killing by silver ions occurred simultaneously. Some viable bacteria were attached to the $(PAH/PSS/Ag^0)_2PAH/PSS$ membrane, as shown in Fig. 2.8 (b).

Only a few bacteria were adhered to the $(PAH/PSS)_3$MPC-co-AEMA membrane (Fig. 2.8 (c)). This membrane did not have embedded Ag nanoparticles, but it was coated with polyzwitterion. This suppressed bacteria adhesion was attributed to the polyzwitterion top layer on the membrane. A layer of polyzwitterion prevents bacterial adhesion on the modified membrane surface because of its high free water content [4, 21].

The $(PAH/PSS/Ag^0)_2PAH/PSS$/MPC-co-AEMA membrane (Fig. 2.8 (d)) remained the cleanest of the membranes. Almost no bacteria were observed on the surface after one week of immersion in the bacterial suspension. In fact, even if some bacteria could survive in the presence of the released Ag ions, the polyzwitterion layer prevented their adherence to the membrane surface. Thus, the membrane incorporating Ag nanoparticles and covered by polyzwitterion had both bacteria release killing and bacteria antiadhesion properties. This membrane had a high antibiofouling property, which could be attributed to the combined effect of release killing and antiadhesion properties.

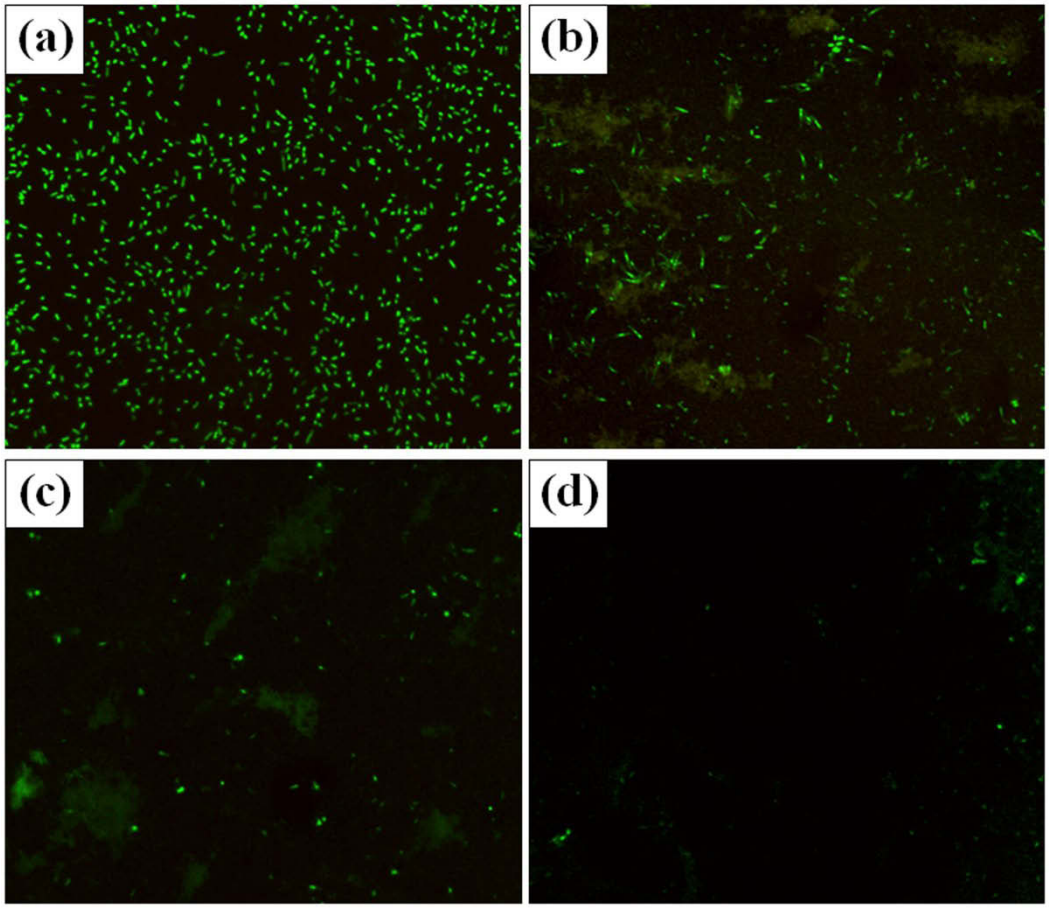

Fig. 2.8. CLSM images of various membrane surfaces, **(a)** unmodified membrane, **(b)** $(PAH/PSS/Ag^0)_2$ PAH/PSS membrane, **(c)** $(PAH/PSS)_3$ MPC-co-AEMA membrane and **(d)** $(PAH/PSS/Ag^0)_2$PAH/PSS/ MPC-co-AEMA membrane. The black background is the membrane surface and green points are stained viable bacteria.

Although the filtration experiment was not carried out in this study, it is expected that the antibiofouling performance of the modified membrane in the real cross flow RO process will be improved because the silver loaded amount into membrane surface would be enough to show antibacterial property and moreover the antiadhesion property of the membrane surface is effective even in the real RO system.

2.3.6. Permeability and rejection of membranes

The membrane performances of the unmodified membrane and modified membranes are given in Table 2.3. These results show the water permeability was decreased by a maximum of about 15% after modification, while the observed rejection was similar to the unmodified membrane. Although the water permeability was decreased, the observed rejection did not decrease and the antibiofouling properties were improved. The flux for unmodified membrane will be decreased by biofouling during RO process. Thus, even if the initial flux for modified membrane is lower than unmodified membrane, the total flux for modified membrane would be higher than unmodified membrane. The water flux will not be decreased by biofouling during RO process because the antibiofouling performance prevents to form biofilm on the membrane surface. Thus, it can be concluded that the surface modification using PEMs and embedded Ag nanoparticles combined with a polyzwitterion top layer is a useful technique for modifying commercial membranes.

Table 2.3. Membrane performance of unmodified and modified membranes

Sample	**Water permeability ($L/m^2.hr.atm$)**	**Observed rejection (NaCl) (%)**
Unmodified Membrane	5.2 ± 0.4	97 ± 1
$(PAH/PSS/Ag^0)_2$	4.8 ± 0.4	98 ± 2
$(PAH/PSS/Ag^0)_2$PAH/PSS/ MPC-co-AEMA	4.4 ± 0.6	97 ± 1

2.4. Conclusion

A commercial RO membrane surface was modified by PEMs deposition with embedded Ag nanoparticles and finally covered by a polyzwitterion. The release killing property was greatly improved by Ag nanoparticles embedded within the PEMs. The polyzwitterion top layer improved the hydrophilicity because of the free water content of this layer and thereby improved the antiadhesion properties towards bacteria. Thus, the antibiofouling performance of the commercial RO membrane was greatly improved by the combined effects of release killing and adhesion resistance. Also, it is expected that the antibiofouling is effective even in real RO process. Although the initial water permeability was decreased by a maximum of about 15% through the surface modification, the observed rejection did not decrease. Furthermore it is expected that the total water flux through modified membranes would be higher than unmodified membrane.

References

[1] D.E.E. L. A. Grab, S. J. Baron, N. A. Smolik, (1990) 309-323., Glutaraldehyde; a new slimicide for paper making, Papermakers Conf., printed by. Atlanta: Tappi Press (1990) 309-323.
[2] I. Sawada, R. Fachrul, T. Ito, Y. Ohmukai, T. Maruyama, H. Matsuyama, Development of a hydrophilic polymer membrane containing silver nanoparticles with both organic antifouling and antibacterial properties, Journal of Membrane Science, 387–388 (2012) 1-6.
[3] R. Bernstein, S. Belfer, V. Freger, Bacterial Attachment to RO Membranes Surface-Modified by Concentration-Polarization-Enhanced Graft Polymerization, Environmental Science & Technology, 45 (2011) 5973-5980.
[4] F. Razi, I. Sawada, Y. Ohmukai, T. Maruyama, H. Matsuyama, The improvement of antibiofouling efficiency of polyethersulfone membrane by functionalization with zwitterionic monomers, Journal of Membrane Science, 401–402 (2012) 292-299.

[5] A. Al-Amoudi, R.W. Lovitt, Fouling strategies and the cleaning system of NF membranes and factors affecting cleaning efficiency, Journal of Membrane Science, 303 (2007) 4-28.
[6] G.-d. Kang, Y.-m. Cao, Development of antifouling reverse osmosis membranes for water treatment: A review, Water Research, 46 (2012) 584-600.
[7] A. Sweity, W. Ying, M.S. Ali-Shtayeh, F. Yang, A. Bick, G. Oron, M. Herzberg, Relation between EPS adherence, viscoelastic properties, and MBR operation: Biofouling study with QCM-D, Water Research, 45 (2011) 6430-6440.
[8] H.-L. Yang, J.C.-T. Lin, C. Huang, Application of nanosilver surface modification to RO membrane and spacer for mitigating biofouling in seawater desalination, Water Research, 43 (2009) 3777-3786.
[9] R. Schneider, L. Ferreira, P. Binder, E. Bejarano, K. Goes, E. Slongo, C. Machado, G. Rosa, Dynamics of organic carbon and of bacterial populations in a conventional pretreatment train of a reverse osmosis unit experiencing severe biofouling, Journal of Membrane Science, 266 (2005) 18-29.
[10] N. Hilal, V. Kochkodan, L. Al-Khatib, T. Levadna, Surface modified polymeric membranes to reduce (bio)fouling: a microbiological study using E. coli, Desalination, 167 (2004) 293-300.
[11] N. Park, B. Kwon, I.S. Kim, J. Cho, Biofouling potential of various NF membranes with respect to bacteria and their soluble microbial products (SMP): Characterizations, flux decline, and transport parameters, Journal of Membrane Science, 258 (2005) 43-54.
[12] J.A. Lichter, K.J. Van Vliet, M.F. Rubner, Design of Antibacterial Surfaces and Interfaces: Polyelectrolyte Multilayers as a Multifunctional Platform, Macromolecules, 42 (2009) 8573-8586.
[13] X. Cao, M. Tang, F. Liu, Y. Nie, C. Zhao, Immobilization of silver nanoparticles onto sulfonated polyethersulfone membranes as antibacterial materials, Colloids and Surfaces B: Biointerfaces, 81 (2010) 555-562.
[14] R. Bai, X. Zhu, K.-H. Wee, C. Liu, S.-L. Tang, Membrane surfaces immobilized with ionic or reduced silver and their anti-biofouling performances, Journal of Membrane Science, 363 (2010) 278-286.
[15] X. Zan, Z. Su, Polyelectrolyte multilayer films containing silver as antibacterial coatings, Thin Solid Films, 518 (2010) 5478-5482.
[16] Z. Li, D. Lee, X. Sheng, R.E. Cohen, M.F. Rubner, Two-Level Antibacterial Coating with Both Release-Killing and Contact-Killing Capabilities, Langmuir, 22 (2006) 9820-9823.
[17] F. Razi, I. Sawada, Y. Ohmukai, T. Maruyama, H. Matsuyama, Surface functionalization by grafting of (2-dimethylamino)ethyl methacrylate methyl chloride quaternary salt (DMAEMAq) onto hollow fiber polyethersulfone (PES) membranes for improvement of antibiofouling properties, Solvent Extr. Res. Dev, 19 (2012) 101-115.
[18] H. Karkhanechi, R. Takagi, Y. Ohmukai, H. Matsuyama, Enhancing the antibiofouling performance of RO membranes using Cu(OH)2 as an antibacterial agent, Desalination, 325 (2013) 40-47.
[19] M. Herzberg, A. Sweity, M. Brami, Y. Kaufman, V. Freger, G. Oron, S. Belfer, R. Kasher, Surface Properties and Reduced Biofouling of Graft-Copolymers That Possess Oppositely Charged Groups, Biomacromolecules, 12 (2011) 1169-1177.

[20] C.X. Liu, D.R. Zhang, Y. He, X.S. Zhao, R. Bai, Modification of membrane surface for anti-biofouling performance: Effect of anti-adhesion and anti-bacteria approaches, Journal of Membrane Science, 346 (2010) 121-130.
[21] K. Ishihara, Bioinspired phospholipid polymer biomaterials for making high performance artificial organs, Science and Technology of Advanced Materials, 1 (2000) 131-138.
[22] J. Yuan, L. Chen, X. Jiang, J. Shen, S. Lin, Chemical graft polymerization of sulfobetaine monomer on polyurethane surface for reduction in platelet adhesion, Colloids and Surfaces B: Biointerfaces, 39 (2004) 87-94.
[23] S. Jiang, S. Chen, Z. Zhang, Y. Chang, Super-low fouling sulfobetaine and carboxybetaine materials and related methods, US 7879444 B2, (Feb.1.2011).
[24] X. Zan, M. Kozlov, T.J. McCarthy, Z. Su, Covalently Attached, Silver-Doped Poly(vinyl alcohol) Hydrogel Films on Poly(l-lactic acid), Biomacromolecules, 11 (2010) 1082-1088.
[25] M. Vaselbehagh, H. Karkhanechi, S. Mulyati, R. Takagi, H. Matsuyama, Improved antifouling of anion-exchange membrane by polydopamine coating in electrodialysis process, Desalination, (2013).
[26] X. Zan, Z. Su, Incorporation of Nanoparticles into Polyelectrolyte Multilayers via Counterion Exchange and in situ Reduction, Langmuir, 25 (2009) 12355-12360.
[27] C.Y. Tang, Y.-N. Kwon, J.O. Leckie, Probing the nano- and micro-scales of reverse osmosis membranes—A comprehensive characterization of physiochemical properties of uncoated and coated membranes by XPS, TEM, ATR-FTIR, and streaming potential measurements, Journal of Membrane Science, 287 (2007) 146-156.
[28] J.-H. Li, M.-Z. Li, J. Miao, J.-B. Wang, X.-S. Shao, Q.-Q. Zhang, Improved surface property of PVDF membrane with amphiphilic zwitterionic copolymer as membrane additive, Applied Surface Science, 258 (2012) 6398-6405.
[29] T. Ishigami, K. Amano, A. Fujii, Y. Ohmukai, E. Kamio, T. Maruyama, H. Matsuyama, Fouling reduction of reverse osmosis membrane by surface modification via layer-by-layer assembly, Separation and Purification Technology, 99 (2012) 1-7.
[30] V.M. Magueijo, L.G. Anderson, A.J. Fletcher, S.J. Shilton, Polysulfone mixed matrix gas separation hollow fibre membranes filled with polymer and carbon xerogels, Chemical Engineering Science, 92 (2013) 13-20.
[31] A. Subramani, E.M.V. Hoek, Direct observation of initial microbial deposition onto reverse osmosis and nanofiltration membranes, Journal of Membrane Science, 319 (2008) 111-125.

Chapter 3

Enhancing the antibiofouling performance of RO membranes using $Cu(OH)_2$ as an antibacterial agent

3.1. Introduction

In the second chapter, I showed that the two main strategies (totally three approaches) that could enhance the antibiofouling properties of membrane surfaces are based on the improved antibacterial and antiadhesion properties. The antibacterial properties of membranes are commonly improved by the antibacterial agents including organic and inorganic compounds [1-6]; however, organic antibacterial agents are limited in their applications because of low heat resistance and short life time. On the other hand, inorganic antibacterial agents have attracted considerable attention [5, 6], because the materials show superior durability, low toxicity, good heat resistance and show high activity at low concentrations [7].

Silver is a well-known inorganic antimicrobial agent with a particularly high antibacterial activity [4, 8, 9]. Sawada et al. improved the antibiofouling properties of a polyethersulfone membrane by forming an acrylamide surface layer embedded with silver nanoparticles [1]. I also improved the antibacterial properties of a commercial RO membrane by embedding silver nanoparticles into polyelectrolyte multilayers as described in the second chapter [2].

Other inorganic materials used for these purposes include metal hydroxide such as $Ca(OH)_2$, $Mg(OH)_2$ and $Cu(OH)_2$. However, only a few researches have been reported using these materials [5]. $Ca(OH)_2$ is a common oral antibacterial agent because of its strong alkaline properties and has been widely used in endodontics for intracanal dressings [10, 11]. Dong et al. have recently investigated the antibacterial activity of $Mg(OH)_2$ by adding $Mg(OH)_2$ nanoparticles to wood pulp to make paper sheets with antibacterial property showing that $Mg(OH)_2$ has high antibacterial activity against *Escherichia coli (E. coli)* bacteria both in a liquid culture and on a dry paper surface [5]. They showed that direct contact of bacteria with $Mg(OH)_2$ nanoparticles was the critical factor for bacteria lysis [11]. This means that contact killing is the dominant mechanism contributing to the antibacterial properties of $Mg(OH)_2$. $Cu(OH)_2$ is also well-known as a fungicide and many thousands of tons are used annually all over the world in agriculture. For this reason, a large amount of the research on $Cu(OH)_2$ has focused on agriculture applications. $Cu(OH)_2$ can also be used as a source of copper ion that may provide antibacterial properties [12, 13].

The solubility product, K_{sp}, is the equilibrium constant for highly insoluble solid substances is given by the product of molar concentration of anions and cations dissolving in saturated aqueous solution. Thus, it is possible to calculate the pH of a saturated aqueous solution of $Ca(OH)_2$, $Mg(OH)_2$ and $Cu(OH)_2$ with knowledge of their solubility products, which are 7.9×10^{-6}, 5.6×10^{-12} and 2.2×10^{-20} in water at 25 °C, respectively [14]. The pH value calculated for $Cu(OH)_2$ is 7.6 and much lower than 12.5 for $Ca(OH)_2$ and 10.4 for $Mg(OH)_2$. It is known that *E. coli* cannot survive at pH higher than 10 and that antibacterial activity increases with pH [11, 15]. This suggests that the

antibacterial activity of $Ca(OH)_2$ and $Mg(OH)_2$ suspensions may derive mainly from their alkaline properties. Antibacterial activity may not be expected from $Ca(OH)_2$ and $Mg(OH)_2$ particle used in drinking water processes (ref. Fig 3.3), as the pH range of drinking water is limited to 6.5–8.5 [16]. However, $Cu(OH)_2$ shows antibacterial properties at pH 7.6. The activity of $Cu(OH)_2$ is not linked to strong alkaline conditions but may be attributed to release of Cu^{2+} ions into aqueous solution. *E. coli* is sensitive to Cu^{2+} ion and has a low survival rate when exposed to copper surfaces or ions [12, 13, 17, 18]. It is expected that $Cu(OH)_2$ particles adsorbed onto a membrane surface may show high antibacterial activity by release of Cu^{2+} ions into the feed solutions used in drinking water processes. In addition, $Cu(OH)_2$ particles adsorbed on a membrane surface would be expected to have higher stability compared with $Ca(OH)_2$ and $Mg(OH)_2$ because of the lower solubility product of $Cu(OH)_2$ as shown above.

The secondary Maximum Contaminant Level (SMCL) set by the US Environmental Protection Agency for silver in drinking water is 0.1 $mg \cdot l^{-1}$, while this level for copper is 1 $mg \cdot l^{-1}$ [16]. This indicates that copper could be used as a disinfectant in drinking water processes with a lower level of risk for human health than silver. $Cu(OH)_2$ is also considerably cheaper than silver, and thus, a better for commercial applications from both environmental and economic standpoints.

Despite the potential of $Cu(OH)_2$ as an antibacterial agent, to the best of my knowledge, there are few reports on the use of $Cu(OH)_2$ to improve antibiofouling properties. In this chapter, I present the result of my attempt to improve the antibiofouling properties of commercial RO membranes with $Cu(OH)_2$ as an inorganic antibacterial agent.

3.2. Experimental

3.2.1. Materials

ES-20 (Nitto Denko, Osaka, Japan) was used as a RO membrane. $Cu(OH)_2$, $Mg(OH)_2$, NaCl, KCl, glutaraldehyde, KH_2PO_4 and Na_2HPO_4 were purchased from Wako Pure Chem. Ind. (Osaka, Japan). $Ca(OH)_2$ was purchased from Nacalai Tesque Inc. (Kyoto, Japan). Silver nanoparticles were purchased from Sigma-Aldrich Company (St. Louis, MO, USA). Difco nutrient broth (NB) (Becton, Dickinson and Company, Franklin Lakes, USA) was used as nutrient agent in experiments. *Escherichia coli* (*E.coli*) (NBRC 3310) and *Pseudomonas putida* (*P.putida*) (NBRC100650) (Biological Resource Center at the National Institute of Technology and Evaluation, Shibuya, Japan) were used as bacteria. Molecular Probes including Syto 9 and Syto propidium iodide (PI) were purchased from Life Technologies Corporation (Tokyo, Japan). All chemicals were used without further purification. Milli-Q water (18.2 MΩ·cm) (Millipore, Billerica, MA, USA) was used to prepare all solutions and for rinsing.

3.2.2. Membrane modification

The $Cu(OH)_2$ suspension was prepared by adding the required amount of $Cu(OH)_2$ powder (mean particle size 195 nm) into water stirring for 10 min, followed by ultrasonication for 10 min. A piece of membrane was then fixed to a glass plate shown in Figure 3.1 and dipped into a $Cu(OH)_2$ suspension at a fixed temperature for a certain period of time. In this way, only the skin layer side of the RO membrane was exposed to the suspension and modified by $Cu(OH)_2$ particles. The effective circular membrane

area was 7.5×10^{-4} m^2 with a diameter of 3.1×10^{-2} m. After dipping for the desired time, the membrane was removed from the suspension and rinsed three times with fresh water to remove excess $Cu(OH)_2$.

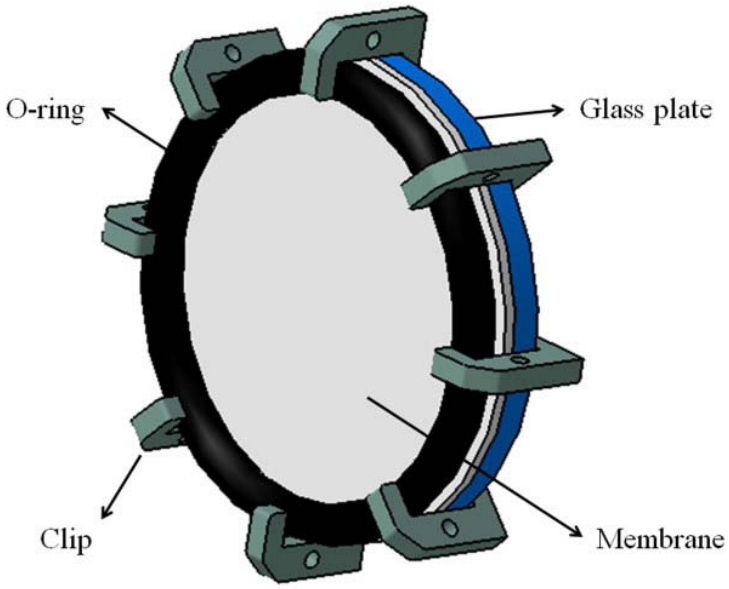

Fig. 3.1. Schematic of fixture for membrane modification technique

3.2.3. Characterization

3.2.3.1. Size distribution and ζ-potential of particles

The size distribution of particles in the $Cu(OH)_2$ suspension was measured with particle size analyzer (ELSZ-0H, Otsuka Electronics, Osaka, Japan) and the ζ-potential of these particles was also measured by the same apparatus using 0.01 M NaCl solution (pH 5.6) at room temperature. Different types of sample cells were used to measure size distribution and ζ-potential measurements.

3.2.3.2. Adsorption amount

A 4×10^{-4} m^2 portion of the membrane modified with $Cu(OH)_2$ particles was immersed in 20 ml of 1.00 M HNO_3 solution and shaken for one week to dissolve all adsorbed $Cu(OH)_2$ particles. Copper concentration of the HNO_3 solution was analyzed with a polarized atomic absorption spectrophotometer (ASS), (Z 2310, Hitachi High-Technologies Corporation, Tokyo, Japan) and then, the amount of adsorbed $Cu(OH)_2$ on the membrane surface was obtained.

3.2.3.3. Morphology and chemical composition of Surface

The membranes were first dried in a freeze dryer (FDU-1200 EYELA; Tokyo Rikakikai Co. Ltd., Tokyo, Japan) overnight and then coated with osmium tetroxide (OsO_4). A thin OsO_4 layer (ca. 5 nm) was formed using an osmium coater (Neoc-STB; MEIWAFOSIS Co. Ltd., Tokyo, Japan). The surface morphology of the modified membrane was then observed using a field emission scanning electron microscope (FE-SEM) (JSF-7500F; JEOL Co. Ltd., Tokyo, Japan) with an accelerating voltage of 5 kV. The chemical composition of membrane surface was also analyzed by the energy dispersive spectroscopy (EDS) with FE-SEM. The accelerating voltage used for EDS analysis was 20 kV.

3.2.3.4. Contact angle and ζ-potential of membrane surface

Water contact angles were measured to evaluate the hydrophilicity of the membrane using a contact angle meter (Drop Master 300, Kyowa Interface Science Co.

Ltd., Niiza, Japan). For water contact angle measurements, 0.5 µl of water was dropped onto the membrane surface. The contact angle was measured 10 times for each sample and the mean was calculated.

The ζ-potential of the membrane surface was obtained from the streaming potential measurement by an ELS-4000K instrument (Otsuka Electronics) using a 0.01 M NaCl solution (pH 5.6) at room temperature.

3.2.3.5. Water permeability and salt rejection

A laboratory scale cross-flow membrane test unit was used to measure water permeability and rejection of the unmodified and modified membranes. The unit was equipped with a membrane cell and a pump (NPL-120, Nihon Seimitsu Kagaku Co., Tokyo, Japan) to control the flow rate of solutions. A back-pressure regulator was used to control the applied pressure. An aqueous solution of 0.05 wt% NaCl was fed at flow rate 1.0×10^{-6} $m^3\cdot min^{-1}$ and applied pressure of 0.75 MPa. The effective membrane area was 7.5×10^{-4} m^2 with a diameter of 3.1×10^{-2} m. The volume of membrane cell for this setup was 1.6×10^{-5} m^3. The feed side of the membrane was stirred at 400 rpm by a magnetic stirrer. The NaCl concentrations of the permeate and retentate flows were used to calculate the NaCl rejection, R_{obs} using Eq. (1). The NaCl concentration was determined using a conductance meter (CM-30R, DKK-TOA Corporation, Tokyo, Japan). The water flux ($l.m^{-2}.h^{-1}.atm^{-1}$) was obtained from the time course of volume of permeated water.

$$R_{obs} = (1 - \frac{2C^{p}_{NaCl}}{(C^{r}_{NaCl} + C^{f}_{NaCl})}) \times 100 \qquad (1)$$

where, C^{p}_{NaCl} , C^{r}_{NaCl} and C^{f}_{NaCl} indicate the NaCl concentrations in the permeate, retentate, and feed, respectively. Generally, R_{obs} is calculated using not $(C^{r}_{NaCl} + C^{f}_{NaCl})/2$, but C^{f}_{NaCl}. However, C^{r}_{NaCl} is higher than C^{f}_{NaCl}. It means that there is a concentration gradient between inlet and outlet of cell. Then, we evaluated R_{obs} using $(C^{r}_{NaCl} + C^{f}_{NaCl})/2$ as an average concentration in the flow cell.

3.2.3.6. Bactericidal property

The bactericidal properties of the unmodified and modified membranes were evaluated by a shake flask test using *E.coli* as a model gram-negative bacteria. The bacteria were cultured in NB media and then placed in an incubator-shaker overnight. The incubation temperature for all steps was 37°C. The bacterial suspension (*E. coli* suspension) was diluted in phosphate buffered saline (PBS) to 1–5 × 10^5 cfu·ml^{-1}. Three pieces of each membrane (unmodified and modified membranes), with a total weight of 10 ± 2 mg, equivalent to an area of 1.1 ± 0.2 cm^2, were immersed in 20 ml of the diluted bacterial suspension. Simultaneously, 20 ml of the diluted bacterial suspension without membrane was used as a control. Diluted bacterial suspensions with and without membranes were incubated and shaken for 8 h at 37°C. After 8 hours, 1 ml of the diluted bacterial suspension was taken from each of samples including a control and added to 27 ml of NB/Agar solution. After solidification, NB/Agar plates were incubated for 2 days. Then, the number of live bacteria of each plate was counted. The bacteria killing ratio (sterilization ratio) was calculated by Eq. (2) [2].

$$bacteria\ killing\ ratio\ (\%) = \left(\frac{N_B - N_S}{N_B} \right) \times 100 \qquad (2)$$

where N_B indicates the number of live bacteria on the control plate and N_S that of the sample plate. N_B reflects the number of live bacteria in the diluted control bacteria suspension and N_S that of the diluted bacteria suspension containing a membrane. Thus, the bacteria killing ratio reflects the bactericidal properties of the membrane.

3.2.3.7. Antiadhesion property

The antiadhesion property of the modified membranes was evaluated using a static adhesion test. In this test, *P. putida* was used as a model gram-negative bacterium, since *P. putida* can form a biofilm more easily than *E. coli.* When *E. coli* was used in this experiment, biofilm formation was slow and did not allow clear comparisons. Thus, the antiadhesion experiments were performed only with *P. putida*. The unmodified and modified membranes were immersed in 40 ml of *P. putida* suspension (1–5 × 10^7 cfu·ml^{-1}) in Vogel Banner Minimum Medium (VBMM) at pH=8 [19], and incubated at 30°C for 4 days. The membrane surface area was about 5 cm^2. The membranes were then taken out of the suspension and rinsed 4 times with NaCl solution (0.85 w/w %). The residual bacteria on each membrane were stained for 15 min by immersion in a staining solution prepared by mixing 1.5 µl of a cell-permeable green fluorescence dye (Syto 9) and 1.5 µl of a viable cell-impermeable red dye (SytoPI) with 1 ml of 0.85 w/w % NaCl solution. The membranes were then rinsed thoroughly with NaCl solution (0.85 w/w %) and immersed in 2.5 v/v % glutaraldehyde solution at 4°C to fix the

adhered bacteria. After 1 h, the amount of total bacteria on the membrane surface was observed using confocal laser scanning microscopy (CLSM, FV 1000 D, Olympus Co. Ltd., Tokyo, Japan).

3.3. Results and discussion

3.3.1. Effect of pH and antibacterial property of metal hydroxides

Prior to studying the antibacterial property of metal hydroxides, the effect of pH on the antibacterial activity was studied by a shake flask test as described in section 3.2.3.6. The pH of the bacterial suspensions was adjusted to 7–12 by addition of 1.0 M NaOH or 1.0 M HCl solutions. The results of the tests are shown in Fig. 3.2, demonstrating that antibacterial activity increased with pH and that *E. coli* could not survive when the suspension pH was higher than 10. These results are consistent with the results of Grab et al. [20], where glutaraldehyde was used as biocide against *E. coli* over a range of pH and the killing rate at pH 8.5 was approximately twenty times higher than the killing rate at pH 5.

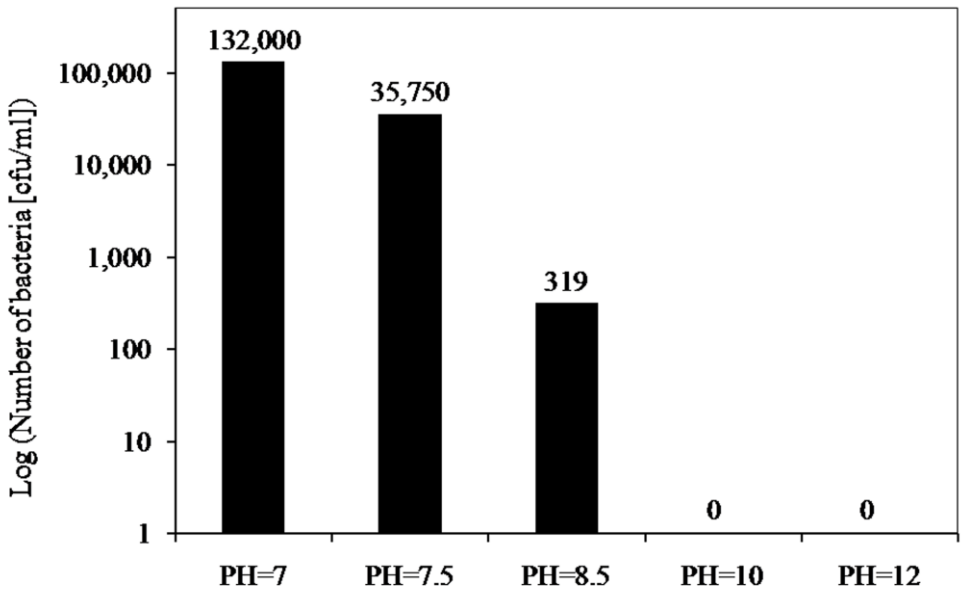

Fig. 3.2. Effect of pH of PBS buffer solution on *E. coli* survival.

The antibacterial properties of the metal hydroxides and silver particles were investigated in a preliminary experiment using a shake flask test to evaluate the bactericidal properties of these materials. In this experiment, the pH of all solutions was adjusted to 7. The concentration of $Ca(OH)_2$, $Mg(OH)_2$, $Cu(OH)_2$ and silver suspensions was 100 $mg \cdot l^{-1}$. The mean particle size of $Ca(OH)_2$, $Mg(OH)_2$, $Cu(OH)_2$ and silver were 15, 0.07, 0.20 and less than 0.1 μm, respectively. Figure 3.3 shows that $Ca(OH)_2$ and $Mg(OH)_2$ had poor antibacterial activity under neutral conditions. This phenomenon is consistent with reports or reduced activity at low pH [8, 13]. $Cu(OH)_2$ and silver maintained excellent antibacterial activity even though the activity of $Cu(OH)_2$ was only slightly lower than silver. $Cu(OH)_2$ is therefore considered a more suitable candidate for RO membrane modification than $Mg(OH)_2$ and $Ca(OH)_2$ because it features good antibacterial activity over the pH range of drinking water (pH 6.5–8.5).

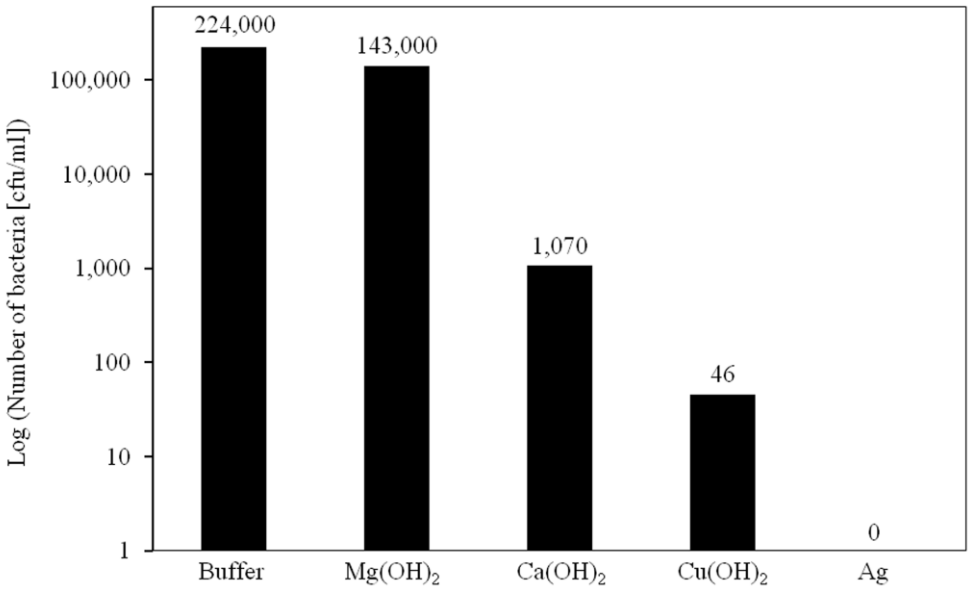

Fig. 3.3. Effect of $Mg(OH)_2$, $Ca(OH)_2$, $Cu(OH)_2$ and silver particles (all at 100 $mg \cdot l^{-1}$) in PBS buffer solution at pH 7 on *E. coli* survival.

3.3.2. $Cu(OH)_2$ particles characterization

A $Cu(OH)_2$ suspension of 500 $mg \cdot l^{-1}$ was prepared according to the method described in section 3.2.2. The particle size distribution is shown in Fig. 3.4. Narrow particle size distributions with mean size of 195 nm were found. The ζ-potential of particles was -63 ± 1 mV. The error values represent the standard deviation from at least 3 separate experiments. From the negative ζ-potential of particles, it may be expected that the negative surface charge density of the modified membrane would be increased by adsorption of $Cu(OH)_2$ particles.

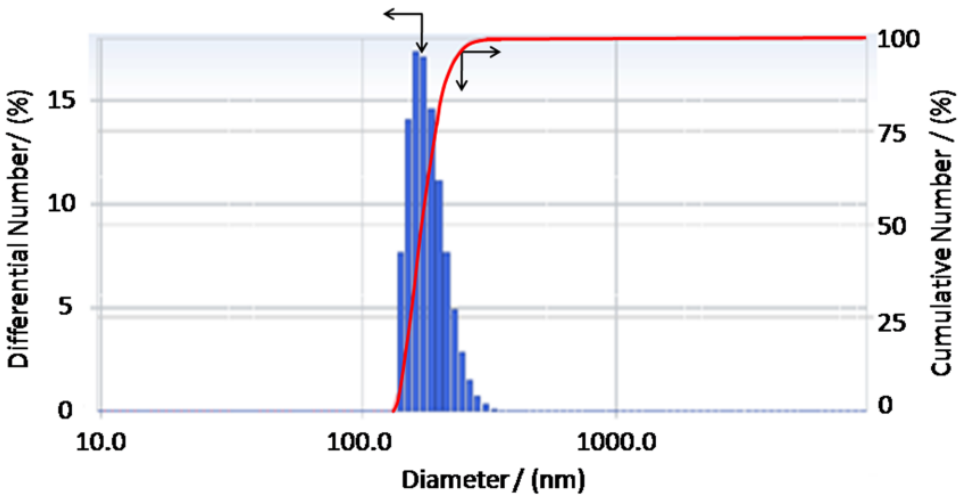

Fig. 3.4. Particle size distribution of 500 $mg \cdot l^{-1}$ $Cu(OH)_2$ suspension. The bar graph shows the differential and the red line the cumulative particle count.

3.3.3. Adsorption property

The optimum deposition time for $Cu(OH)_2$ particles on the membrane surface was examined in initial studies. In this experiment, the membrane was immersed in $Cu(OH)_2$ suspension of 500 $mg \cdot l^{-1}$ for different periods at 25°C. The amount of adsorbed $Cu(OH)_2$ was measured as described in Section 3.2.3.2 and plotted as a function of time. Figure 3.5 shows that the adsorption saturated after 60 min which was used in all following experiments.

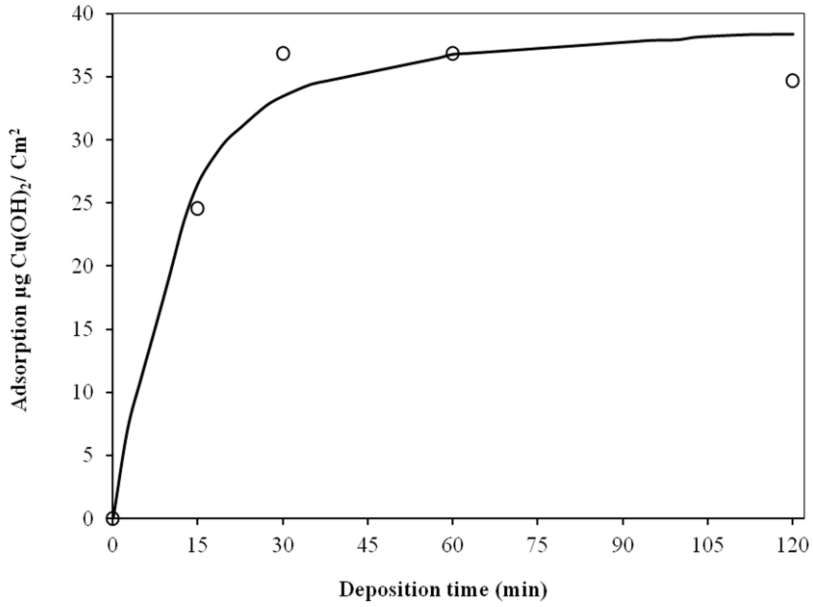

Fig. 3.5. Adsorption of $Cu(OH)_2$ particles as a function of deposition time. The membrane was immersed in a 500 $mg \cdot l^{-1}$ $Cu(OH)_2$ suspension at 25°C.

The adsorption isotherms of $Cu(OH)_2$ were measured at different temperatures to determine the adsorption energy. The adsorption amount of $Cu(OH)_2$ increased with the increase of $Cu(OH)_2$ concentration and saturated at high concentration. This is the Langmuir type isotherm. Thus, these data were analyzed by the Langmuir adsorption isotherm given by Eq. (3).

$$C_{adsorbed} = \frac{\alpha C_{saturated} C_{bulk}}{1 + \alpha C_{bulk}} \qquad (3)$$

where $C_{adsorbed}$ ($\mu g \cdot cm^{-2}$) indicates the adsorbed amount of $Cu(OH)_2$, $C_{saturated}$ ($\mu g \cdot cm^{-2}$) the saturated adsorbed amount, C_{bulk} ($mg \cdot l^{-1}$) the bulk concentration and α the adsorption coefficient. The relation between α and adsorption energy, ΔΦ ($J \cdot mol^{-1}$) is given by Arrhenius relationship, Eq. (4) [21]:

$$\alpha \propto \exp(\Delta\Phi/RT) \qquad (4)$$

where R denotes the gas constant ($J \cdot K^{-1} \cdot mol^{-1}$) and T the absolute temperature (K).

The adsorption coefficient, α, at each different temperature was obtained from a best fit of Eq. (3). Figure 3.6 shows *ln α* as a function of 1/T. The adsorption energy, ΔΦ was determined to be 6.5 $kJ \cdot mol^{-1}$ suggesting that $Cu(OH)_2$ was physically adsorbed to the membrane surface as the adsorption energy was less than 42 $kJ \cdot mol^{-1}$ [21].

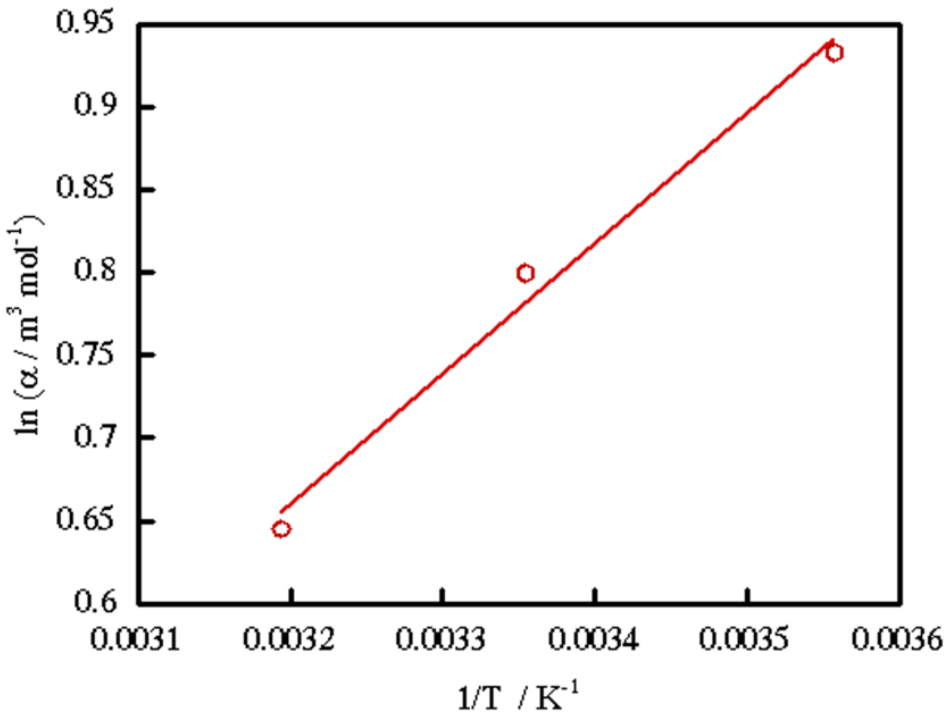

Fig. 3.6. Adsorption coefficient of $Cu(OH)_2$ particles on the membrane surface as a function of inverse of temperature.

3.3.4. Membrane surface characterization and membrane performance

Figure 3.7 (a) shows an SEM image of the treated surface of the RO membrane modified by $Cu(OH)_2$ particles (500 $mg \cdot l^{-1}$). It is clear from Fig. 3.7 (a) that particles were deposited onto the membrane surface, however, the particles size appears larger than the mean particle size of $Cu(OH)_2$ suspension (195 nm), which may be because of aggregation of particles. Figure 3.7 (b) shows the EDS spectra of Cu from a line scan of the membrane surface. The spectrum showed clear Cu peaks at site of particle, strongly suggesting that the adsorbed particles on the membrane surface were $Cu(OH)_2$ particles, as this was the only Cu source.

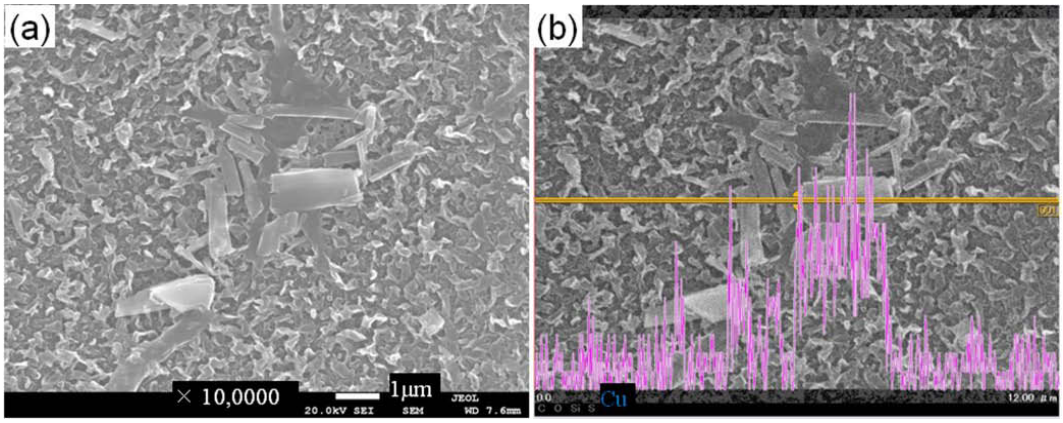

Fig. 3.7. (a) FE-SEM image and (b) EDS spectrum of membrane modified with 500 $mg \cdot l^{-1}$ $Cu(OH)_2$ suspension. Straight line in Fig. 3.7(b) shows scanning position.

It was expected that the adsorption of $Cu(OH)_2$ would increase the hydrophilicity and the negative charge density of the membrane surface. The increase of hydrophilicity increases the free water content at the membrane surface and then may enhance the antiadhesion properties by decreasing the hydrophobic interactions between bacteria

and the membrane surface [19, 22-24]. The increase of negative surface charge density may also increase the antiadhesion properties by increasing electrostatic repulsion between negatively charged bacteria and the membrane. The hydrophilicity was evaluated by the water contact angle and the negative surface charge density by the ζ-potential as described in section 3.2.3.4. The water contact angle and ζ-potential of the unmodified and $Cu(OH)_2$ modified membranes (treated with $Cu(OH)_2$ suspensions of 100 and 500 $mg \cdot l^{-1}$) surfaces are listed in Table 3.1. The water contact angle was decreased by modification with $Cu(OH)_2$ particles suggesting an increase in hydrophilicity attributed to the presence of –OH groups from $Cu(OH)_2$ particles adsorbed to the membrane surface. The contact angle of the membranes treated with 100 and 500 $mg \cdot l^{-1}$ $Cu(OH)_2$ suspensions were similar. However, the ζ-potential of the membrane modified by the 500 $mg \cdot l^{-1}$ suspension was more negative than that of unmodified membrane, likely because of the presence of negatively charged $Cu(OH)_2$ particles as described in section 3.3.2.

Table 3.1. Water contact angle and ζ-potential of unmodified and modified membranes

Sample	**Water contact angle (°)**	**ζ– potential (mV)**
Unmodified RO	40 ± 3	-10.5 ± 0.8
RO/$Cu(OH)_2$-100 $mg \cdot l^{-1}$	30 ± 2	-11 ± 2
RO/$Cu(OH)_2$-500 $mg \cdot l^{-1}$	28 ± 1	-21 ± 2

The effect of surface modification on water permeability and salt rejection was evaluated by the way shown in section 3.2.3.5. Table 3.2 shows the results. It was found

from Table 3.2 that both the water permeability and the rejection were slightly reduced by the surface modification. The decrease in water permeability was only 0.2-0.3 [l.m-2.h-1.atm-1] and that in rejection was only about 1%. Thus, it was clear that the surface modification with $Cu(OH)_2$ did not strongly affect the membrane performance.

Table 3.2. Water permeability and rejection of unmodified and modified membranes

Sample	**Permeability ($l \cdot m^{-2} \cdot h^{-1} \cdot atm^{-1}$)**	**Rejection (%)**
Unmodified RO	5.3 ± 0.04	97.8 ± 0.3
RO/$Cu(OH)_2$-100 $mg \cdot l^{-1}$	5.0 ± 0.1	96.3 ± 0.4
RO/$Cu(OH)_2$-500 $mg \cdot l^{-1}$	5.1 ± 0.1	96.7 ± 0.4

3.3.5. Bactericidal properties

Table 3.3 shows the results of a shake flask test used to evaluate the bactericidal properties of modified membranes. The modified membranes showed good antibacterial properties over a range of pH (i.e., from 6.5 to 7.5) compared with the unmodified membranes. It was found from that the killing ratio depended only weakly on the pH, with a slightly higher killing ratio at high pH as shown in Table 3.3. The membrane modified with the both 100 and 500 $mg \cdot l^{-1}$ $Cu(OH)_2$ suspensions showed almost the same killing ratios at the same pH.

Two probable mechanisms were proposed for the antibacterial properties of the modified membranes, contact killing and release killing [25, 26]. Contact killing is based on direct contact of bacteria with the biocide, whereas release killing depends

upon the release of ions from the biocide materials, which then come into contact with and kill bacteria. In order to clarify the dominant antibacterial mechanism of the modified membranes, three pieces of the membrane modified with the 500 $mg \cdot l^{-1}$ $Cu(OH)_2$ suspension (total weight: 10±2 mg) were immersed in a 20 ml of PBS solution (without bacteria) and shaken in an incubator shaker at 200 rpm for 8 h. The resultant PBS solution was expected to contain Cu^{2+} ion released from the $Cu(OH)_2$ particles adsorbed on the membrane surface. The membranes were removed from the solution and 200 µl of an *E. coli* suspension ($1–5\times10^7$ $cfu \cdot ml^{-1}$) was added to the solution which was again incubated and shaken for 8 h at 37°C. The bacteria killing ratios were calculated by Eq. (2). In this experiment, a killing ratio was 99.8%, which compares well with the results where the membranes were maintained in the solutions as shown in Table 3.3. This suggests that the $Cu(OH)_2$ adsorbed on the membrane surface released Cu^{2+} ion in sufficient amounts to kill the bacteria. It can therefore be concluded that a release killing mechanism is the main contribution to the bactericidal properties of the modified membranes.

The saturated amount of $Cu(OH)_2$ adsorbed to the membrane modified with 500 $mg \cdot l^{-1}$ suspension was about 38.4 $\mu g \cdot cm^{-2}$ as shown in Figure 3.5. The membrane area immersed in 20 ml of diluted bacterial suspension in shake flask test was about 1.1 cm^2, thus the total amount of $Cu(OH)_2$ present in each flask was 42.2 µg. We prepared the bacterial suspension which contained 42.2 µg/20ml (2.11 $mg \cdot l^{-1}$) $Cu(OH)_2$ to investigate the effects of particle size aggregation on antibacterial properties and evaluated the killing ratio at pH 7.5. The killing ratio of this suspension was 99.85 ± 0.02%, and the same as that of the modified membrane within experimental error. Considering the

solubility constant of $Cu(OH)_2$ is 2.2×10^{-20} at 25°C, the saturated amount of $Cu(OH)_2$ dissolved in the 20 ml solution at pH 7.5 is 0.43 μg (0.28 μg as Cu^{2+} ion) suggesting that the amount of $Cu(OH)_2$ adsorbed on the membrane surface (42.2 μg) was sufficient to release 0.43μg $Cu(OH)_2$ into 20 ml of suspension. I found no effect on the killing ratio from particle size even though the solutions may be expected to take different times to reach saturation, depending on particle size. These results suggest that a Cu^{2+} ion concentration of 0.014 $mg \cdot l^{-1}$ (0.28 μg/20ml) is sufficient to give high antibacterial activity. While the antibacterial activity of $Cu(OH)_2$ is slightly lower than silver as shown [2], the secondary maximum contaminant level for copper is 10 times higher than silver [16], suggesting that $Cu(OH)_2$ may be good alternative for use in drinking water processes.

Table 3.3. Killing ratio measured by the shaking flask test in different pH

Sample	**Killing ratio (%)**		
	pH		
	6.5	7	7.5
Unmodified RO membrane	0	0	0
RO membrane+ $Cu(OH)_2$ – 100 $mg \cdot l^{-1}$	90 ± 3	95 ± 2	99.7 ± 0.1
RO membrane+ $Cu(OH)_2$ – 500 $mg \cdot l^{-1}$	90 ± 3	98.1 ± 0.1	98 ± 2

3.3.6. Antiadhesion resistance

A static adhesion test was performed to evaluate the antiadhesion property of the unmodified and modified membranes against bacteria as shown in section 3.2.3.7. The

membrane surface was observed by CLSM after immersion in bacteria suspension for 4 days. *P. putida* was used in this test because as could form biofilms easily than *E. coli*. Figure 3.8 shows the CLSM images, with the black background showing the membrane surface and green points indicating bacteria. The number of bacteria adsorbed onto the modified membranes surfaces (Fig. 3.8 (b) and (c)) was significantly less than the unmodified membrane surface (Fig. 3.8 (a)).

The number of bacteria in the suspensions was lowered by interactions with the Cu^{2+} ions released into the solution from $Cu(OH)_2$ particles adsorbed on the membrane surface as shown in Table 3.3. While this effect may decrease the number of bacteria that could potential attach to the modified membrane surface, the hydrophilicity of the membrane surface was also increased by modification with $Cu(OH)_2$ particles as shown in Table 3.1. The increase of hydrophilicity could contribute to the improvement of the membrane antiadhesion properties through the induction of higher free water content at the membrane surface. In addition, the higher negative surface charge density could improve the antiadhesion property of the membranes as *P. putida* has an overall negative potential (ζ-potential = -33 mv) [27]. The number of adsorbed bacteria may decrease through the electrostatic repulsion between the bacteria and membrane. Then, even if a small amount of bacteria survived, they were prevented to adhere the membrane surface.

The number of bacteria that attached to the membrane modified with $Cu(OH)_2$ 100 $mg \cdot l^{-1}$ (Fig. 3.8 (b)) was larger than that of the membrane modified with $Cu(OH)_2$ 500 $mg \cdot l^{-1}$ in Fig. 3.8 (c). This may be explained by the higher negative surface charge density of membrane modified with $Cu(OH)_2$ 500 $mg \cdot l^{-1}$ than that of the membrane

modified with $Cu(OH)_2$100 $mg \cdot l^{-1}$, as the hydrophilicity (contact angles) were almost same as shown in Table 3.1. The electrostatic repulsion between bacteria and membrane surface modified with $Cu(OH)_2$ 500 $mg \cdot l^{-1}$ was higher than that between bacteria and membrane surface modified with $Cu(OH)_2$ 100 $mg \cdot l^{-1}$. Thus, the antibiofouling properties of the modified membranes may be attributed to a combination of antibacterial and antiadhesion properties.

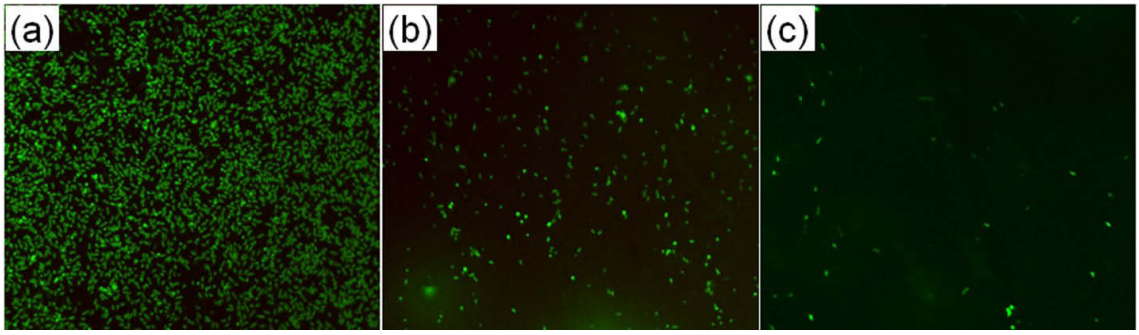

Fig. 3.8. CLSM images of different membrane surfaces, **(a)** unmodified membrane, **(b)** membrane modified with 100 $mg \cdot l^{-1}$ $Cu(OH)_2$ suspension, **(c)** membrane modified with 500 $mg \cdot l^{-1}Cu(OH)_2$ suspension. Black background is membrane surface and green points are bacteria.

3.3.7. Stability of modified membrane

The membrane modified with $Cu(OH)_2$ 500 $mg \cdot l^{-1}$ suspension was immersed into 250 ml of water for 8 and 16 days in refrigerator at 5°C to evaluate the stability of the $Cu(OH)_2$ modified membranes. The samples were kept in the refrigerator to avoid the effect of variations in temperature. After that, the antiadhesion properties were evaluated as described in section 3.2.3.7 Figure 3.9 shows that the modified membranes maintained their anti-adhesion properties after 8 days' immersion in water (Fig. 3.9 (b)).

After 16 days of immersion in water, there was a slight increase in the number of bacteria that attached to the membrane (Fig. 3.9 (c)) which may be attributed to desorption of $Cu(OH)_2$ during dipping into water. However, the membrane maintained good antiadhesion resistance compared with the unmodified membrane (Fig. 3.9 (a)). Whereas the stability of the modified membranes may not be adequate for a long term applications at present, it is clear that $Cu(OH)_2$ has good potential as an antibacterial agent for improving the antibiofouling properties of RO membranes.

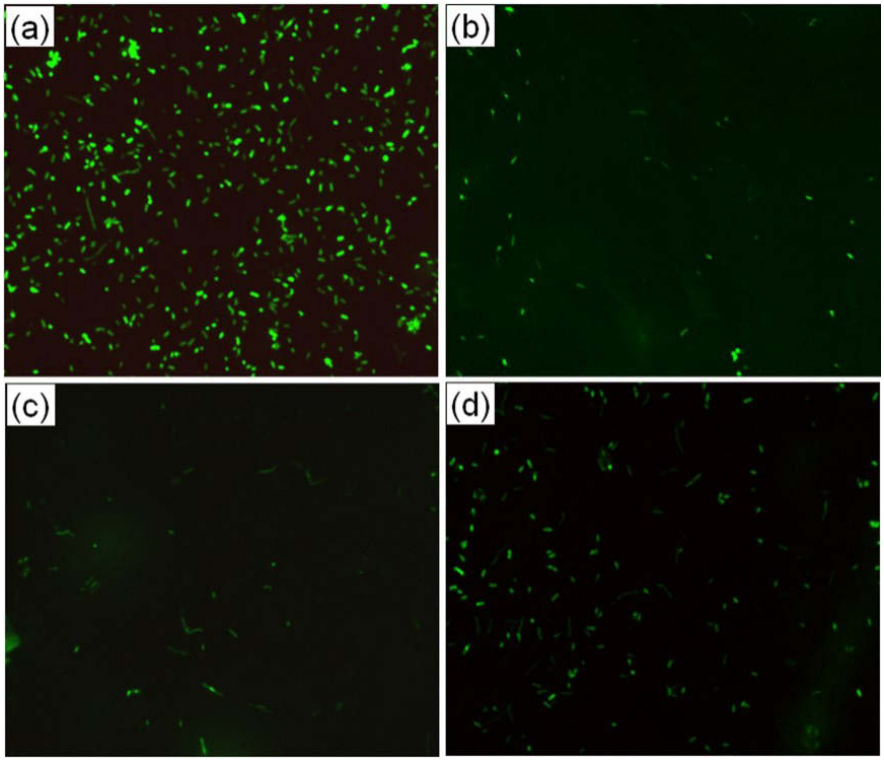

Fig 3.9. CLSM images of different membrane surfaces, **(a)** unmodified membrane, **(b)** RO modified with $Cu(OH)_2$ 500 $mg \cdot l^{-1}$ suspension, just after modification **(c)** RO modified with $Cu(OH)_2$ 500 $mg \cdot l^{-1}$ suspension, after 8 days in water **(d)** RO modified with $Cu(OH)_2$ 500 $mg \cdot l^{-1}$suspension, after 16 days in water. Black background represents the membrane surface and green points indicate bacteria.

3.4. Conclusion

I show that $Cu(OH)_2$ particles have superior antibacterial properties under neutral conditions compared with $Ca(OH)_2$ and $Mg(OH)_2$. $Cu(OH)_2$ particles were used to modify commercial RO membranes improving the antibacterial properties. It was found that the $Cu(OH)_2$ particles physically adsorbed on the membrane surface, and bactericidal activity may be attributed to release of Cu^{2+} ions from the membrane surface into solution. The hydrophilicity of modified membrane and the negative charge density of membrane surface were also increased by adsorption of $Cu(OH)_2$ particles. Antiadhesion properties towards bacteria were improved attributed to an increase in the free water content at the membrane surface from the high surface hydrophilicity and the increase of electrostatic repulsion between bacteria and negative surface charge. Thus, the antibiofouling performance of a commercial RO membrane was greatly improved by the enhancement of antibacterial and antiadhesion effects.

References

[1] I. Sawada, R. Fachrul, T. Ito, Y. Ohmukai, T. Maruyama, H. Matsuyama, Development of a hydrophilic polymer membrane containing silver nanoparticles with both organic antifouling and antibacterial properties, Journal of Membrane Science, 387–388 (2012) 1-6.
[2] H. Karkhanechi, F. Razi, I. Sawada, R. Takagi, Y. Ohmukai, H. Matsuyama, Improvement of antibiofouling performance of a reverse osmosis membrane through biocide release and adhesion resistance, Separation and Purification Technology, 105 (2013) 106-113.
[3] R. Bai, X. Zhu, K.-H. Wee, C. Liu, S.-L. Tang, Membrane surfaces immobilized with ionic or reduced silver and their anti-biofouling performances, Journal of Membrane Science, 363 (2010) 278-286.

[4] R. Bai, C.X. Liu, D.R. Zhang, Y. He, X.S. Zhao, Modification of membrane surface for anti-biofouling performance: Effect of anti-adhesion and anti-bacteria approaches, Journal of Membrane Science, 346 (2010) 121-130.
[5] Y. Deng, C. Dong, J. Cairney, Q. Sun, O.L. Maddan, G. He, Investigation of Mg(OH)2 nanoparticles as an antibacterial agent, Journal of Nanoparticle Research, 12 (2009) 2101-2109.
[6] M. Fang, J. Chen, X. Xu, P. Yang, H. Hildebrand, Antibacterial activities of inorganic agents on six bacteria associated with oral infections by two susceptibility tests, International Journal of Antimicrobial Agents, 27 (2006) 513-517.
[7] H. R. Nawaz, B. A. Solangi, B. Zehra, U. Nadeem, Preparation of Nano Zinc Oxide and its Application in Leather as a Retanning and Antibacterial Agent, Canadian Journal on Scientific and Industrial Research, 2 (2011) 164-170.
[8] C. Marambio-Jones, E.V. Hoek, A review of the antibacterial effects of silver nanomaterials and potential implications for human health and the environment, J Nanopart Res, 12 (2010) 1531-1551.
[9] Q.L. Feng, J. Wu, G.Q. Chen, F.Z. Cui, T.N. Kim, J.O. Kim, A mechanistic study of the antibacterial effect of silver ions on Escherichia coli and Staphylococcus aureus, Journal of Biomedical Materials Research, 52 (2000) 662-668.
[10] J.F. Siqueira, H.P. Lopes, Mechanisms of antimicrobial activity of calcium hydroxide: a critical review, International Endodontic Journal, 32 (1999) 361-369.
[11] C. Dong, D. Song, J. Cairney, O.L. Maddan, G. He, Y. Deng, Antibacterial study of Mg(OH)2 nanoplatelets, Materials Research Bulletin, 46 (2011) 576-582.
[12] J.A. Narciso, C.M. Ference, M.A. Ritenour, W.W. Widmer, Effect of copper hydroxide sprays for citrus canker control on wild-type Escherichia coli, Letters in Applied Microbiology, 54 (2012) 108-111.
[13] J.G. Gadi Borkow, Copper, An Ancient Remedy Returning to Fight Microbial, Fungal and Viral Infections, Current Chemical Biology, 3 (2009) 272-278.
[14] P. Patnaik, Handbook of Inorganic Chemicals, (2002).
[15] A.F. Mendonca, T.L. Amoroso, S.J. Knabel, Destruction of gram-negative food-borne pathogens by high pH involves disruption of the cytoplasmic membrane, Applied AND Environmental Microbiology, 60 (1994) 4009.
[16] U.S.E.P. Agency, National secondary drinking water regulations, The agency, washington, DC, (1984).
[17] C.E. Santo, N. Taudte, D.H. Nies, G. Grass, Contribution of Copper Ion Resistance to Survival of Escherichia coli on Metallic Copper Surfaces, Applied AND Environmental Microbiology, 74 (2007) 977-986.
[18] J.O. Noyce, H. Michels, C.W. Keevil, Use of Copper Cast Alloys To Control Escherichia coli O157 Cross-Contamination during Food Processing, Applied AND Environmental Microbiology, 72 (2006) 4239-4244.
[19] F. Razi, I. Sawada, Y. Ohmukai, T. Maruyama, H. Matsuyama, The improvement of antibiofouling efficiency of polyethersulfone membrane by functionalization with zwitterionic monomers, Journal of Membrane Science, 401–402 (2012) 292-299.
[20] T.R. Bott, Industrial Biofouling, Elsevier, 2011.
[21] G. M.Barrow, Physical Chemistry, 1961.
[22] Z. Su, X. Zan, Counterions in polyelectrolyte multilayers: A vehicle for introducing functionalities, Thin Solid Films, 518 (2009) 116-119.

[23] J.-H. Li, M.-Z. Li, J. Miao, J.-B. Wang, X.-S. Shao, Q.-Q. Zhang, Improved surface property of PVDF membrane with amphiphilic zwitterionic copolymer as membrane additive, Applied Surface Science, 258 (2012) 6398-6405.
[24] T. Ishigami, K. Amano, A. Fujii, Y. Ohmukai, E. Kamio, T. Maruyama, H. Matsuyama, Fouling reduction of reverse osmosis membrane by surface modification via layer-by-layer assembly, Separation and Purification Technology, 99 (2012) 1-7.
[25] J.A. Lichter, K.J. Van Vliet, M.F. Rubner, Design of Antibacterial Surfaces and Interfaces: Polyelectrolyte Multilayers as a Multifunctional Platform, Macromolecules, 42 (2009) 8573-8586.
[26] Z. Li, D. Lee, X. Sheng, R.E. Cohen, M.F. Rubner, Two-Level Antibacterial Coating with Both Release-Killing and Contact-Killing Capabilities, Langmuir, 22 (2006) 9820-9823.
[27] A. Subramani, E.M.V. Hoek, Direct observation of initial microbial deposition onto reverse osmosis and nanofiltration membranes, Journal of Membrane Science, 319 (2008) 111-125.

Chapter 4

Biofouling resistance of reverse osmosis membrane modified with polydopamine

4.1. Introduction

Biofouling is the undesired attachment of microorganism communities to a membrane surface. Bacteria adhered to the surface release extracellular polymeric substances (EPS) and consequently, a biofilm EPS matrix with embedded bacteria is formed. Because biofilms reduce salt rejection and flux [1, 2], biofouling is a serious obstacle in reverse osmosis (RO), and other membrane processes. Several methods have been reported to overcome membrane biofouling. Most of these methods have been based on enhancing the antimicrobial and antiadhesion properties [3-5]. An antimicrobial property improves bacteria lysis, while the antiadhesion property increases the adhesion resistance of the surface against bacterial attachment.

Surface modifications such as coating, deposition and grafting are general approaches that improve membrane biofouling resistance by increasing antimicrobial or antiadhesion properties. Using organic and inorganic antimicrobial agents is a common method to increase the antibacterial property of the membrane surface. The adhesion resistance against bacteria could be improved by improving hydrophilicity and

smoothness, and also by increasing the negative charge density of the membrane surface [6-8].

To improve the antibacterial properties, silver is an inorganic agent used in many studies as a strong biocide. Silver nanoparticles can release Ag ions, which are biocidal and consequently lyse the bacteria [4, 9-11]. Sawada et al. enhanced the antibiofouling properties of a polyethersulfone (PES) hollow fiber (HF) membrane by forming an acrylamide surface layer embedded with silver nanoparticles [10]. In the second chapter, the antibacterial property of a commercial RO membrane was improved by silver nanoparticles embedded into polyelectrolyte multilayers using the Layer-by-Layer (LbL) method [4]. Metal hydroxides such as $Ca(OH)_2$, $Mg(OH)_2$ and $Cu(OH)_2$ were also used as inorganic antimicrobial agents [12-14]. We recently reported that the antibacterial property of an RO membrane surface was improved by the deposition of $Cu(OH)_2$ particles that released Cu ions [14]. The other approach to improve the antibacterial property is the formation of a material surface with antibiotic functional groups such as antimicrobial peptides or compounds that present positive charges such as the quaternary ammonium (QA) group. Razi et al. improved the antibiofouling properties of a PES-HF membrane by grafting (2-dimethylamino) ethyl methacrylate methyl chloride quaternary salt (DMAEMAq) onto the membrane surface [15]. The QA groups have positive charges that penetrate the cell wall of bacteria or induce disruption of the cell membrane integrity and lyse the cell.

Many investigations have reported that the improvement of membrane surface hydrophilicity improves the antiadhesion property and effectively reduces membrane biofouling [4, 16, 17]. Surface modification with hydrophilic substances such as

zwitterions is a promising method. Zwitterionic monomers, such as methacryloyloxyethyl phosphorylcholine (MPC), are electrically neutral chemicals with cationic and anionic groups on their backbone structures. We coated a commercial RO membrane surface with polyzwitterion (PZ) using the LbL method and improved the antiadhesion property of the membrane surface [4]. Organic fouling and biofouling resistances of a PES-HF membrane were also improved by grafting zwitterionic monomers [17].

However, the methods mentioned above have a number of shortcomings, such as high cost (e.g. Silver or PZ), risks to human health (Low value of secondary maximum contaminant level, for example, 0.1 mg/L for silver), complexity (such as LbL method), low reproducibility and poor stability. Thus, an attractive method should feature low toxicity, simplicity, low cost and good stability in addition to good antiadhesion and antimicrobial properties.

Dopamine coating is a relatively new surface modification method. A polydopamine (PDA) layer is formed on any substrate that is immersed in dopamine solution [18]. Surface modification with PDA has been reported for several kinds of membranes, including electrodialysis (ED) [19], microfiltration (MF) [20], ultrafiltration (UF) and RO membranes [20-22]. It is well known that PDA is a super-hydrophilic material that improves the hydrophilicity of hydrophobic surfaces such as polyethylene (PE), poly (vinyl fluoride) (PVDF) and polytetrafluoroethylene (PTFE) [23-26]. The PDA layer tightly adheres to the surface by strong covalent and non-covalent interactions with the substrate, giving a highly stable PDA coating [27]. Xi et al. showed that PDA had very good stability on the membrane surface [23]. Kasemset et

al. showed that the organic fouling resistance of a commercial RO membrane was sufficiently improved by PDA modification [21]. Also, Azari and Zou showed that the organic fouling resistance of an RO membrane was enhanced by L-PDA coating through a marked improvement of hydrophilicity [22].

Considering the experimental results shown above, surface modification with PDA would also be a promising modification method to improve the antibiofouling potential of an RO membrane. The PDA coating is a simpler method than the LbL method we used for the surface modification with silver nanoparticles and PZ. The dopamine is cheaper than silver and PZ. In addition, it is expected that the PDA coating is more stable than the $Cu(OH)_2$ coating we have already reported, since $Cu(OH)_2$ adsorbed by physical adsorption. Furthermore, recently, PDA has attracted considerable interest for various types of biomedical applications [28] indicating that PDA can be used safely to modify membranes for producing drinking water. To the best my knowledge, the improvement of antibiofouling properties of RO membranes with PDA coating has not been reported. So in this chapter, I attempted to improve the antibiofouling properties of an RO membrane by PDA coating. The optimal conditions and mechanism behind the improvement of the antibiofouling performance are discussed. Finally, I show, for the first time, the antibacterial property of PDA.

4.2. Experimental

4.2.1. Materials

A commercial RO membrane (ES20, Nitto Denko, Osaka, Japan) was used as the base membrane. This is an ultra-low pressure RO membrane with an aromatic

polyamide selective layer. The nominal value of rejection stated in the company catalog is 99.7% for 0.05% NaCl. NaCl (Wako Pure Chem. Ind., Osaka, Japan) was used as an electrolyte. Glutaraldehyde, ethanol and [Bis(trimethylsilyl)amine] (Wako Pure Chem. Ind.) were used in antiadhesion experiments. Dopamine hydrochloride (Sigma-Aldrich, St. Louis, MO, USA) was used for surface modification of the RO membrane. The chemical structure of dopamine is shown in Fig. 4.1. Tryptic Soya Broth (TSB) and Difco Nutrient Broth (NB) (Becton, Dickinson and Company, Franklin Lakes, NJ, USA) were used as nutrient agents. *Escherichia coli* (*E.coli*) (NBRC 3310) and *Pseudomonas putida* (*P. putida*) (NBRC 100650) (Biological Resource Center at the National Institute of Technology and Evaluation, Shibuya, Japan) were used as model Gram-negative bacteria, because most bacteria in water treatment processes are Gram-negative bacteria [29]. Syto 9 and Syto propidium iodide (PI) (Life Technologies Corporation, Tokyo, Japan) were used as molecular probes for bacteria. All chemicals were used without further purification. Milli-Q water (18.2 MΩ·cm) (Millipore, Billerica, MA, USA) was used to prepare all solutions and for rinsing.

4.2.2. Membrane modification

The RO membrane was modified by dopamine. Dopamine solutions were prepared by dissolving dopamine hydrochloride at several concentrations (i.e., 0.1, 0.5, 1, 1.5, and 2 kg/m^3) in 15 mM Tris–HCl buffer (pH 8.8). Dopamine spontaneously polymerizes and forms PDA by contacting with oxygen in an alkaline aqueous solution [30]. Figure 4.1 shows a mechanism for dopamine oxidative self-polymerization [18, 31-34]. The PDA interacts with membrane surface by covalent and noncovalent

interactions [27], and strongly adheres to the membrane surface. A membrane was fixed to a customized fixture [14] and only the active layer was exposed to the aqueous dopamine solution since the fouling takes place only on the active layer of membrane. Otherwise PDA coating deposited on the support layer will lead to a decline membrane performance. The fixture was horizontally placed in a beaker containing 600 ml of dopamine solution, and then the solution was thoroughly stirred for the desired modification time (i.e., 1.5, 3, 6, 15 and 24 hours) at 28°C.

After modification for the desired time, the membrane was removed from the beaker and rinsed three times with fresh water. To remove excess or weakly-bound PDA from the membrane surface, the modified membrane was immersed in 25% (v/v) isopropyl alcohol (IPA) solution for 10 min. The membrane was then thoroughly rinsed with Milli-Q water for one day.

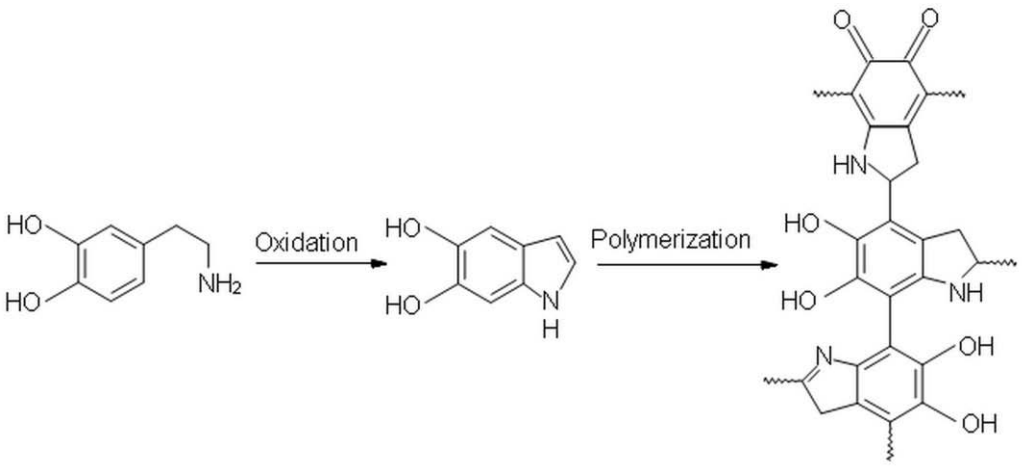

Fig. 4.1. Dopamine polymerization [31, 34]

4.2.3. Characterization

4.2.3.1. FT-IR and XPS

The surface chemical structures of the unmodified membrane and PDA-modified membranes were analyzed by Fourier-transform infrared spectroscopy (FT-IR) and the chemical composition by X-ray photoelectron spectroscopy (XPS). FT-IR measurements were carried out by an FT-IR spectrometer (ALPHA, Bruker Co., Billerica, MA, USA) with attenuated total reflectance (ATR). XPS measurements were carried out with an ESCA-850 spectrometer (Shimadzu Co., Kyoto, Japan). The sample surface was irradiated by Mg Kα radiation, generated at 8 kV and 30 mA. The membranes were dried in a freeze dryer (FDU-1200 EYELA; Tokyo Rikakikai Co. Ltd., Tokyo, Japan) overnight prior to FT-IR and XPS measurements.

4.2.3.2. Surface Morphology

The surface morphology of the PDA-modified membrane was observed using a field emission scanning electron microscope (FE-SEM) (JSF-7500F; JEOL Co. Ltd., Tokyo, Japan) with an accelerating voltage of 5 kV. The membranes were dried overnight in a freeze dryer in the same way as described in Section 4.2.3.1 and then coated with osmium tetroxide (OsO_4) prior to FE-SEM measurements. A thin OsO_4 layer (ca. 5 nm) was formed using an osmium coater (Neoc-STB; MEIWAFOSIS Co. Ltd., Tokyo, Japan).

4.2.3.3. Air contact angle and ζ-potential of membrane surface

The hydrophilicity of the membrane was evaluated by air contact angle using a contact angle meter (Drop Master 300, Kyowa Interface Science Co. Ltd., Niiza, Japan). Membrane samples were horizontally immersed into Milli-Q water facing the active layer down. Air bubble was attached onto the active layer using a micro liter syringe equipped with a J-hook needle, and then the contact angle was measured. The static contact angle was measured at least10 times for each sample and then the mean value was calculated.

The ζ-potential of the membrane surface was obtained from the streaming potential measurement by an ELS-4000K instrument (Otsuka Electronics, Osaka, Japan) using a 0.01 M NaCl solution (pH 5.9) at room temperature.

4.2.3.4. Water permeability and salt rejection

The laboratory scale cross-flow membrane test unit shown in Fig. 2.2 was used to measure the salt rejection and water permeability of the unmodified and PDA-modified membranes [4, 14]. The NaCl rejection, R_{obs}, was calculated using Eq. (1). The NaCl concentration was determined from a conductance measurement (CM-30R, DKK-TOA Corporation, Tokyo, Japan) using calibration curve between concentration and conductivity.

$$R_{obs} = (1 - \frac{2C^{p}_{NaCl}}{(C^{r}_{NaCl} + C^{f}_{NaCl})}) \times 100 \qquad (1)$$

where, C^{p}_{NaCl} , C^{r}_{NaCl} and C^{f}_{NaCl} indicate the NaCl concentrations in the permeate, retentate, and feed, respectively. Generally, R_{obs} is calculated using not $(C^{r}_{NaCl}+C^{f}_{NaCl})/2$, but C^{f}_{NaCl}. However, C^{r}_{NaCl} is higher than C^{f}_{NaCl}. It means that there is a concentration gradient between inlet and outlet of cell. Then, we evaluated R_{obs} using $(C^{r}_{NaCl}+C^{f}_{NaCl})/2$ as an average concentration in the flow cell.

The water permeability ($m^3 \cdot m^{-2} \cdot h^{-1} \cdot atm^{-1}$) was obtained from the volume of permeated water accumulated with time. The mass of permeate was measured using an analytical balance and recorded by computer connected to the balance.

4.2.3.5. Biofouling potential

4.2.3.5.1. Filtration experiment with a bacterial suspension

The time course of water flux through the unmodified membrane and the PDA-modified membranes were measured by cross-flow filtration of a bacterial suspension to evaluate the antibacterial potential. In addition, bacterial adhesion to the membrane surface was measured by FE-SEM after 1200 minute continuous filtration. This filtration experiment was carried out using the laboratory-scale apparatus shown in Fig. 2.2. The system was cleaned with bleach solution (250 mg/l of NaClO) for 30 minutes to disinfect the system prior to each filtration. The system was then rinsed for at least 1 hour with Milli-Q water. It is reported that the water flux affects the progress of fouling [35, 36]. This is probably because the amount of foulants filtered by the membrane depends on the water flux through the membrane. This situation will be the same for biofouling. Thus, the initial flux of all membranes was adjusted to 2.2×10^{-2} $m^3.h^{-1}.m^{-2}$

by controlling the transmembrane pressure difference (TMP) using sterilized NaCl (0.085 w/w %) before feeding the bacterial suspension at the flow rate, 1.0×10^{-6} $m^3.min^{-1}$. The same flow rate was applied for bacterial filtration. A bacterial suspension of *P. putida* was used as the feed solution. *P. putida* was first cultured in TSB medium overnight and then diluted in sterilized NaCl (0.085 w/w %). The final concentrations of *P. putida* in the bacterial suspension for all filtration experiments were closely similar, (10^7- 10^8) cfu/ml. The concentration of bacterial suspensions was evaluated by an optical density measurement just before feeding. The optical density was measured by UV-VIS spectrophotometer (V-650 KE, JASCO Analytical instruments, Japan) prior to filtration and the average was 0.135 at 660 nm wavelength.

After 1200 minute of continuous bacterial filtration, the bacteria attached on the membrane surface were observed by FE-SEM, as described in Section 4.2.3.2. After the bacterial filtration test, the membrane samples were thoroughly washed with phosphate buffered saline (PBS) solution (pH 7.5), and then the bacteria on the membrane surface were fixed by dipping the membrane into a 2.5 v/v % glutaraldehyde PBS solution for 4 hours at 4°C [17, 37]. After fixation, the membranes were rinsed with PBS to remove residual glutaraldehyde from the surfaces. To reduce the water content of the membrane samples, they were then dehydrated with ethanol. Dehydration steps were performed by immersing each of the membrane samples into 50, 70, 90 and 99.5% ethanol solutions for 10 minutes in series, followed by immersion into a 99.5% ethanol solution for 10 minutes twice. Finally, the membrane samples were immersed in [Bis(trimethylsilyl)amine] solution for 1 minute to coat them to avoid water adsorption,

dried in air, then stored in a desiccator. The dried membrane samples were used in FE-SEM observations.

4.2.3.5.2. Static adhesion test

The antiadhesion properties of the unmodified and PDA-modified membranes were evaluated using a static adhesion test. In this test, *P. putida* was used as a model bacterium because *P. putida* can form a biofilm more easily than *E. coli* [38]. When *E. coli* was used in this experiment, the biofilm formation was slow and did not allow clear comparisons. Thus, the antiadhesion experiments were performed only with *P. putida*. The unmodified and PDA-modified membranes were immersed in 40 ml of *P. putida* suspension (1–5 × 10^7 cfu/ml) in Vogel Banner minimum medium (VBMM) at pH = 8 [17] and incubated at 30°C for 4 days. The membrane surface area was about 5×10^{-4} m^2. The membranes were then removed from the suspension and rinsed four times with NaCl solution (0.85 w/w%). The residual bacteria on each type of membrane were stained for 15 min by immersion in a staining solution. The staining solution was prepared by dissolving 1.5 µl of a cell-permeable green fluorescence dye (Syto 9) and 1.5 µl of a viable cell-impermeable red dye (Syto PI) in 1 ml of 0.85 w/w % NaCl solution. The membranes were then rinsed thoroughly with NaCl solution (0.85 w/w %) and immersed in 2.5 v/v % glutaraldehyde solution at 4°C to fix the adhered bacteria [17, 37]. After 1 hour, the amount of total bacteria on the membrane surface was observed using confocal laser scanning microscopy (CLSM) (FV 1000 D, Olympus Co. Ltd., Tokyo, Japan).

4.2.3.5.3. Antibacterial property

The bactericidal properties of the unmodified and PDA-modified membranes were evaluated by a shake flask test using *E. coli* as a model Gram-negative bacterium because *E. coli* is more resistant against antibacterial agents than the *P. putida* [4, 39]. Thus, the evaluation condition with *E. coli* was more severe than with *P. putida*. The bacteria were cultured in NB media and then placed in an incubator-shaker overnight. The incubation temperature for all steps was 37°C. The bacterial suspension (*E. coli* suspension) was diluted in phosphate buffered saline (PBS) (pH= 7.5) to 1–5 × 10^5 cfu.ml^{-1}. Three pieces of each membrane (unmodified or modified membranes), with a total weight of 10 ± 2 mg, equivalent to an area of 1.1 ± 0.2 cm^2, were immersed in 20 ml of the diluted bacterial suspension. Simultaneously, 20 ml of the diluted bacterial suspension without membrane was used as a control. Diluted bacterial suspensions with and without membranes were incubated and shaken for 8 h at 37°C. After 8 hours, 1 ml of the diluted bacterial suspension was taken from each sample, including the control, and added to 27 ml of NB/Agar solution. After solidification, NB/Agar plates were incubated for 2 days and the number of live bacteria on each plate was counted. The bactericidal ratio (sterilization ratio) was calculated by Eq. (2).

$$bactericidal\ ratio\ (\%) = \left(\frac{N_B - N_S}{N_B} \right) \times 100\,, \qquad (2)$$

where N_B indicates the number of live bacteria on the control plate and N_S that of the sample plate. N_B reflects the number of live bacteria in the diluted control bacteria suspension and N_S that of the diluted bacteria suspension containing a membrane. Thus,

the bactericidal ratio reflects the bactericidal properties of the membrane, assuming the bacteria adsorption on membranes does not affect the bactericidal ratio.

4.3. Results and discussion

4.3.1. Surface characterization

4.3.1.1. Analysis of membrane chemical structure

The surface chemical structure of the membranes was analyzed by FT-IR spectroscopy. FT-IR spectra of an unmodified and PDA-modified membrane are shown in Figs. 4.2a-4.2c. New peaks observed for the PDA-modified membrane and their assignment are summarized in Table 4.1. The small peak at 1738 cm^{-1} was assigned to the >C=O group [40, 41] that is formed by oxidation of the catechol groups into quinine during the self-polymerization, as shown in Fig. 4.1. The peaks attributed to >C=O, –O–H and >N–H confirm the existence of PDA on the RO membrane surface.

Table 4.1. New FT-IR peaks observed in PDA-modified membrane.

Wavenumber (cm^{-1})	Bond and functional group
1218	–C–O stretching [24]
1368	phenolic –O–H bending and stretching vibration [24]
1738	>C=O group [40, 41]
3100- 2900	–N–H/–O–H stretching vibrations [41, 42]

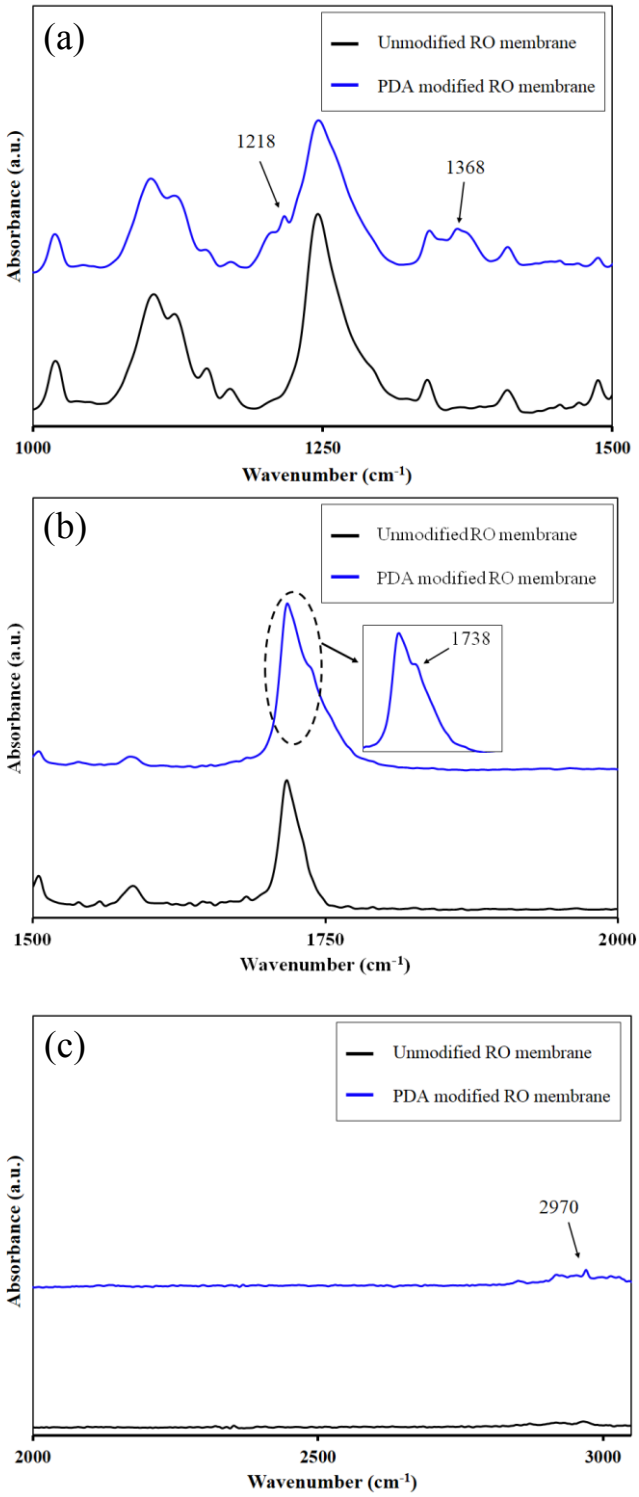

Fig. 4.2. FT-IR spectra of unmodified and PDA-modified membranes. The concentration of dopamine solution was 0.5 kg/m^3 and the dopamine coating time was 24 hours at pH 8.8.

To determine the chemical composition of the unmodified and PDA-modified membranes, XPS analysis was carried out. The composition ratios for the unmodified and PDA-modified membranes are shown in Table 4.2. The C:O and C:N ratios for the unmodified membrane were 4.4 and 6.4, respectively, in agreement with the typical composition of aromatic polyamide membranes [43]. The theoretical values of C1s for the unmodified membrane and dopamine are similar, at 72%. The O1s content of PDA-modified membranes (20.7 % for RO+PDA and 20.9 % after 3 months) are higher than the theoretical value (18.2%) that is considered as experimental error. Thus, the N1s content is the main criterion used to confirm the deposition of PDA. The C:N ratio was increased from 6.4 to 9.2 after PDA coating. This increase could be attributed to PDA deposition on the membrane surface. In addition, the result of XPS analysis was not noticeably changed, as shown in Table 4.2, after immersing the PDA-modified membrane in water for three months. This indicates that the PDA coating is stable on the membrane surface and can probably be attributed to the high adhesion property of PDA [18, 27, 32].

Table 4.2. Chemical composition (in atomic percent) of the unmodified and PDA-modified membranes, measured by high-resolution XPS.

Membrane	C1s (%)	N1s (%)	O1s (%)	C: O	C:N
Unmodified RO	72.2	11.3	16.5	4.4	6.4
Dopamine (theoretic value)	72.7	9.1	18.2	4.0	8.0
RO + PDA	71.5	7.8	20.7	3.5	9.2
RO + PDA (after 3 months)	71.0	8.2	20.9	3.4	8.7

4.3.1.2. Surface color changes

Figure 4.3 shows the color change of the modified membranes as a function of dopamine concentration. PDA is spontaneously formed in the aerobic and alkaline dopamine aqueous solution and simultaneously deposited on the membrane surface. The brown color of the PDA-modified membrane also indicates that PDA was successfully deposited on the membrane surface [44]. It was found from Fig. 4.3 that the color was unchanged above a 1 kg/m^3 concentration of dopamine. This indicates that the membrane surface was fully covered by 1 kg/m^3 dopamine solution.

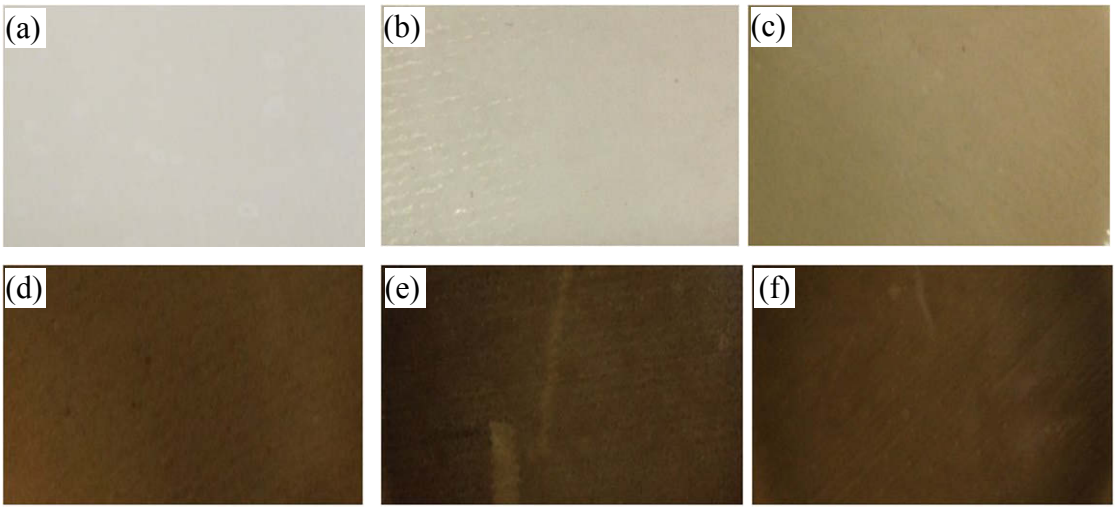

Fig. 4.3. Color change of membrane surface as a function of dopamine concentration; the dopamine concentrations (kg/m^3) were 0 (a), 0.1 (b), 0.5 (c), 1(d), 1.5 (e) and 2 (f). The surface modification time was 24 h at pH 8.8. Fig. 4.3 (a) shows the unmodified membrane.

4.3.1.3. Surface morphology

Because the membrane surface morphology is often affected by a surface modification, the surface of the unmodified and PDA-modified membranes were observed by FE- SEM, as shown in Fig. 4.4. The membranes were modified with different dopamine concentrations for 24 hours at pH 8.8. It is known that the active layer of RO membrane has a specific waved morphology due to interfacial polymerization as shown in Fig. 4.4a. By contrast, the surface of the modified membrane was changed in morphology by PDA coating as shown in Figs. 4.4b-4.4d. Thus, it was confirmed that PDA was successfully deposited on the membrane surface.

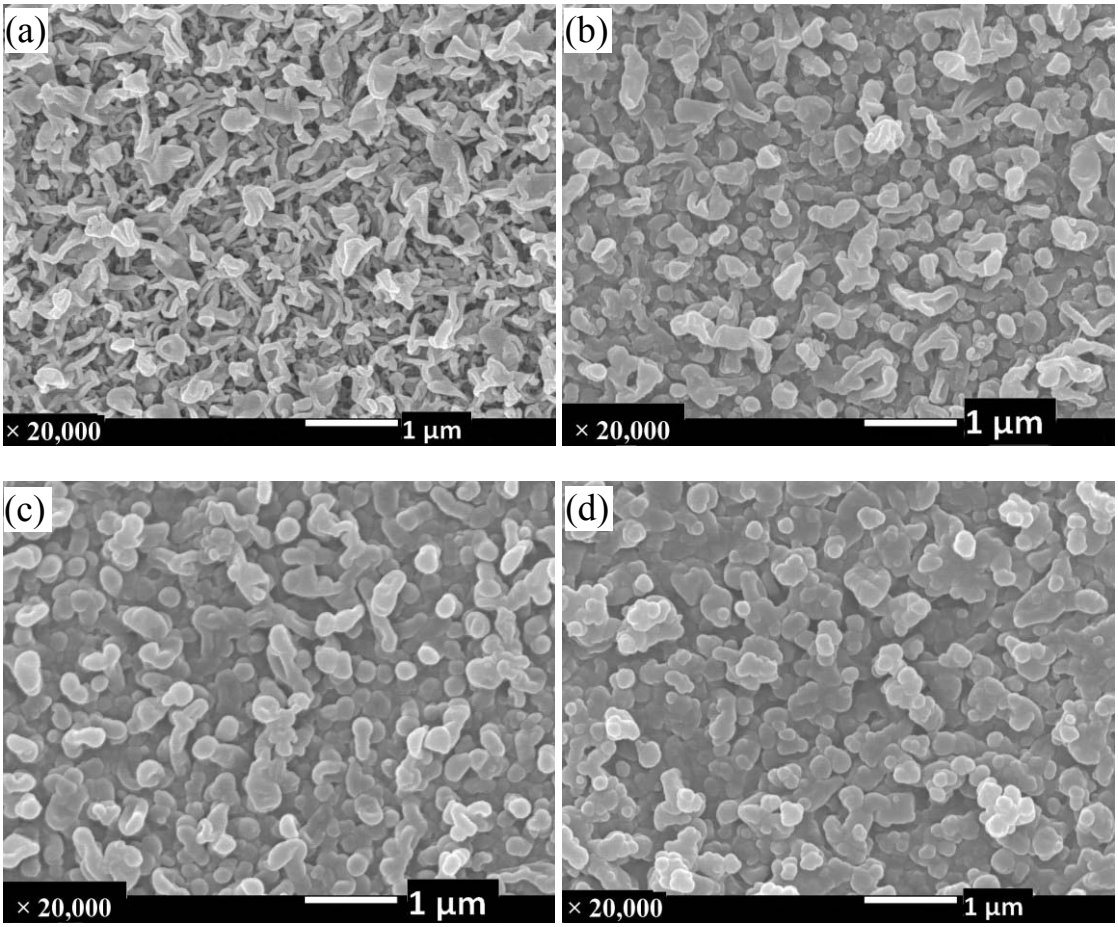

Fig. 4.4. FE-SEM images of the membrane surface. The dopamine concentration (kg/m^3) was 0 (a), 0.5 (b), 1 (c) and 2 (d). The dopamine deposition time was 24 h at pH 8.8. Fig. 4.4 (a) shows the unmodified membrane.

4.3.1.4. Effect of modification condition on air contact angle

The hydrophilicity of the membrane surface is usually evaluated by water or air contact angles. In this study, the hydrophilicity was evaluated with air contact angle, because the RO membrane is always used in contact with water. An increase in the air contact angle indicates an improvement in hydrophilicity. The static air contact angles of the unmodified and PDA-modified membranes are shown in Table 4.3. It has been

reported that PDA coating can improve the hydrophilicity of the membrane surface through the introduction of new groups, such as hydroxyl, catechol and amine groups [23, 45]. However, the PDA coating was not very effective at improving the hydrophilicity in my case, although the deposition of PDA on the membrane surface was confirmed, as described in Sections 4.3.1.1–4.3.1.2.

The change in hydrophilicity strongly depends on the substrate. The surface of the unmodified membrane is already highly hydrophilic due to the carboxylic acid groups of the active layer. Thus, surface modification with PDA could not dramatically improve the hydrophilicity of the RO membrane. A similar phenomenon was observed by Kasemset et al. [21].

Table 4.3. Air contact angle of PDA modified membranes at different dopamine concentrations. The dopamine deposition time was 24 h at pH 8.8.

Dopamine concentration (kg/m^3)	**Air contact angle (^{o})**
0 (unmodified)	145.0 ± 0.5
0.1	146.3 ± 0.4
0.5	152.6 ± 0.4
1	145.4 ± 0.4
1.5	147 ± 1
2	144.9 ± 0.5

4.3.1.5. Surface Charge

PDA is as an amphoteric material [46]. This property is attributed to amine groups and phenolic hydroxyl groups. As shown in Fig. 4.5, PDA is positively charged and its ζ- potential is 16.0 mV in a pH 3 solution because of protonation of amine groups, while in pH 11 solution, it has a negative charge and its ζ- potential is −20.8 mV because of deprotonation of the phenolic groups [46]. The isoelectric point (Isp) of PDA was reported as pH 3.4 [47] or pH 4.0 ± 0.5 [48]. Because the pH of the NaCl solution in my ζ- potential measurements was 5.9, a negative surface charge would be expected on the PDA-modified membrane. The ζ- potentials for PDA-modified membranes with different dopamine concentrations are shown in Table 4.4. As expected, the ζ-potential of the PDA-modified membrane was negative over the entire concentration range of dopamine. However, the ζ-potential of the PDA-modified membrane was almost the same as that of the unmodified membrane. The difference between modified membranes by 1 and 1.5 kg/m^3 dopamine and unmodified membrane is about ±2 mV and within the accuracy of experimental apparatus. This is probably because the unmodified membrane surface already had a high negative charge density because of the carboxylic acid groups. This phenomenon is similar to the hydrophilicity outcomes described above. Thus, the PDA coating did not also appreciably increase the membrane surface charge density.

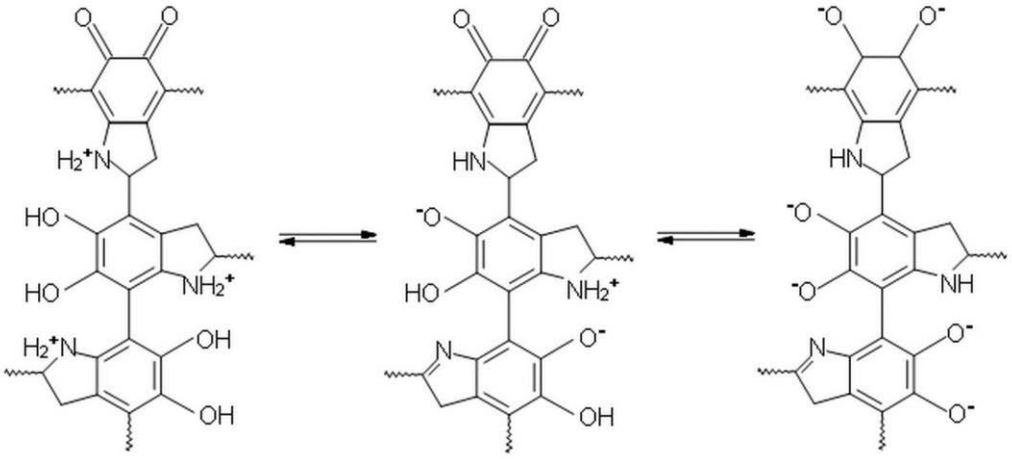

Fig. 4.5. The structure of PDA at different pH values (modified from Yu et al. report [46])

Table 4.4. The ζ-potential of the unmodified and PDA-modified membranes surfaces. The dopamine coating time was 24 hours at pH 8.8. The ζ-potential was measured at pH 5.9.

Dopamine concentration (kg/m^3)	**ζ– potential (mV)**
0	-10.5 ± 0.8
0.5	-10.6 ± 0.9
1	-12.7 ± 0.7
1.5	-8.9 ± 0.6

4.3.2. Water permeability and salt rejection of membranes

The water permeability and salt rejection of unmodified and PDA-modified membranes were measured by the cross-flow filtration setup described in Section

4.2.3.4. The results are shown in Fig. 4.6. The salt rejections for unmodified and PDA-modified membranes were similar, indicating that the modification did not affect salt rejection. Polydopamine formation is a mild oxidative self-polymerization at pH 8.8. According to the information mentioned in the membrane manufacturer's catalog, the permissible pH range for the commercial RO membrane (i.e., ES-20) is between 2 and 10 [49]. This means that the modification method applying PDA may not damage the structure of the active layer (i.e., top layer). The salt rejection is governed by the active layer and was not affected by PDA coating.

Conversely, the water permeability decreased with modification time. It has already been reported that water permeation through an RO membrane consists of two main steps. First, water molecules are adsorbed onto the membrane surface and, second, these molecules diffuse through the PDA coating and polyamide active layers [50]. This implies that the hydrophilicity and diffusion resistance of the membrane surface play major roles in water permeability through an RO membrane. The thickness of the PDA layer on the membrane surface was gradually increased with increasing modification time. Consequently, the water diffusion resistance increased with modification time. However, the hydrophilicity of the PDA-modified membranes is almost the same as the unmodified membrane, as shown in Table 4.3. Thus, the increase in the surface layer by PDA coating increased the diffusional resistance for water permeation and decreased the water flux.

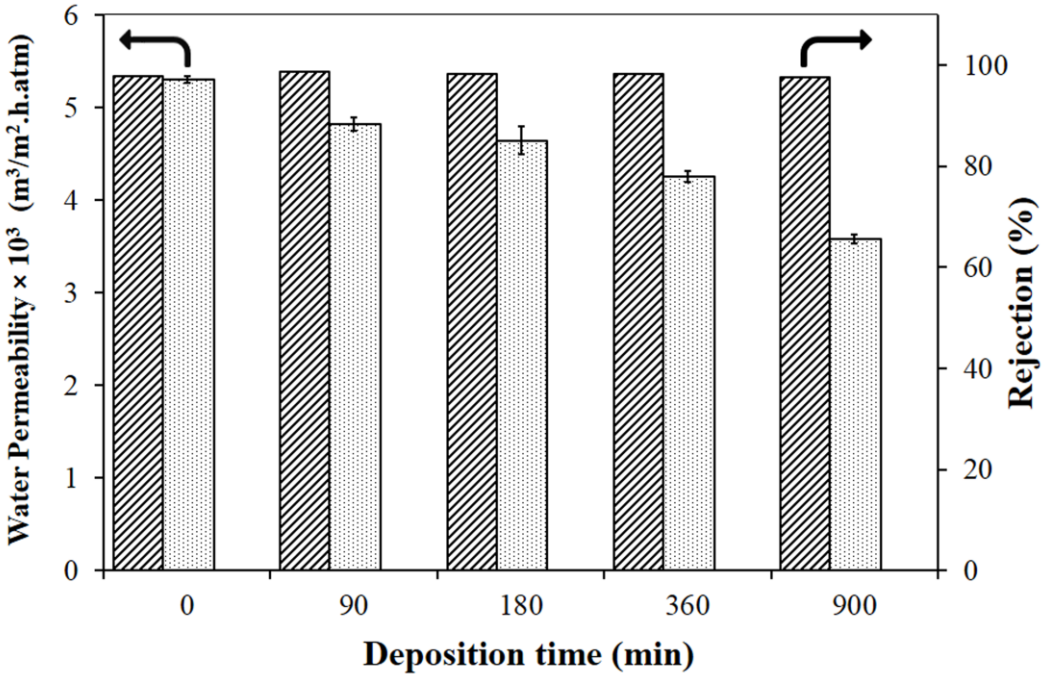

Fig. 4.6. Water permeability (⁘) and salt rejections (▨) of the unmodified membrane and the PDA-modified membranes with the different dopamine coating time. The dopamine solution contained 0.5 kg/m^3 at pH 8.8.

4.3.3. Antibiofouling evaluation

4.3.3.1. Bacteria filtration

The antibiofouling performance of the unmodified and the PDA-modified membranes was evaluated by cross-flow filtration of a bacterial suspension as described in Section 4.2.3.5.1. The filtration was continuously carried out for 1200 minutes using the bacterial suspension of (10^7- 10^8) cfu/ml as a feed solution. The water flux was initially adjusted to 2.2×10^{-2} m^3.h^{-1}.m^{-2} by controlling the transmembrane pressure difference (TMP), because this is known to affect biofouling. The results of the bacterial filtration are shown in Figs. 4.7 and 4.8. Figures 4.7 and 4.8 show the effect of modification time on the flux decline and the effect of the dopamine concentration in

the modification solution, respectively. In these figures, the water flux is shown as a normalized flux (J/J_0). Here, J is the real water flux of the bacterial suspension filtration with time and J_0 is the initial water flux.

It can be seen in Fig. 4.7 that the water flux of the unmodified membrane retained just 61% of its initial flux after 1200 minutes of bacterial filtration, while the water flux of the PDA-modified membranes retained about 80% of initial flux after 1200 minutes filtration. These results clearly show that the RO membranes modified with PDA have high antibiofouling properties.

According to Figs. 4.7 and 4.8, the progress in biofouling of the unmodified membrane can be divided into two steps. During the first step, the water flux sharply decreased, while in the second step the water decline rate is lower than during the first step. Conversely, the water flux of PDA-modified membranes decreased linearly and the flux decline rate was almost the same as that of the unmodified membrane in the second step. In addition, FE-SEM images of the membrane surface showed that numerous bacteria adsorbed and formed a biofilm on the surface of the unmodified membrane (Fig. 4.9a); however, almost no bacteria adsorbed on the surface of PDA-modified membranes (Fig. 4.9b). Thus, it is reasonable to assume that the first step of flux decline with the unmodified membrane involved the direct deposition of bacteria on the membrane surface. However, the water flux decline in the second step of the unmodified membrane was not due to the deposition, but due to the accumulation of bacteria near the membrane surface. In case of PDA-modified membranes, their antibiofouling properties prevent bacteria from depositing on the membrane surface, but bacteria accumulate near the membrane surface due to TMP.

Therefore, it was concluded that antibiofouling was improved by surface modification with PDA through the increase of antiadhesion properties, even though the hydrophilicity and negative charge density of the membrane surface were not markedly improved by PDA coating, as shown in Tables 4.3 and 4.4.

Furthermore, as shown in Fig. 4.7, the modification time barely affected the antibiofouling property. In addition, as discussed in Section 4.3.2, the modification time should be as short as possible. Therefore, 180 minutes was identified as the optimal modification time for subsequent experiments. Figure 4.8 shows that increasing the dopamine concentration did not enhance the antibiofouling performance. Thus, a 0.5 kg/m^3 dopamine concentration was identified as the concentration to use in my subsequent experiments, because there is a possibility that PDA will agglomerate in solutions with high dopamine concentrations.

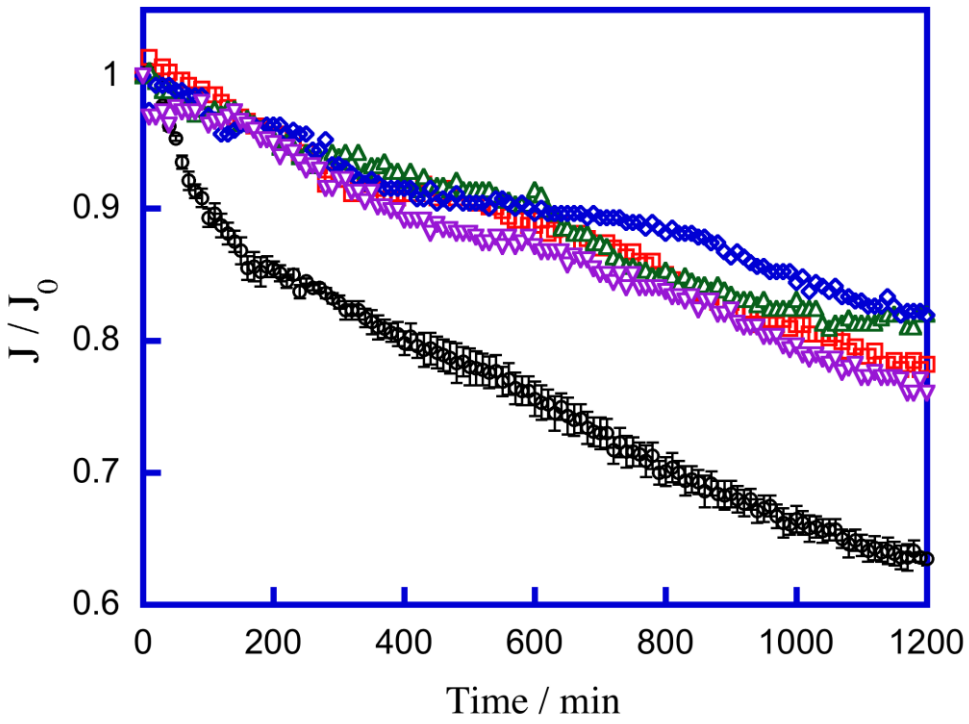

Fig. 4.7. Normalized flux of the unmodified membrane (○) and PDA-modified membranes with different dopamine modification times (minutes) (□ 90, △ 180, ◇ 900 and ▽1440) as a function of time during bacterial filtration. The membranes were modified with a 0.5 kg/m^3 dopamine solution at pH 8.8. The bacterial concentration was (10^7- 10^8) cfu/ml.

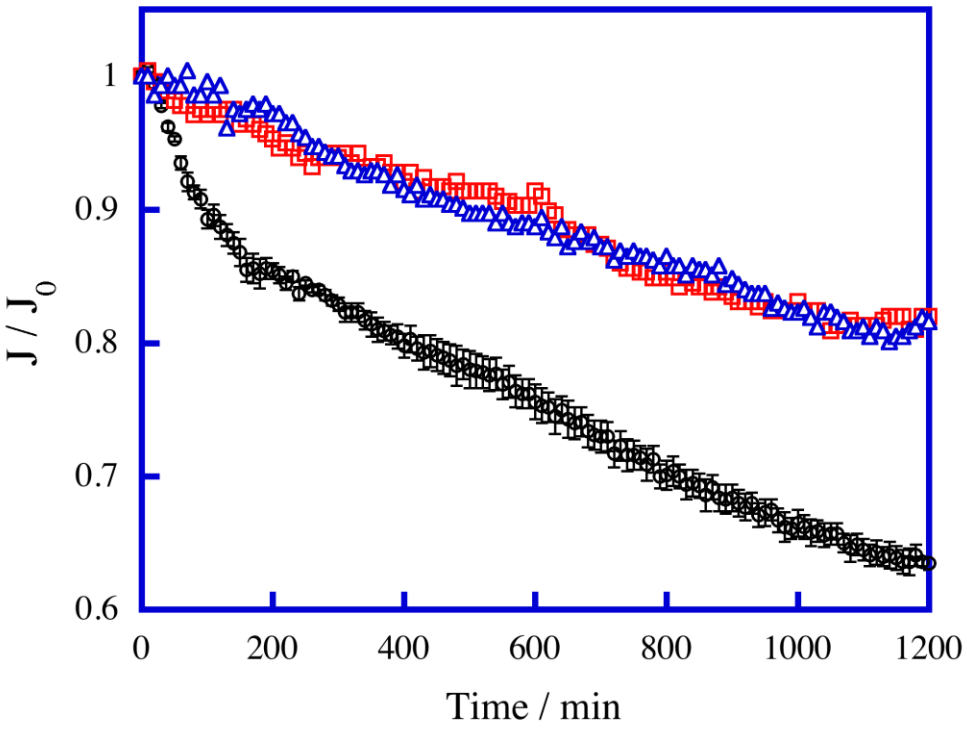

Fig. 4.8. Normalized flux of the unmodified membrane (○) and PDA-modified membranes with different dopamine concentrations (□ 0.5 and △ 2 kg/m^3) as a function of time during bacterial filtration. The membranes were modified for 180 minutes at pH 8.8. The bacterial concentration was (10^7- 10^8) cfu/ml.

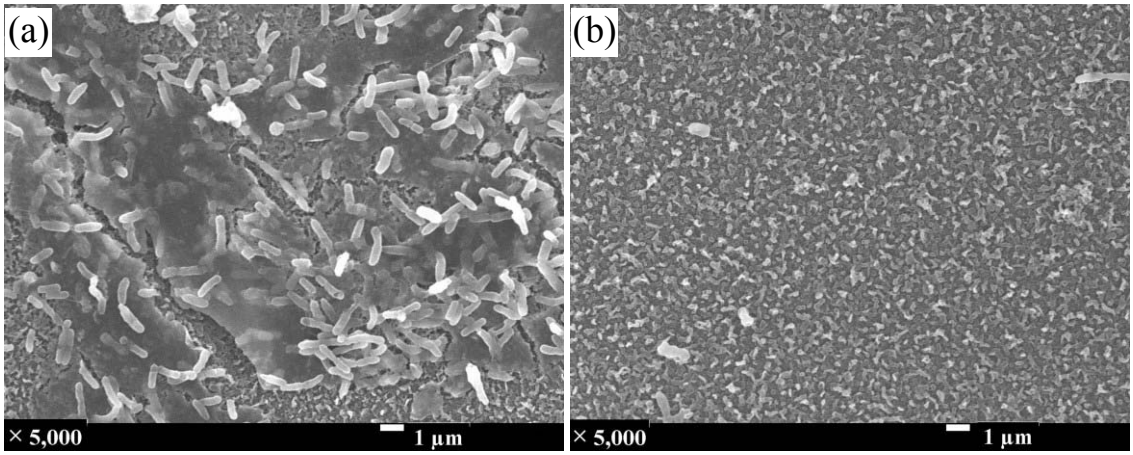

Fig. 4.9. FESEM images of the unmodified membrane surface (a) and PDA-modified membrane surface (b) after 1200 minutes bacterial filtration shown in Fig.4.9. The membrane was modified with a 0.5 kg/m^3 dopamine solution for 180 minutes at pH 8.8.

4.3.3.2. Static adhesion test

For further clarification of bacterial adhesion, the antiadhesion properties of the unmodified and PDA-modified membranes (with 0.5 kg/m^3 dopamine solution for 24 hours at pH 8.8) against bacteria were evaluated using a static adhesion test, as described in Section 4.2.3.5.2. In this experiment, the membrane was modified for 24 hours to enhance the effect of PDA modification. Figure 4.10 shows the membrane surface observed by CLSM after 4 days of immersion in a bacterial suspension. *P. putida* was used for this test because it can easily form a biofilm. In this figure, the membrane surface is the black background and the green points are stained bacteria. It can be seen from Fig. 4.10 that the number of bacteria adsorbed onto the surface of the PDA-modified membrane was significantly lower than that of the unmodified membrane. Thus, it is clear that the antiadhesion property of the membrane was markedly improved by PDA coating and thus, the antibiofouling property was improved.

It is well known that organic fouling and biofouling are reduced by improving hydrophilicity and increasing negative charge density [6-8]. However, the hydrophilicity and negative surface charge density were not noticeably increased as shown in Tables 4.3 and 4.4. It means that the improvement of adhesion property by PDA coating is not due to the improvement of hydrophilicity and negative charge density, but due to other factors. Thus, we attempted to evaluate bactericidal properties of PDA modified membrane. If the PDA modified membrane has the bactericidal properties, the number of live bacteria will be reduced and, as a result, the bacteria adhesion is reduced.

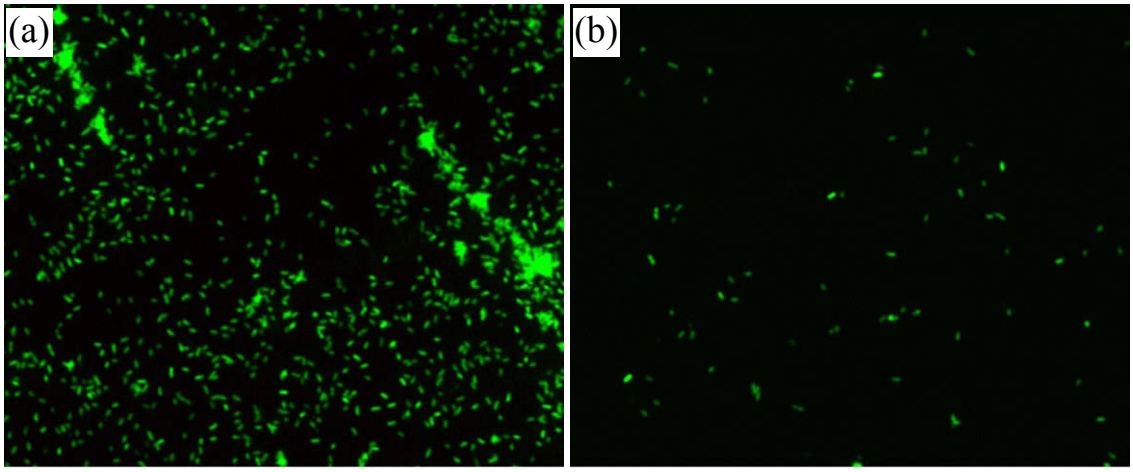

Fig. 4.10. CLSM images of (a) unmodified membrane, (b) PDA-modified membrane after 4 days of immersion in a bacterial (*P. putida)* suspension. The membrane was modified with a 0.5 kg/m^3 dopamine solution for 24 hours at pH 8.8. The black background is the membrane surface and green points are stained viable bacteria.

4.3.3.3. Antibacterial property

Another possibility to improve the antibiofouling is through improvement of antibacterial properties. The bactericidal ratio (sterilization ratio) was measured by the shake flask test to evaluate the antibacterial property for unmodified and PDA-modified membranes. This experiment was carried out using *E.coli* as a model Gram-negative bacterium, because it is more resistant against antibacterial agents than the *P. putida*, as described in Section 4.2.3.5.3. It was impossible to evaluate the bactericidal ratio correctly in a pH range lower than 6, because the number of surviving bacteria was too low. In addition the growth rate of *E. coli* drastically decreases above pH 8 [14]. Thus, the bactericidal ratio was evaluated between pH 6 and 7.5.

In this experiment, the membrane was modified with a 0.5 kg/m^3 dopamine solution at pH 8.8 for 24 hours to enhance the effect of PDA modification. The

bactericidal ratios were calculated with Eq. (2) and are shown in Table 4.5. The bactericidal ratio of unmodified membrane is zero, even though bacteria easily adsorb on the unmodified membrane as shown in Figs. 4.9 and 4.10. It means that the assumption for bactericidal experiment that is "the bacteria adsorption on membranes does not affect the bactericidal ratio" is clearly satisfied in this experiment. Thus, Table 4.5 shows the correct bactericidal property of PDA modified membrane. The bactericidal ratio of the PDA-modified membrane was 29 ± 8 % at pH 7.5 and 46 ± 3 % at pH 6. These results reveal that PDA coating conveys an antibacterial property, although these values are not high in comparison with silver nanoparticles or $Cu(OH)_2$ particles (i.e., > 90%).

Because PDA is amphoteric, with an isoelectric point of around pH 4 [47, 48], -OH groups dissociate to $-O^-$ and >NH to $>NH_2^+$ depending on pH (refer to Fig. 4.5). Even though the total charge of membrane surface is negative at pH >4, there are protonated amine groups in PDA. It was supposed that the protonated amine groups might cause the antibacterial property, because it is known that positively charged functional groups can cause bacteria lysis by contacting the cell wall of bacteria [15, 38]. The pK_b of amine groups of PDA was reported to be 5.3 [48], so the dissociation degree (protonation degree), α, of PDA is expressed by Eq. (3), where K_b is the base dissociation constant. Therefore, the protonation degree at pH 7.5 was obtained as 94% and almost 100% at pH 6 with Eq. (3).

$$\alpha = \left(\frac{10^{(14-pH-pK_b)}}{1+10^{(14-pH-pK_b)}}\right)\times 100 \qquad (3)$$

The change in α of amino groups is qualitatively consistent with the change in bactericidal ratio shown in Table 4.5. Thus, the antibacterial property of PDA modified membrane would be attributed to the bactericidal property of protonated amine groups of PDA. This property of PDA coating might expand the future application of PDA coating.

Table 4.5 Killing ratio measured by the shaking flask test at different pH values

Sample	Killing ratio %	
	pH = 6	pH = 7.5
Unmodified RO membrane	0	0
RO membrane + PDA (0.5 kg/m^3, 24 h)	46 ± 3	29 ± 8

The improvement in antibacterial properties can indirectly improve the antiadhesion property by suppressing the number of bacteria in the feed solution. Thus, it was concluded that the improvement in antibiofouling properties of the PDA-modified membrane was mainly due to the bactericidal property of the PDA layer.

4.4. Conclusion

A commercial RO membrane was modified with PDA using various dopamine concentrations and modification times under alkaline conditions to improve antibiofouling properties. The deposition of PDA on the membrane surface was confirmed by XPS, FT-IR, FE-SEM and the change in color of PDA-modified membrane. The hydrophilicity and surface charge were not appreciably changed by surface modification with PDA. The salt rejection of PDA-modified membranes was

not also affected by modification with PDA. However, the pure water permeability was decreased, presumably because the PDA coating layer increased the resistance to water transport through the modified membrane. Dynamic bacterial filtration showed that membrane modification with PDA clearly enhanced the biofouling resistance of RO membranes. Also, a static adhesion test showed an improvement in the bacterial adhesion resistance. Moreover, by shake flask tests, we demonstrated that the PDA coating layer had good antibacterial properties. The pH dependence of the antibacterial property proved that the bactericidal property of protonated amine groups in PDA contributed to the antibacterial property of the PDA layer. According to the results described above, modification with a 0.5 kg/m^3 dopamine solution for 180 minutes at pH 8.8 was sufficient to impart a high antibiofouling property to an RO membrane by surface modification with PDA.

References

[1] R. Bernstein, S. Belfer, V. Freger, Bacterial Attachment to RO Membranes Surface-Modified by Concentration-Polarization-Enhanced Graft Polymerization, Environmental Science & Technology, 45 (2011) 5973-5980.

[2] T.R. Bott, Industrial Biofouling, Elsevier, 2011.

[3] C.X. Liu, D.R. Zhang, Y. He, X.S. Zhao, R. Bai, Modification of membrane surface for anti-biofouling performance: Effect of anti-adhesion and anti-bacteria approaches, Journal of Membrane Science, 346 (2010) 121-130.

[4] H. Karkhanechi, F. Razi, I. Sawada, R. Takagi, Y. Ohmukai, H. Matsuyama, Improvement of antibiofouling performance of a reverse osmosis membrane through biocide release and adhesion resistance, Separation and Purification Technology, 105 (2013) 106-113.

[5] Z. Li, D. Lee, X. Sheng, R.E. Cohen, M.F. Rubner, Two-Level Antibacterial Coating with Both Release-Killing and Contact-Killing Capabilities, Langmuir, 22 (2006) 9820-9823.
[6] C. Hobbs, S. Hong, J. Taylor, Effect of surface roughness on fouling of RO and NF membranes during filtration of a high organic surficial groundwater, Aqua- Journal of Water Supply: Research and Technology, 55 (2006) 559.
[7] J.S. Louie, I. Pinnau, I. Ciobanu, K.P. Ishida, A. Ng, M. Reinhard, Effects of polyether–polyamide block copolymer coating on performance and fouling of reverse osmosis membranes, Journal of Membrane Science, 280 (2006) 762-770.
[8] W. Lee, C.H. Ahn, S. Hong, S. Kim, S. Lee, Y. Baek, J. Yoon, Evaluation of surface properties of reverse osmosis membranes on the initial biofouling stages under no filtration condition, Journal of Membrane Science, 351 (2010) 112-122.
[9] C. Zhao, X. Cao, M. Tang, F. Liu, Y. Nie, Immobilization of silver nanoparticles onto sulfonated polyethersulfone membranes as antibacterial materials, Colloids and Surfaces B: Biointerfaces, 81 (2010) 555-562.
[10] I. Sawada, R. Fachrul, T. Ito, Y. Ohmukai, T. Maruyama, H. Matsuyama, Development of a hydrophilic polymer membrane containing silver nanoparticles with both organic antifouling and antibacterial properties, Journal of Membrane Science, 387–388 (2012) 1-6.
[11] Z. Su, X. Zan, Polyelectrolyte multilayer films containing silver as antibacterial coatings, Thin Solid Films, 518 (2010) 5478-5482.
[12] Y. Deng, C. Dong, J. Cairney, Q. Sun, O.L. Maddan, G. He, Investigation of $Mg(OH)_2$ nanoparticles as an antibacterial agent, Journal of Nanoparticle Research, 12 (2009) 2101-2109.
[13] C. Dong, D. Song, J. Cairney, O.L. Maddan, G. He, Y. Deng, Antibacterial study of Mg(OH)2 nanoplatelets, Materials Research Bulletin, 46 (2011) 576-582.
[14] H. Karkhanechi, R. Takagi, Y. Ohmukai, H. Matsuyama, Enhancing the antibiofouling performance of RO membranes using Cu(OH)2 as an antibacterial agent, Desalination, 325 (2013) 40-47.
[15] F. Razi, I. Sawada, Y. Ohmukai, T. Maruyama, H. Matsuyama, Surface functionalization by grafting of (2-dimethylamino)ethyl methacrylate methyl chloride

quaternary salt (DMAEMAq) onto hollow fiber polyethersulfone (PES) membranes for improvement of antibiofouling properties, Solvent Extr. Res. Dev, 19 (2012) 101-115.
[16] K. Ishihara, Bioinspired phospholipid polymer biomaterials for making high performance artificial organs, Science and Technology of Advanced Materials, 1 (2000) 131-138.
[17] F. Razi, I. Sawada, Y. Ohmukai, T. Maruyama, H. Matsuyama, The improvement of antibiofouling efficiency of polyethersulfone membrane by functionalization with zwitterionic monomers, Journal of Membrane Science, 401–402 (2012) 292-299.
[18] H. Lee, S.M. Dellatore, W.M. Miller, P.B. Messersmith, Mussel-Inspired Surface Chemistry for Multifunctional Coatings, Science, 318 (2007) 426-430.
[19] M. Vaselbehagh, H. Karkhanechi, S. Mulyati, R. Takagi, H. Matsuyama, Improved antifouling of anion-exchange membrane by polydopamine coating in electrodialysis process, Desalination, 332 (2014) 126-133.
[20] B.D. McCloskey, H.B. Park, H. Ju, B.W. Rowe, D.J. Miller, B.J. Chun, K. Kin, B.D. Freeman, Influence of polydopamine deposition conditions on pure water flux and foulant adhesion resistance of reverse osmosis, ultrafiltration, and microfiltration membranes, Polymer, 51 (2010) 3472-3485.
[21] S. Kasemset, A. Lee, D.J. Miller, B.D. Freeman, M.M. Sharma, Effect of polydopamine deposition conditions on fouling resistance, physical properties, and permeation properties of reverse osmosis membranes in oil/water separation, Journal of Membrane Science, 425-426 (2013) 208-216.
[22] S. Azari, L. Zou, Using zwitterionic amino acid l-DOPA to modify the surface of thin film composite polyamide reverse osmosis membranes to increase their fouling resistance, Journal of Membrane Science, 401-402 (2012) 68-75.
[23] Z.-Y. Xi, Y.-Y. Xu, L.-P. Zhu, Y. Wang, B.-K. Zhu, A facile method of surface modification for hydrophobic polymer membranes based on the adhesive behavior of poly(DOPA) and poly(dopamine), Journal of Membrane Science, 327 (2009) 244-253.
[24] L.-P. Zhu, J.-H. Jiang, B.-K. Zhu, Y.-Y. Xu, Immobilization of bovine serum albumin onto porous polyethylene membranes using strongly attached polydopamine as a spacer, Colloids and Surfaces B: Biointerfaces, 86 (2011) 111-118.

[25] J.-H. Jiang, L.-P. Zhu, X.-L. Li, Y.-Y. Xu, B.-K. Zhu, Surface modification of PE porous membranes based on the strong adhesion of polydopamine and covalent immobilization of heparin, Journal of Membrane Science, 364 (2010) 194-202.
[26] L.-P. Zhu, J.-Z. Yu, Y.-Y. Xu, Z.-Y. Xi, B.-K. Zhu, Surface modification of PVDF porous membranes via poly(DOPA) coating and heparin immobilization, Colloids and Surfaces B: Biointerfaces, 69 (2009) 152-155.
[27] H. Lee, N.F. Scherer, P.B. Messersmith, Single-molecule mechanics of mussel adhesion, Proceedings of the National Academy of Sciences, 103 (2006) 12999-13003.
[28] M.E. Lynge, R. van der Westen, A. Postma, B. Stadler, Polydopamine-a nature-inspired polymer coating for biomedical science, Nanoscale, 3 (2011) 4916-4928.
[29] L.A. Bereschenko, G.H.J. Heilig, M.M. Nederlof, M.C.M. van Loosdrecht, A.J.M. Stams, G.J.W. Euverink, Molecular Characterization of the Bacterial Communities in the Different Compartments of a Full-Scale Reverse-Osmosis Water Purification Plant, Applied and Environmental Microbiology, 74 (2008) 5297-5304.
[30] C. Foppoli, R. Coccia, C. Cini, M.A. Rosei, Catecholamines oxidation by xanthine oxidase, Biochimica et Biophysica Acta (BBA) - General Subjects, 1334 (1997) 200-206.
[31] Y. Liao, R. Wang, A.G. Fane, Engineering superhydrophobic surface on poly(vinylidene fluoride) nanofiber membranes for direct contact membrane distillation, Journal of Membrane Science, 440 (2013) 77-87.
[32] J. Jiang, L. Zhu, L. Zhu, B. Zhu, Y. Xu, Surface Characteristics of a Self-Polymerized Dopamine Coating Deposited on Hydrophobic Polymer Films, Langmuir, 27 (2011) 14180-14187.
[33] D.R. Dreyer, D.J. Miller, B.D. Freeman, D.R. Paul, C.W. Bielawski, Elucidating the Structure of Poly(dopamine), Langmuir, 28 (2012) 6428-6435.
[34] W. Wang, R. Li, M. Tian, L. Liu, H. Zou, X. Zhao, L. Zhang, Surface Silverized Meta-Aramid Fibers Prepared by Bio-inspired Poly(dopamine) Functionalization, ACS Applied Materials & Interfaces, 5 (2013) 2062-2069.
[35] R.W. Field, D. Wu, J.A. Howell, B.B. Gupta, Critical flux concept for microfiltration fouling, Journal of Membrane Science, 100 (1995) 259-272.

[36] D.J. Miller, S. Kasemset, L. Wang, D.R. Paul, B.D. Freeman, Constant flux crossflow filtration evaluation of surface-modified fouling-resistant membranes, Journal of Membrane Science, 452 (2014) 171-183.
[37] X. Zhu, R. Bai, K.-H. Wee, C. Liu, S.-L. Tang, Membrane surfaces immobilized with ionic or reduced silver and their anti-biofouling performances, Journal of Membrane Science, 363 (2010) 278-286.
[38] V. Kochkodan, S. Tsarenko, N. Potapchenko, V. Kosinova, V. Goncharuk, Adhesion of microorganisms to polymer membranes: a photobactericidal effect of surface treatment with TiO2, Desalination, 220 (2008) 380-385.
[39] T. Urquidy, O. Hernando, Copper Resistant Bacteria Better Tolerate Commercially Available Antimicrobial Treatments Based in Silver and Silver–Copper ions, The University of Arizona, Dissertation (2011).
[40] A. Nguyen, S. Azari, L. Zou, Coating zwitterionic amino acid l-DOPA to increase fouling resistance of forward osmosis membrane, Desalination, 312 (2013) 82-87.
[41] G. Han, S. Zhang, X. Li, N. Widjojo, T.-S. Chung, Thin film composite forward osmosis membranes based on polydopamine modified polysulfone substrates with enhancements in both water flux and salt rejection, Chemical Engineering Science, 80 (2012) 219-231.
[42] C. Cheng, S. Li, W. Zhao, Q. Wei, S. Nie, S. Sun, C. Zhao, The hydrodynamic permeability and surface property of polyethersulfone ultrafiltration membranes with mussel-inspired polydopamine coatings, Journal of Membrane Science, 417-418 (2012) 228-236.
[43] C.Y. Tang, Y.-N. Kwon, J.O. Leckie, Probing the nano- and micro-scales of reverse osmosis membranes—A comprehensive characterization of physiochemical properties of uncoated and coated membranes by XPS, TEM, ATR-FTIR, and streaming potential measurements, Journal of Membrane Science, 287 (2007) 146-156.
[44] S.M. Kang, J. Rho, I.S. Choi, P.B. Messersmith, H. Lee, Norepinephrine: Material-Independent, Multifunctional Surface Modification Reagent, Journal of the American Chemical Society, 131 (2009) 13224-13225.

[45] Y. Liao, Y. Wang, X. Feng, W. Wang, F. Xu, L. Zhang, Antibacterial surfaces through dopamine functionalization and silver nanoparticle immobilization, Materials Chemistry and Physics, 121 (2010) 534-540.
[46] B. Yu, J. Liu, S. Liu, F. Zhou, Pdop layer exhibiting zwitterionicity: a simple electrochemical interface for governing ion permeability, Chemical Communications, 46 (2010) 5900-5902.
[47] Q. Liu, B. Yu, W. Ye, F. Zhou, Highly Selective Uptake and Release of Charged Molecules by pH-Responsive Polydopamine Microcapsules, Macromolecular Bioscience, 11 (2011) 1227-1234.
[48] V. Ball, Impedance spectroscopy and zeta potential titration of dopa-melanin films produced by oxidation of dopamine, Colloids and Surfaces A: Physicochemical and Engineering Aspects, 363 (2010) 92-97.
[49] Nitto Denko Corporation, Japan, Osaka, data sheet, http://www.nittodenko.com/cn/datasheet/membrane/005/index.html
[50] R. Yang, J. Xu, G. Ozaydin-Ince, S.Y. Wong, K.K. Gleason, Surface-Tethered Zwitterionic Ultrathin Antifouling Coatings on Reverse Osmosis Membranes by Initiated Chemical Vapor Deposition, Chemistry of Materials, 23 (2011) 1263-1272.

Chapter 5

Enhanced antibiofouling of RO membranes via polydopamine coating and polyzwitterion immobilization

5.1. Introduction

Fouling, which includes organic and biofouling, is a major problem in bio-separation, artificial organs, and water and wastewater treatment [1-3]. Reverse osmosis (RO) membranes are one of the most popular water purifying materials because of their high salt rejection and permeation rates as well as their excellent chemical, thermal, and mechanical stability. However, they face fouling problems [4] that can lead to reductions in water flux, salt rejection, and membrane life time [5-7].

It is generally known that hydrophilic surfaces are less prone to fouling than hydrophobic surfaces [2, 8]. Thus, surface hydrophilization is an approach used to improve fouling resistance. Hydrophilic materials such as poly(ethylene glycol) (PEG) [9] or oligo(ethylene glycol) (OEG) [10, 11] are widely used to improve fouling resistance through hydration via hydrogen bounding. However, their antifouling properties decline during long-term application because of oxidative degradation and enzymatic cleavage [12]. Over recent years, a new type of antifouling and anti-

biofouling material, polyzwitterions (PZs), have attracted increasing attention because of their high hydration capability and consequently excellent antiadhesion properties against proteins and bacteria. Typically, PZs contain both positively and negatively charged functional groups within the same segment side chains but maintain overall charge neutrality [13]. PZs are able to bind water molecules strongly and increase the free water content around bonded water on the membrane surface. Improved fouling and biofouling resistance would be expected as a result of this high free water content [14-18]. Thus, surface modification with an ideal PZ layer is a promising approach to inhibiting the attachment of proteins or bacteria to a membrane surface.

Until now, several surface modification methods have been used to modify membrane surfaces with zwitterionic monomers or PZs, including surface-initiated atom transfer radical polymerization (ATRP) [19, 20], self-assembled monolayers (SAMs) [21], plasma-induced interfacial polymerization [22], chemical vapor deposition (CVD) [23], Layer-by-Layer (LbL) coating [5], UV-initiated grafting polymerization [24], and grafting by click chemistry [25]. In membrane engineering group of Kobe University, the antifouling properties of hollow fiber polyethersulfone (PES) membranes were improved by functionalizing the PES membrane with zwitterionic monomers using UV irradiation-induced graft polymerization [24]. The zwitterionic monomers used for grafting were 2-(methacryloyloxy)ethyl-dimethyl-(3-sulfopropyl) ammonium hydroxide (MEDSAH) and 2-(methacryloyloxy)ethyl phosphorylcholine (MPC). In the second chapter, it was shown that the active layer of an RO membrane modified with a copolymer of MPC and 2-aminoethyl methacrylate (AEMA) (MPC-co-AEMA) by the LbL method to improve antibiofouling properties [5].

However, existing methods for using zwitterionic monomers or PZ have shortcomings, such as low stability, complexity, and difficulty in scale up [25]. In addition, zwitterionic monomers and PZs are expensive chemicals. Thus, from a commercial point of view, an ideal modification method should be efficient and easy to control and scale up. In addition, the coated PZ layer must be stable and durable during storage and water treatment.

Application of a precursor layer is a technique used in surface modification to change substrate properties for further modification [26, 27]. A polydopamine (PDA) coating is a precursor layer that is used for surface modification. The polar groups in a PDA coating, such as hydroxyl and amine groups, improve the hydrophilicity, antifouling, and antibiofouling properties of a substrate [28-30]. Moreover, a PDA layer containing reactive groups endows a versatile platform for further surface functionalization and immobilization [28, 31]. Silver immobilization using a PDA coating as a precursor layer has been reported [32-34]. In addition, it was reported that hydrophobic poly(vinyl fluoride) (PVDF) and polyethylene (PE) membrane surfaces were initially modified by a PDA coating to enable covalent immobilization heparin [31, 35]. In another attempt, Zhu et al. immobilized bovine serum albumin (BSA) onto porous PE membranes using a PDA coating as a precursor layer [28].

In chapter 4, a commercial RO membrane was modified with a PDA coating to improve its antibiofouling properties [30]. The modification conditions, such as dopamine concentration and deposition time, were then optimized. In addition, a cross-flow bacterial suspension filtration and shake flask test showed that the PDA coating markedly improved anti-adhesion and antibacterial properties. In this chapter, I attempt

to enhance the antibiofouling properties of a PDA-modified membrane through a PZ (MPC-co-AEMA) immobilization. It was expected that the PZ would be covalently immobilized on the PDA surface and that the PZ layer would show a high stability compared with modification without using the PDA precursor layer.

5.2. Experimental

5.2.1. Materials

ES-20 (Nitto Denko, Osaka, Japan) was used as an RO membrane. This is an ultra-low pressure RO membrane with an aromatic polyamide selective layer. The nominal value of rejection in company catalogue is 99.7% for 0.05% NaCl. NaCl (Wako Pure Chem. Ind., Osaka, Japan) was used as an electrolyte. Glutaraldehyde, ethanol, and [bis(trimethylsilyl)amine] (Wako Pure Chem. Ind.) were used in antiadhesion experiments. Dopamine hydrochloride (Sigma-Aldrich, St. Louis, MO, USA) was used for surface modification of the RO membrane. A 2-(methacryloyloxy)ethyl phosphorylcholine (MPC) copolymer with 2-aminoethyl methacrylate (AEMA) (MPC-co-AEMA) was kindly provided by NOF Corporation (Tokyo, Japan), and used as the PZ. The weight average of molecular weight was 9.7×10^5 [36] and the molar ratio of MPC to AEMA was 9:1. The chemical structure of dopamine and MPC-co-AEMA is illustrated in Fig. 5.1. Tryptic Soya Broth (TSB) (Becton, Dickinson and Company, Franklin Lakes, USA) was used to provide nutrient agents. *Pseudomonas putida (P.putida)* (NBRC100650) (Biological Resource Center at the National Institute of Technology and Evaluation, Shibuya, Japan) was used as a model Gram-negative

bacterium. Milli-Q water (18.2 MΩ·cm) (Millipore, Billerica, MA, USA) was used to prepare all solutions and for rinsing.

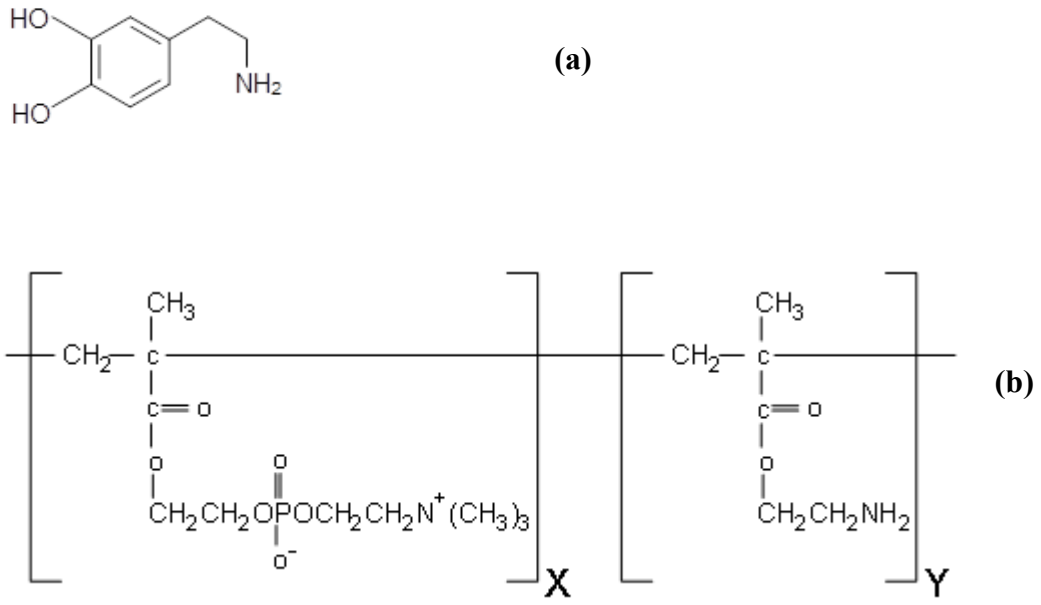

Fig. 5.1. Chemical structures of (a) dopamine and (b) MPC-co-AEMA; X:Y = 9:1.

5.2.2. Membrane modification

The RO membrane was modified with dopamine. The dopamine solutions were prepared by dissolving 0.5 kg/m^3 of the dopamine hydrochloride in 15 mM Tris-HCl buffer (pH 8.8). Dopamine spontaneously polymerizes and forms PDA by contacting with oxygen in an alkaline aqueous solution [37]. Figure 5.2 shows a mechanism for dopamine oxidative self-polymerization [33, 38-41]. A membrane was fixed to a customized fixture [1] so that only the active layer was exposed to the dopamine aqueous solution. The fixture was horizontally placed in a beaker containing 600 mL of dopamine solution and then the solution was thoroughly stirred for 3 hours at 28°C. The dopamine concentration and modification time were optimized in chapter 4 [30]. After

modification, the membrane was removed from the beaker and rinsed three times with fresh water. To remove excess or weakly bound PDA from the membrane surface, the modified membrane was immersed in 25% (v/v) isopropyl alcohol (IPA) for 10 min. The membrane was then thoroughly rinsed with Milli-Q water for one day.

PZ solution was prepared by dissolving 1 kg/m^3 of MPC-co-AEMA and 0.5 M NaCl as a PZ and supporting electrolyte, respectively, in 15 mM Tris-HCl buffer (pH 8.8). A layer of PZ was then deposited onto the active layer of membrane by immersing the samples for 24 hours in PZ solution. Thereafter, the membrane was thoroughly rinsed with Milli-Q water for one day.

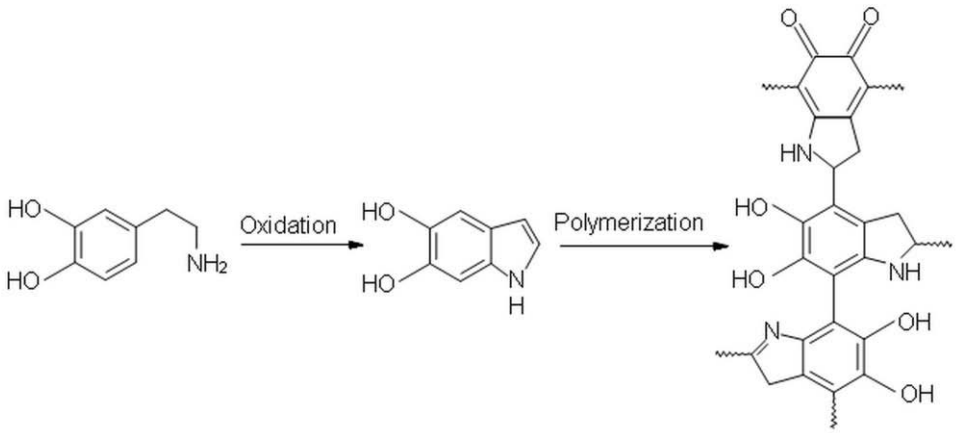

Fig. 5.2. The scheme for dopamine self-polymerization [33, 38]

5.2.3. Characterization

5.2.3.1. X-ray photoelectron spectroscopy

The chemical compositions of unmodified and modified membrane surfaces were analyzed by X-ray photoelectron spectroscopy (XPS). XPS measurements were carried out with an ESCA-850 spectrometer (Shimadzu Co., Kyoto, Japan). The sample surface

was irradiated by Mg Kα radiation, generated at 8 kV and 30 mA. The membranes were dried in a freeze dryer (FDU-1200 EYELA; Tokyo Rikakikai Co. Ltd., Tokyo, Japan) overnight prior to XPS measurements.

5.2.3.2. Surface Morphology

The surface morphology of the unmodified and modified membranes after bacterial suspension filtration was observed using a field emission scanning electron microscope (FE-SEM, JSF-7500F; JEOL Co. Ltd., Tokyo, Japan) with an accelerating voltage of 5 kV. The bacteria were fixed on the membrane surface as described in Section 5.2.3.5. The membranes were then dried overnight in a freeze dryer in the same way as described in Section 5.2.3.1, then coated with osmium tetroxide (OsO_4) prior to FE-SEM measurements. A thin OsO_4 layer (ca. 5 nm) was formed using an osmium coater (Neoc-STB; MEIWAFOSIS Co. Ltd., Tokyo, Japan).

5.2.3.3. Air Contact angle and ζ-potential of membrane surface

The hydrophilicity of the membrane was evaluated by air contact angle using a contact angle meter (Drop Master 300, Kyowa Interface Science Co. Ltd., Niiza, Japan). Membrane samples were horizontally immersed into Milli-Q water facing the active layer down. Air bubble was attached onto the active layer using a micro liter syringe equipped with a J-hook needle, and then the contact angle was measured. The static contact angle was measured at least10 times for each sample and then the mean value was calculated.

A surface charge density was evaluated by a ζ-potential, since the ζ-potential reflected the surface charge density. The ζ-potential of the membrane surface was obtained from a streaming potential measurement using an ELS-4000K instrument (Otsuka Electronics, Osaka, Japan) with a 0.01 M NaCl solution (pH 5.9) at room temperature.

5.2.3.4. Water permeability and salt rejection

The laboratory-scale cross-flow membrane test unit shown in Fig. 5.3 was used to measure the salt rejection and water permeability of the unmodified and PDA-modified membranes. An aqueous solution of 0.05 wt% NaCl was fed at a flow rate 1.0×10^{-6} m^3/min at 25°C and applied pressure of 0.75 MPa. The effective membrane area was 7.5×10^{-4} m^2 with the diameter of 3.1×10^{-2} m. The volume of membrane cell for this setup was 1.6×10^{-5} m^3. The feed side of the membrane was stirred at 400 rpm by a magnetic stirrer [1, 5]. The NaCl rejection, R_{obs}, was calculated using Eq. (1). The NaCl concentration was determined from a conductance measurement (CM-30R, DKK-TOA Corporation, Tokyo, Japan) using a calibration curve between concentration and conductivity.

$$R_{obs} = (1 - \frac{2C^{p}_{NaCl}}{(C^{r}_{NaCl} + C^{f}_{NaCl})}) \times 100 \qquad (1)$$

where, C^{p}_{NaCl}, C^{r}_{NaCl} and C^{f}_{NaCl} indicate the NaCl concentrations in the permeate, retentate, and feed, respectively. Generally, R_{obs} is calculated using not (+)/2, but . However, is higher than . It means that there is a concentration

gradient between the inlet and the outlet of cell. Then, I evaluated R_{obs} using $(C^{r}_{NaCl}+C^{f}_{NaCl})/2$ as an average concentration in the flow cell.

The water permeability ($m^3 \cdot m^{-2} \cdot h^{-1} \cdot atm^{-1}$) was obtained from the volume of permeated water accumulated with time. The mass of permeate was measured using an analytical balance and recorded by computer connected to the balance.

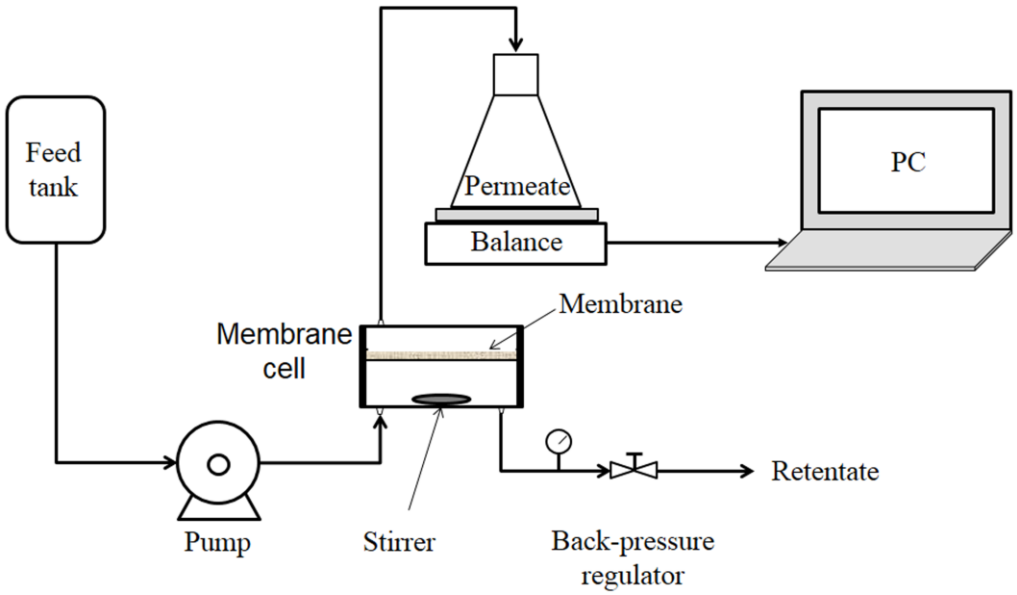

Fig. 5.3. Diagram of the cross-flow setup.

5.2.3.5. Biofouling potential- Filtration experiment with a bacterial suspension

The time course of water flux through the unmodified and modified membranes was measured by cross-flow filtration of a bacterial suspension to evaluate the antibacterial potential. In addition, bacterial adhesion to the membrane surface was observed by FE-SEM after 1200 minutes filtration. This filtration experiment was carried out using the laboratory-scale apparatus shown in Fig. 5.3. The system was cleaned with bleach solution (250 mg/l of NaClO) for 30 minutes to disinfect the system

prior to each filtration. The system was then rinsed for at least 1 hour with Milli-Q water. Because the water flux affects the progress of biofouling [30], the initial flux of all membranes was adjusted to 2.2×10^{-2} $m^3.h^{-1}.m^{-2}$ by controlling the trans-membrane pressure difference (TMP). A bacterial suspension of *P. putida* was used as the feed solution. *P. putida* was first cultured in TSB medium overnight and then diluted in sterilized NaCl (850 g/m^3). The final concentrations of *P. putida* in the bacterial suspensions for all filtration experiments were closely similar. The optical density of all bacterial suspensions was measured prior to filtration and the average was 0.112 at 660 nm wavelength.

After 1200 min of bacterial suspension filtration, the bacteria attached on the membrane surface were observed by FE-SEM, as described in Section 5.2.3.2. After the bacterial suspension filtration test, the membrane samples were thoroughly washed with phosphate buffered saline (PBS) solution (pH 7.5), and then the bacteria on the membrane surface were fixed by dipping the membrane into a 2.5 v/v % glutaraldehyde PBS solution for 4 hours at 4°C. After fixation, the membranes were rinsed with PBS to remove residual glutaraldehyde from the surfaces. To reduce the water content of the membrane samples, they were then dehydrated with ethanol. Dehydrations steps were performed by immersing each of the membrane samples into 50, 70, 90, and 99.5% ethanol solutions for 10 minutes in series, followed by immersion into a 99.5% ethanol solution for 10 minutes twice. Finally, the membrane samples were immersed in [bis(trimethylsilyl)amine] solution for 1 minute to coat them to avoid water adsorption, dried in air, and then stored in a desiccator. The dried membrane samples were used in FE-SEM observations.

To evaluate the stability of modified membranes during storage, the membranes modified with PDA and/or PZ were immersed into 2 M NaCl aqueous solution for one month. After one month immersion, their antibiofouling potentials were evaluated by cross-flow filtration of bacterial suspensions for 1200 minutes, as described above. The stability during storage will also reflect the stability during filtration.

5.3. Results and discussion

5.3.1. Surface characterization

5.3.1.1. Analysis of membrane chemical composition

To determine the chemical composition of unmodified and modified membrane surfaces, XPS analysis was carried out. The results are shown in Table 5.1. The C:N and C:O ratios for the unmodified membrane were 6.4 and 4.4, respectively, in agreement with the typical composition of aromatic polyamide membranes [42]. The measured values of C1s for the unmodified membrane and the theoretical value for dopamine are similar, at about 72%. However, their N1s values differ. Thus, N1s content was the main criterion used to confirm the deposition of PDA. The C:N ratio was increased from 6.4 to 9.2 after the PDA coating, which could be attributed to PDA deposition on the membrane surface.

For the membranes modified with PZ, a large peak due to phosphorus was detected at around 134 eV (Fig. 5.4a). This peak is attributed to the phosphorus element in the PZ structure (refer to Fig. 5.1b). Moreover, high-resolution XPS spectra for the N1s component showed a single strong band at 400 eV that was assigned to the amide N from the unmodified membrane structure, while a band at around 402.5 eV referred to

a quaternary nitrogen [5] (Fig. 5.4b) and the latter band became stronger when the membrane was modified with MPC-co-AEMA layers (Fig. 5.4c). The percentages of each peak at 400 and at 402.5 eV are shown in Table 5.1. The phosphorus peak and the increase in the peak at around 402.5 eV implied the successful deposition of PZ onto the membrane surface.

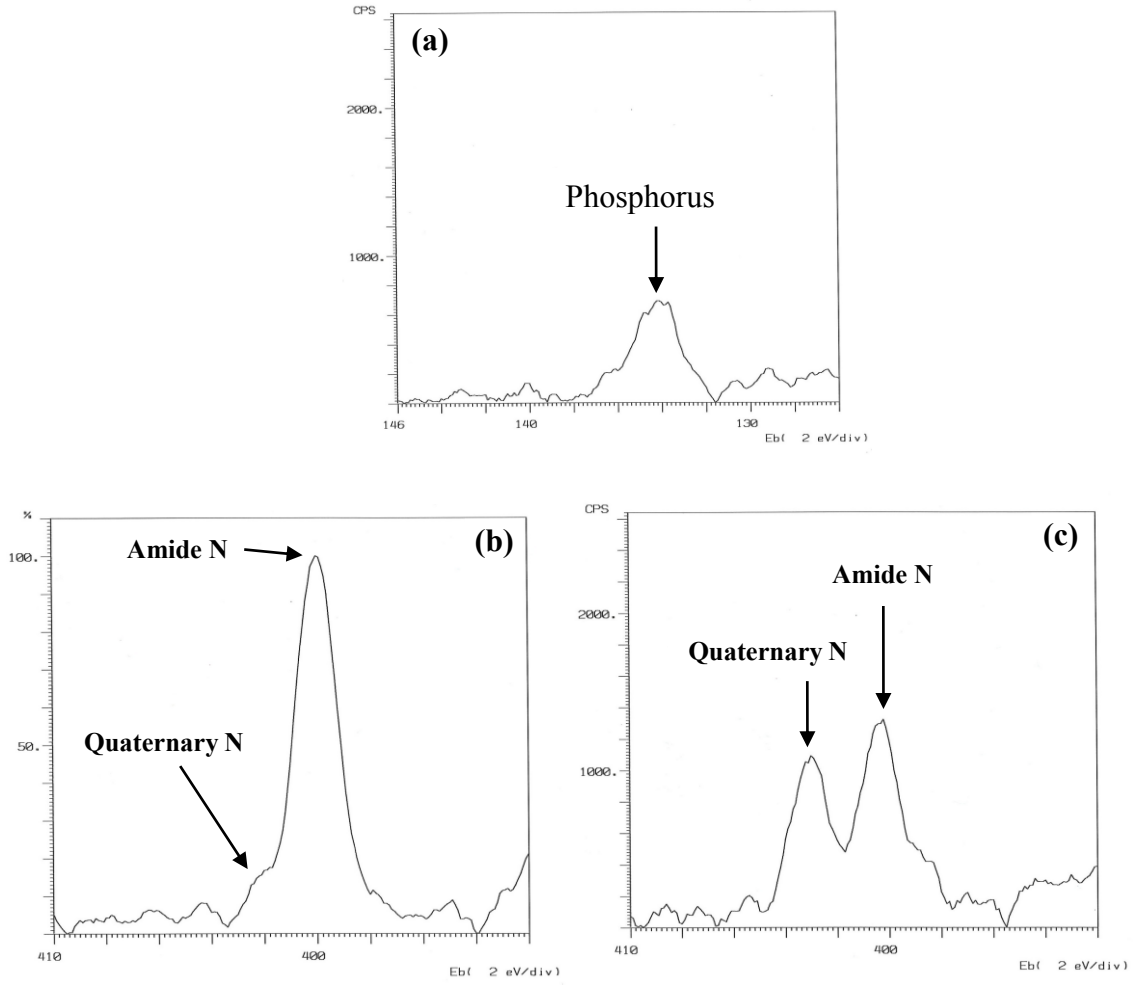

Fig. 5.4. The high-resolution XPS spectra for (a) P2p of PZ immobilized RO membrane, (b) N1s of unmodified membrane and (c) N1s of PZ immobilized RO membrane.

In addition, a quantitative comparison of the phosphorus and quaternary nitrogen components presented in Table 5.1 show that the amount of PZ deposited on the PDA-

modified membrane was higher than on the unmodified membrane. This difference can probably be attributed to different deposition mechanisms. The quinine species in PDA coatings are able to bond with the amine groups of PZ and thus PZ is probably covalently immobilized onto the PDA-modified membrane. Figure 5.5 shows the scheme for PZ immobilization on a PDA-modified substrate as speculated in the literature [31, 35]. However, the PZ layer on the unmodified membrane would be predominantly electrostatically and/or physically adsorbed onto the membrane surface.

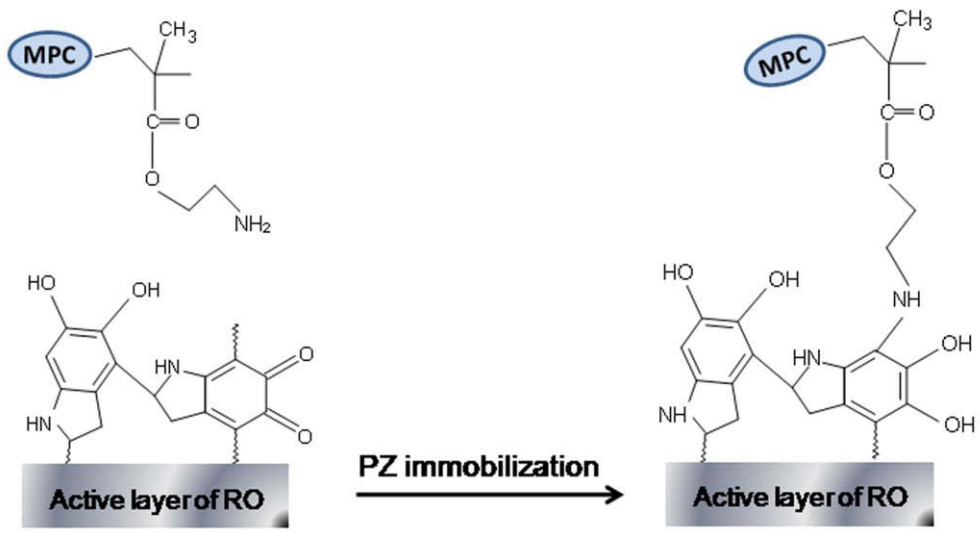

Fig. 5.5. The scheme for PZ immobilization on a PDA-modified RO membrane.

Table 5.1. Chemical composition (in atomic percent) of the unmodified and PDA-modified membranes, measured by high-resolution XPS.

Membrane	C1s	N1s	O1s	P2p	C:N	C:O	N, % of total N	
							400 eV	402.5 eV
Unmodified RO	72.2	11.3	16.5	0.0	6.4	4.4	98.5	1.5
Dopamine (theoretic value)	72.7	9.1	18.2	0.0	8.0	4.0	-	-
RO + PDA	71.5	7.8	20.7	0.0	9.2	3.5	91.5	8.6
RO + PDA+ MPC-co-AEMA	64.5	6.4	25.5	3.7	10.1	2.5	51.9	48.1
RO + MPC-co-AEMA	66.4	7.4	23.4	2.8	9.0	2.8	67.8	32.2

5.3.1.2. Effect of modification on air contact angle and surface charge

The hydrophilicity of the membrane surface is usually evaluated by water or air contact angles. In this study, the hydrophilicity was evaluated through the air contact angle as described in Section 5.2.3.3, because the RO membrane is always used in contact with water. An increase in air contact angle indicates an improvement in hydrophilicity. The static air contact angles of unmodified and modified membranes are shown in Table 5.2. It has been reported that PDA and/or PZ coatings can markedly improve the hydrophilicity of a membrane surface [2, 43-45]. However, as seen in Table 5.2, the air contact angle was scarcely affected by surface modification with PDA and PZ. The change in hydrophilicity strongly depends upon the substrate involved. The surface of the unmodified membrane (i.e., RO membrane) was already highly hydrophilic because of the carboxylic acid groups in the active layer. Thus, surface modification with PDA and PZ would not significantly improve the hydrophilicity of

the RO membrane. A similar phenomenon was previously reported for an RO membrane modified with PDA [30, 46].

Table 5.2. The air contact angle and ζ-potential of the unmodified and modified membranes surfaces. The ζ-potential was measured at pH 5.9.

Membrane	Air contact angle (°)	ζ– potential (mV)
Unmodified RO	145.0 ± 0.5	-10.5 ± 0.8
RO + PDA	152.6 ± 0.4	-10.6 ± 0.9
RO + MPC-co-AEMA	146.2 ± 0.6	1 ± 2
RO + PDA+ MPC-co-AEMA	147.0 ± 0.5	0 ± 1

The ζ-potentials of unmodified and modified membranes are presented in Table 5.2. The PDA is as an amphoteric material [47] and its isoelectric point is reported to be around pH 4 [48, 49]. The structure of PDA at different pH values was discussed in detail in chapter 4 [30]. Thus, the ζ-potential of the PDA-modified membrane was negative, as shown in Table 5.2, because the pH of the NaCl solution in my ζ- potential measurements was 5.9. However, the ζ-potential of the PDA-modified membrane was almost the same as that of the unmodified membrane. This is probably because the unmodified membrane surface already had a high negative charge density because of the carboxylic acid groups. This explanation is similar to that regarding hydrophilicity discussed above.

Because PZs are neutral materials, with both positively and negatively charged functional groups within the same segment side chains, a neutral surface charge would be expected for the PZ immobilized membranes. As expected, the ζ-potentials of the

(RO+PZ) and (RO+PDA+PZ) membranes were almost neutral, as shown in Table 5.2. Thus, it could be concluded that PZ covered the membrane surface.

5.3.2. Water permeability and salt rejection of membranes

The water permeability and salt rejection of unmodified and modified membranes were measured by the cross-flow filtration setup described in Section 5.2.3.4. The results are presented in Table 5.3. It was found that modification with PDA and/or PZ did not affect salt rejection because the salt rejections of the unmodified and modified membranes were similar. The PDA formation is a mild oxidative self-polymerization at pH 8.8 and PZ was also immobilized at the same pH. According to the information mentioned in the membrane manufacturer's catalogue, the permissible pH range for commercial RO membranes (i.e., ES-20) is between 2 and 10 [50]. This means that the methods used for modification with PDA and/or PZ might not damage the structure of the active layer (i.e., top layer). Salt rejection is governed by the active layer and was not affected by the PDA coating and PZ immobilization.

Table 5.3. The water permeability and salt rejection of unmodified and modified membranes.

Membrane	**Permeability ($L/m^2.h.atm$)**	**Δ Perm***	**Rejection (%)**
Unmodified RO	5.3 ± 0.1	0	97.8 ± 0.3
RO + PDA	4.6 ± 0.2	- 0.7 ± 0.2	98.4 ± 0.2
RO + MPC-co-AEMA	5.2 ± 0.1	- 0.1 ± 0.1	98.0 ± 0.2
RO + PDA+ MPC-co-AEMA	4.8 ± 0.1	- 0.5 ± 0.1	97.7 ± 0.1

* $\Delta Perm = P_{modified} - P_{unmodified}$

On the other hand, it is clear from Table 5.3 that the permeability of modified membrane with PDA (RO + PDA and RO + PDA+ MPC-co-AEMA) is a little lower than that of unmodified membrane. This indicates that only PDA coating caused the decrease in permeability. This is probably because the PDA coating layer was dense and governed the water permeability through the membrane modified with PDA.

5.3.3. Antibiofouling

5.3.3.1. Bacterial suspension filtration

The antibiofouling performance of the unmodified and modified membranes (RO+PDA, RO + PZ and RO+PDA+PZ) was evaluated by cross-flow filtration of a bacterial suspension, as described in Section 5.2.3.5. The water flux was initially adjusted to 2.2×10^{-2} $m^3.h^{-1}.m^{-2}$ by controlling the TMP, because the water flux is known to affect biofouling. The time courses of normalized water flux, J/J_0, during the filtration of the bacterial suspension are shown in Fig. 5.6, in which J is the real water flux of the bacterial suspension filtration with time and J_0 is the initial water flux.

It can be observed from Fig. 5.6 that the unmodified membrane retained just 61% of its initial water flux after 1200 minutes of filtration, while the PDA-modified membranes retained about 80% of its initial water flux. Figure 5.6 clearly shows that membranes immobilized with PZ with or without the precursor layer (i.e., PDA layer) have higher antibiofouling potentials than a membrane modified only with PDA. In addition, the PDA precursor layer was effective at increasing the antibiofouling potential of the PZ layer. This effect can probably be attributed to the higher amount of

PZ deposited on the substrate during the immobilization process as shown in Table 5.1. Therefore, it was concluded that antibiofouling was improved by PZ immobilization through the increase of antiadhesion properties, because PZs strongly bind to water molecules via electrostatically induced hydration [14-16]. Such hydration can greatly prevent the attachment of proteins or bacteria to the membrane surface [5, 17, 18].

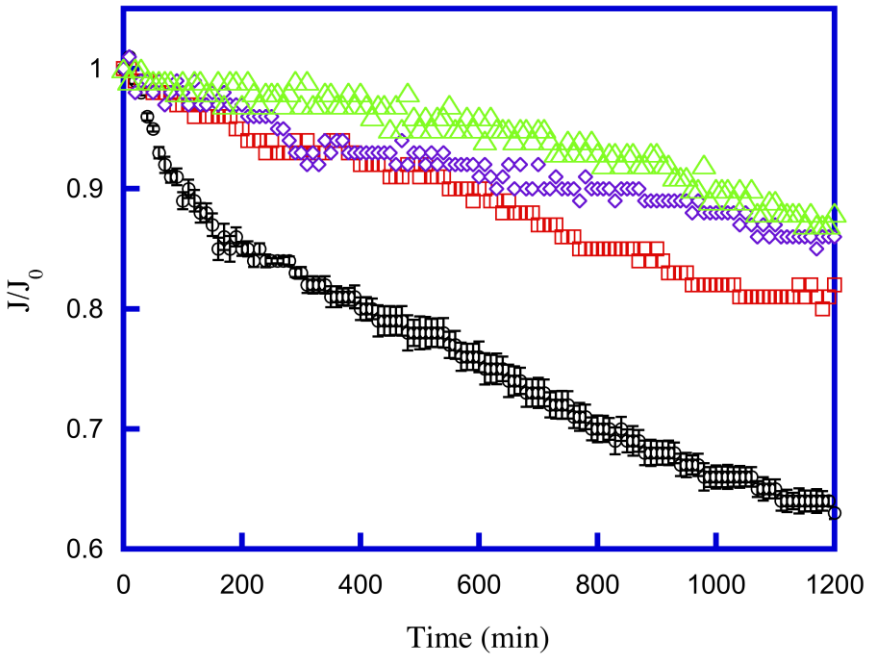

Fig. 5.6. Normalized fluxes of the unmodified membrane (○), PDA-modified membrane (□), RO+MPC-co-AEMA (◇) and RO+PDA+MPC-co-AEMA (△) as a function of time during the filtration of the bacterial suspension.

Figure 5.7 shows SEM images of the membrane surfaces after 1200 minutes filtration of the bacterial suspension. Numerous bacteria adsorbed and formed a biofilm on the surface of the unmodified membrane (Fig. 5.7a). Conversely, few bacteria were adsorbed on the surface of the modified membranes (Figs. 5.7b–5.7d)). These results clearly show that these surface modifications were useful in reducing bacterial

adsorption, although the differences between these modified membranes were not very marked.

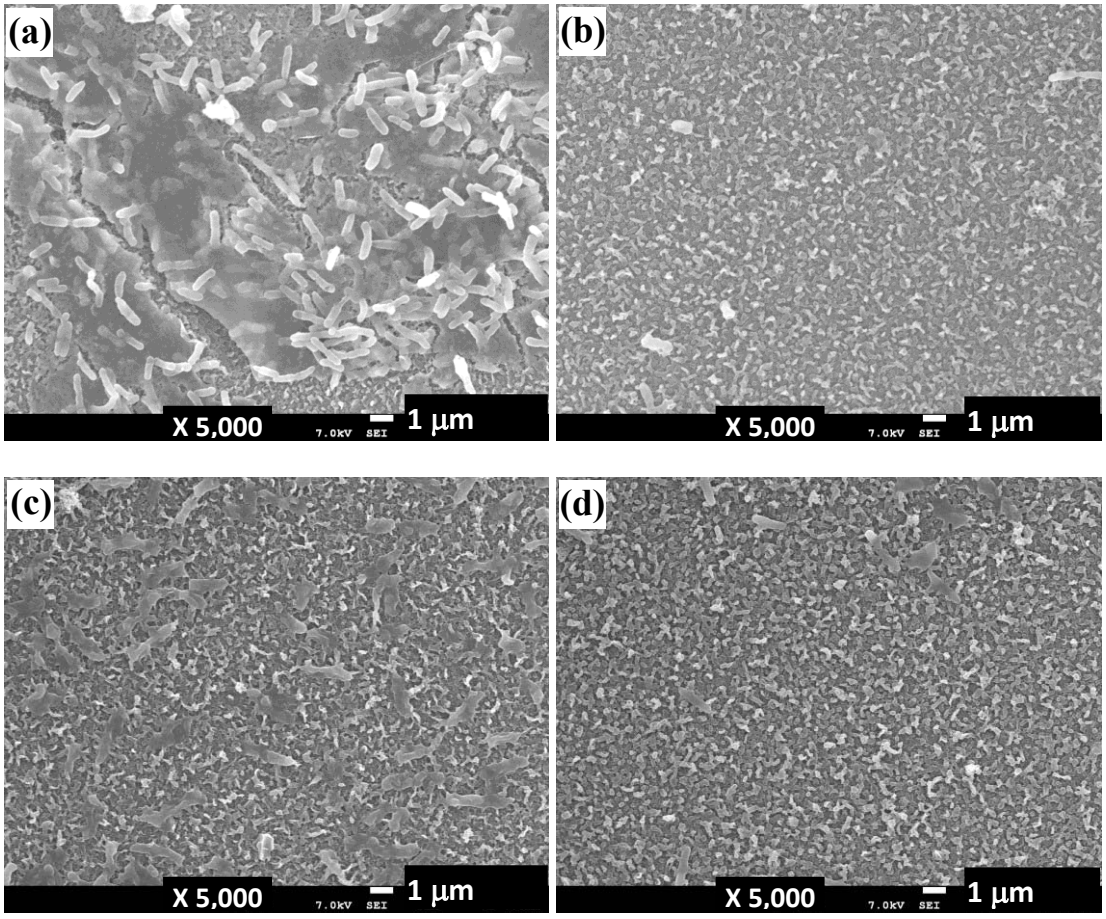

Fig. 5.7. FE-SEM images of (a) the unmodified membrane surface, and the modified membranes (b) RO+PDA, (c) RO +MPC-co-AEMA, and (d) RO+PDA+MPC-co-AEMA after 1200 minutes bacterial suspension filtration.

5.3.3.2. Stability

It has been reported that the PDA coating is stable on the membrane surface and its stability can probably be attributed to the high adhesion property of PDA [29, 39, 41, 51]. To investigate the effect of the PDA precursor layer, PZ was immobilized on the

unmodified membrane and a PDA-modified membrane. These modified membranes were kept under harsh condition by immersing into a 2 M NaCl aqueous solution to evaluate the stability during storage. This NaCl concentration is about 3 times higher than seawater. This data will also reflect the stability during real cross-flow filtration. After one month of immersion, their antibiofouling potential was evaluated by cross-flow filtration of the bacterial suspension, as described in Section 5.2.3.5. The results of the bacterial suspension filtration are shown in Fig. 5.8. It was found from Fig. 5.8a that the antibiofouling potential of the PZ-immobilized membrane without the PDA precursor layer (RO +MPC-co-AEMA) declined after one month of immersion in the 2M NaCl aqueous solution. However, the antibiofouling potential of the PZ-immobilized membrane with the PDA precursor layer (RO +PDA + MPC-co-AEMA) was not markedly changed (Fig. 5.8b). These results reveal that PZ layer immobilized onto a PDA-modified membrane is more stable than that on an unmodified membrane under static (storage) condition, because PZ is covalently immobilized on the PDA-modified membrane [43]. It is expected that the PZ layer immobilized onto a PDA-modified membrane as precursor layer would also show higher stability than PZ layer immobilized without precursor layer even under dynamic condition (real filtration).

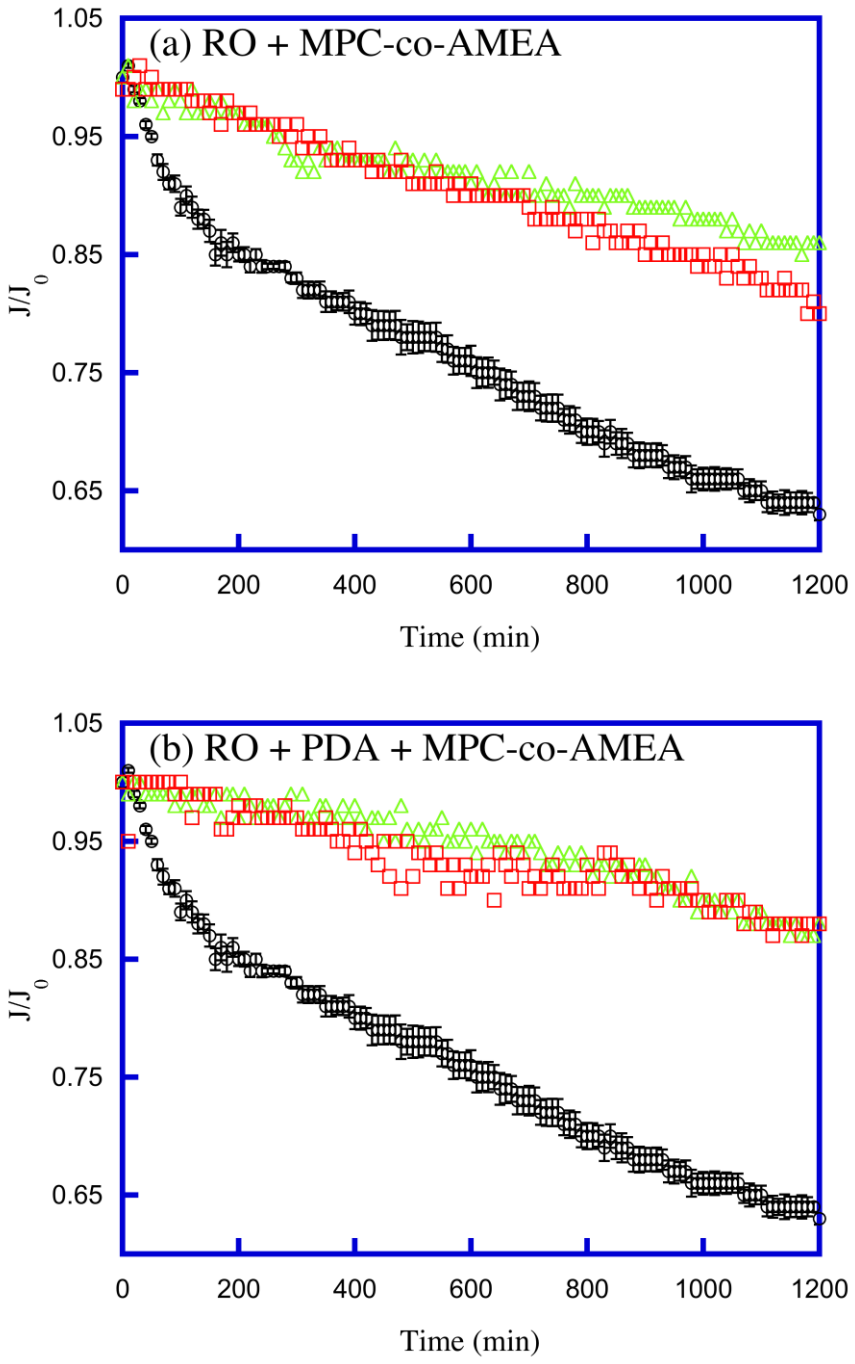

Fig. 5.8. Normalized flux of modified membranes before immersion (△) and after immersion (□) in 2 M NaCl aqueous solution for one month as a function of time during bacterial suspension filtration; **(a)** RO+MPC-co-AEMA membrane and **(b)** RO+PDA+MPC-co-AEMA membrane. Open circles (○) correspond to the unmodified membrane.

5.4. Conclusion

A commercial RO membrane was modified by PZ immobilization to improve antibiofouling properties. In addition, the membrane was initially modified with a PDA coating as a precursor layer to enhance the amount of PZ immobilized and its stability. The deposition of PDA and PZ on the membrane surface was confirmed by XPS. The hydrophilicity was not appreciably changed by surface modification with PDA and/or PZ. The surface charge was changed from negative to neutral by PZ immobilization, even when using a PDA precursor layer. The salt rejection of membranes was not affected by modification with PDA and/or PZ. Water permeability was not changed by PZ immobilization, while it was slightly decreased by PDA modification. This is probably because the PDA coating layer increased the resistance to water transport through the modified membrane. Dynamic bacterial suspension filtration showed that surface modification with PZ clearly enhanced the biofouling resistance of the RO membranes. Moreover, SEM images showed that numerous bacteria were attached to the unmodified membrane, while few bacteria were attached to the membrane modified with PDA and/or PZ. The filtration of a bacterial suspension through modified membranes that had been immersed in a 2 M NaCl aqueous solution for one month revealed that the PZ layer immobilized on a PDA-modified membrane was more stable than that immobilized on a membrane without a PDA precursor layer. The higher stability of the former was probably due to covalent bonding between PZ and the PDA coating.

References

[1] H. Karkhanechi, R. Takagi, Y. Ohmukai, H. Matsuyama, Enhancing the antibiofouling performance of RO membranes using Cu(OH)2 as an antibacterial agent, Desalination, 325 (2013) 40-47.

[2] Y.-F. Yang, Y. Li, Q.-L. Li, L.-S. Wan, Z.-K. Xu, Surface hydrophilization of microporous polypropylene membrane by grafting zwitterionic polymer for anti-biofouling, Journal of Membrane Science, 362 (2010) 255-264.

[3] N. Hilal, V. Kochkodan, L. Al-Khatib, T. Levadna, Surface modified polymeric membranes to reduce (bio)fouling: a microbiological study using E. coli, Desalination, 167 (2004) 293-300.

[4] M.A. Shannon, P.W. Bohn, M. Elimelech, J.G. Georgiadis, B.J. Marinas, A.M. Mayes, Science and technology for water purification in the coming decades, Nature, 452 (2008) 301-310.

[5] H. Karkhanechi, F. Razi, I. Sawada, R. Takagi, Y. Ohmukai, H. Matsuyama, Improvement of antibiofouling performance of a reverse osmosis membrane through biocide release and adhesion resistance, Separation and Purification Technology, 105 (2013) 106-113.

[6] M. Herzberg, M. Elimelech, Biofouling of reverse osmosis membranes: Role of biofilm-enhanced osmotic pressure, Journal of Membrane Science, 295 (2007) 11-20.

[7] T. Ishigami, K. Amano, A. Fujii, Y. Ohmukai, E. Kamio, T. Maruyama, H. Matsuyama, Fouling reduction of reverse osmosis membrane by surface modification via layer-by-layer assembly, Separation and Purification Technology, 99 (2012) 1-7.

[8] K. Ishihara, Bioinspired phospholipid polymer biomaterials for making high performance artificial organs, Science and Technology of Advanced Materials, 1 (2000) 131-138.

[9] C.S. Gudipati, J.A. Finlay, J.A. Callow, M.E. Callow, K.L. Wooley, The Antifouling and Fouling-Release Perfomance of Hyperbranched Fluoropolymer (HBFP)−Poly(ethylene glycol) (PEG) Composite Coatings Evaluated by Adsorption of Biomacromolecules and the Green Fouling Alga Ulva, Langmuir, 21 (2005) 3044-3053.

[10] T.L. Clare, B.H. Clare, B.M. Nichols, N.L. Abbott, R.J. Hamers, Functional Monolayers for Improved Resistance to Protein Adsorption: Oligo(ethylene glycol)-Modified Silicon and Diamond Surfaces, Langmuir, 21 (2005) 6344-6355.

[11] H. Ma, J. Hyun, P. Stiller, A. Chilkoti, "Non-Fouling" Oligo(ethylene glycol)-Functionalized Polymer Brushes Synthesized by Surface-Initiated Atom Transfer Radical Polymerization, Advanced Materials, 16 (2004) 338-341.

[12] S. Krishnan, C.J. Weinman, C.K. Ober, Advances in polymers for anti-biofouling surfaces, Journal of Materials Chemistry, 18 (2008) 3405-3413.

[13] J. Liu, Y. Zhan, T. Xu, G. Shao, Preparation and characterizations of novel zwitterionic membranes, Journal of Membrane Science, 325 (2008) 495-502.

[14] K. Futamura, R. Matsuno, T. Konno, M. Takai, K. Ishihara, Rapid Development of Hydrophilicity and Protein Adsorption Resistance by Polymer Surfaces Bearing Phosphorylcholine and Naphthalene Groups, Langmuir, 24 (2008) 10340-10344.

[15] H. Kitano, T. Mori, Y. Takeuchi, S. Tada, M. Gemmei-Ide, Y. Yokoyama, M. Tanaka, Structure of Water Incorporated in Sulfobetaine Polymer Films as Studied by ATR-FTIR, Macromolecular Bioscience, 5 (2005) 314-321.

[16] S. Chen, J. Zheng, L. Li, S. Jiang, Strong Resistance of Phosphorylcholine Self-Assembled Monolayers to Protein Adsorption: Insights into Nonfouling Properties of Zwitterionic Materials, Journal of the American Chemical Society, 127 (2005) 14473-14478.

[17] I. Eshet, V. Freger, R. Kasher, M. Herzberg, J. Lei, M. Ulbricht, Chemical and Physical Factors in Design of Antibiofouling Polymer Coatings, Biomacromolecules, 12 (2011) 2681-2685.

[18] M. Zhou, H. Liu, J.E. Kilduff, R. Langer, D.G. Anderson, G. Belfort, High-Throughput Membrane Surface Modification to Control NOM Fouling, Environmental Science & Technology, 43 (2009) 3865-3871.

[19] Z. Zhang, S. Chen, Y. Chang, S. Jiang, Surface Grafted Sulfobetaine Polymers via Atom Transfer Radical Polymerization as Superlow Fouling Coatings, The Journal of Physical Chemistry B, 110 (2006) 10799-10804.

[20] W. Feng, J.L. Brash, S. Zhu, Non-biofouling materials prepared by atom transfer radical polymerization grafting of 2-methacryloloxyethyl phosphorylcholine: Separate

effects of graft density and chain length on protein repulsion, Biomaterials, 27 (2006) 847-855.

[21] G. Li, G. Cheng, H. Xue, S. Chen, F. Zhang, S. Jiang, Ultra low fouling zwitterionic polymers with a biomimetic adhesive group, Biomaterials, 29 (2008) 4592-4597.

[22] Y. Chang, W.-J. Chang, Y.-J. Shih, T.-C. Wei, G.-H. Hsiue, Zwitterionic Sulfobetaine-Grafted Poly(vinylidene fluoride) Membrane with Highly Effective Blood Compatibility via Atmospheric Plasma-Induced Surface Copolymerization, ACS Applied Materials & Interfaces, 3 (2011) 1228-1237.

[23] R. Yang, J. Xu, G. Ozaydin-Ince, S.Y. Wong, K.K. Gleason, Surface-Tethered Zwitterionic Ultrathin Antifouling Coatings on Reverse Osmosis Membranes by Initiated Chemical Vapor Deposition, Chemistry of Materials, 23 (2011) 1263-1272.

[24] F. Razi, I. Sawada, Y. Ohmukai, T. Maruyama, H. Matsuyama, The improvement of antibiofouling efficiency of polyethersulfone membrane by functionalization with zwitterionic monomers, Journal of Membrane Science, 401–402 (2012) 292-299.

[25] H.-Y. Yu, Y. Kang, Y. Liu, B. Mi, Grafting polyzwitterions onto polyamide by click chemistry and nucleophilic substitution on nitrogen: A novel approach to enhance membrane fouling resistance, Journal of Membrane Science, 449 (2014) 50-57.

[26] C. Peng, Y.S. Thio, R.A. Gerhardt, Effect of Precursor-Layer Surface Charge on the Layer-by-Layer Assembly of Polyelectrolyte/Nanoparticle Multilayers, Langmuir, 28 (2011) 84-91.

[27] R. Steitz, T. Gutberlet, T. Hauss, B. Klösgen, R. Krastev, S. Schemmel, A.C. Simonsen, G.H. Findenegg, Nanobubbles and Their Precursor Layer at the Interface of Water Against a Hydrophobic Substrate, Langmuir, 19 (2003) 2409-2418.

[28] L.-P. Zhu, J.-H. Jiang, B.-K. Zhu, Y.-Y. Xu, Immobilization of bovine serum albumin onto porous polyethylene membranes using strongly attached polydopamine as a spacer, Colloids and Surfaces B: Biointerfaces, 86 (2011) 111-118.

[29] M. Vaselbehagh, H. Karkhanechi, S. Mulyati, R. Takagi, H. Matsuyama, Improved antifouling of anion-exchange membrane by polydopamine coating in electrodialysis process, Desalination, 332 (2014) 126-133.

[30] Hamed Karkhanechi, Ryosuke Takagi, H. Matsuyama, Biofouling resistance of reverse osmosis membrane modified with polydopamine, Desalination, (2014), http://dx.doi.org/10.1016/j.desal.2013.12.033.

[31] L.-P. Zhu, J.-Z. Yu, Y.-Y. Xu, Z.-Y. Xi, B.-K. Zhu, Surface modification of PVDF porous membranes via poly(DOPA) coating and heparin immobilization, Colloids and Surfaces B: Biointerfaces, 69 (2009) 152-155.

[32] Y. Liao, Y. Wang, X. Feng, W. Wang, F. Xu, L. Zhang, Antibacterial surfaces through dopamine functionalization and silver nanoparticle immobilization, Materials Chemistry and Physics, 121 (2010) 534-540.

[33] W. Wang, R. Li, M. Tian, L. Liu, H. Zou, X. Zhao, L. Zhang, Surface Silverized Meta-Aramid Fibers Prepared by Bio-inspired Poly(dopamine) Functionalization, ACS Applied Materials & Interfaces, 5 (2013) 2062-2069.

[34] T.S. Sileika, H.-D. Kim, P. Maniak, P.B. Messersmith, Antibacterial Performance of Polydopamine-Modified Polymer Surfaces Containing Passive and Active Components, ACS Applied Materials & Interfaces, 3 (2011) 4602-4610.

[35] J.-H. Jiang, L.-P. Zhu, X.-L. Li, Y.-Y. Xu, B.-K. Zhu, Surface modification of PE porous membranes based on the strong adhesion of polydopamine and covalent immobilization of heparin, Journal of Membrane Science, 364 (2010) 194-202.

[36] D. Saeki, T. Tanimoto, H. Matsuyama, Prevention of bacterial adhesion on polyamide reverse osmosis membranes via electrostatic interactions using a cationic phosphorylcholine polymer coating, Colloids and Surfaces A: Physicochemical and Engineering Aspects, 443 (2014) 171-176.

[37] C. Foppoli, R. Coccia, C. Cini, M.A. Rosei, Catecholamines oxidation by xanthine oxidase, Biochimica et Biophysica Acta (BBA) - General Subjects, 1334 (1997) 200-206.

[38] Y. Liao, R. Wang, A.G. Fane, Engineering superhydrophobic surface on poly(vinylidene fluoride) nanofiber membranes for direct contact membrane distillation, Journal of Membrane Science, 440 (2013) 77-87.

[39] J. Jiang, L. Zhu, L. Zhu, B. Zhu, Y. Xu, Surface Characteristics of a Self-Polymerized Dopamine Coating Deposited on Hydrophobic Polymer Films, Langmuir, 27 (2011) 14180-14187.

[40] D.R. Dreyer, D.J. Miller, B.D. Freeman, D.R. Paul, C.W. Bielawski, Elucidating the Structure of Poly(dopamine), Langmuir, 28 (2012) 6428-6435.
[41] H. Lee, S.M. Dellatore, W.M. Miller, P.B. Messersmith, Mussel-Inspired Surface Chemistry for Multifunctional Coatings, Science, 318 (2007) 426-430.
[42] C.Y. Tang, Y.-N. Kwon, J.O. Leckie, Probing the nano- and micro-scales of reverse osmosis membranes—A comprehensive characterization of physiochemical properties of uncoated and coated membranes by XPS, TEM, ATR-FTIR, and streaming potential measurements, Journal of Membrane Science, 287 (2007) 146-156.
[43] Z.-Y. Xi, Y.-Y. Xu, L.-P. Zhu, Y. Wang, B.-K. Zhu, A facile method of surface modification for hydrophobic polymer membranes based on the adhesive behavior of poly(DOPA) and poly(dopamine), Journal of Membrane Science, 327 (2009) 244-253.
[44] B.D. McCloskey, H.B. Park, H. Ju, B.W. Rowe, D.J. Miller, B.J. Chun, K. Kin, B.D. Freeman, Influence of polydopamine deposition conditions on pure water flux and foulant adhesion resistance of reverse osmosis, ultrafiltration, and microfiltration membranes, Polymer, 51 (2010) 3472-3485.
[45] J. Zhao, Q. Shi, S. Luan, L. Song, H. Yang, H. Shi, J. Jin, X. Li, J. Yin, P. Stagnaro, Improved biocompatibility and antifouling property of polypropylene non-woven fabric membrane by surface grafting zwitterionic polymer, Journal of Membrane Science, 369 (2011) 5-12.
[46] S. Kasemset, A. Lee, D.J. Miller, B.D. Freeman, M.M. Sharma, Effect of polydopamine deposition conditions on fouling resistance, physical properties, and permeation properties of reverse osmosis membranes in oil/water separation, Journal of Membrane Science, 425-426 (2013) 208-216.
[47] B. Yu, J. Liu, S. Liu, F. Zhou, Pdop layer exhibiting zwitterionicity: a simple electrochemical interface for governing ion permeability, Chemical Communications, 46 (2010) 5900-5902.
[48] V. Ball, Impedance spectroscopy and zeta potential titration of dopa-melanin films produced by oxidation of dopamine, Colloids and Surfaces A: Physicochemical and Engineering Aspects, 363 (2010) 92-97.

[49] Q. Liu, B. Yu, W. Ye, F. Zhou, Highly Selective Uptake and Release of Charged Molecules by pH-Responsive Polydopamine Microcapsules, Macromolecular Bioscience, 11 (2011) 1227-1234.

[50] Nitto Denko Corporation, Japan, Osaka, data sheet, http://www.nittodenko.com/cn/datasheet/membrane/005/index.html

[51] H. Lee, N.F. Scherer, P.B. Messersmith, Single-molecule mechanics of mussel adhesion, Proceedings of the National Academy of Sciences, 103 (2006) 12999-13003.

Chapter 6

Conclusion

The water shortage problem is a serious problem in the world. Among different desalinations methods, reverse osmosis (RO) membrane technology is one of the most popular water purification technologies, because of its properties such as the high salt rejection and permeation rates as well as their excellent chemical, thermal and mechanical stability. However, fouling including inorganic fouling, organic fouling and biofouling is a major obstacle in membrane process. In this work, I attempted to improve biofouling resistance of commercial RO membrane (ES-20, Ntitto Denko Co.) with surface modification through different methods. These modification methods were based on improving of antibacterial and/or antiadhesion properties. The modified membranes were characterization by water and air contact angle, ζ-potential, FTIR, XPS, TEM and FE-SEM. Also, the antibacterial and antiadhesion properties were evaluated for modified membranes. The results described in chapters 2-5 are summarized as follows:

6.1. Improvement of antibiofouling performance of RO membranes through biocide release and adhesion resistance

In this chapter, I attempted to improve the antibiofouling properties of a commercial RO membrane through surface modification by polyelectrolyte multilayers (PEMs) deposition. The Poly(allylamine hydrochloride) (PAH) and poly(sodium 4-styrene sulfonate) (PSS) were used as a polycation and polyanion, respectively. The silver nanoparticles were embedded into PEMs and finally covered by a 2-methacryloyloxyethyl phosphorylcholine (MPC) copolymer with 2-aminoethyl methacrylate (AEMA) (MPC-co-AEMA) as the polyzwitterion (PZ).

The antibacterial properties were evaluated by a shake flask test. The results confirmed that the antibacterial properties were greatly improved by Ag nanoparticles embedded within PEMs and further experiment showed that the dominant mechanism is release killing. Moreover, the PZ top layer improved the hydrophilicity because of the free water content of this layer and thereby improved the antiadhesion properties towards bacteria. Thus, the antibiofouling potential of RO membrane greatly improved by the combined effects of two strategies including improved antibacterial and antiadhesion properties.

Furthermore, it was experimentally confirmed that the surface modification did not decrease the observed rejection. However, the initial water permeability was decreased by a maximum of about 15% through the surface modification. However, considering, the marked antibiofouling properties of modified membrane, it was expected that the

total water flux through modified membranes would be higher than unmodified membrane.

6.2. Enhancing the antibiofouling performance of RO membranes using $Cu(OH)_2$ as an antibacterial agent

The improvement of antibacterial properties is one of the main strategies to increase the antibiofouling properties of membranes. The antibacterial properties are commonly improved by the antibacterial agents including organic and inorganic compounds. In this chapter, I used $Cu(OH)_2$ instead of silver nanoparticles, because the secondary maximum contaminant level of $Cu(OH)_2$ is higher than Ag and cheaper than Ag. Then, I showed that $Cu(OH)_2$ particles have superior antibacterial properties under neutral conditions compared with other metal hydroxides such as $Ca(OH)_2$ and $Mg(OH)_2$.

The results confirmed that the deposited $Cu(OH)_2$ particles improved the antibacterial properties of commercial RO membrane. It was found that the $Cu(OH)_2$ particles physically adsorbed on the membrane surface. The bactericidal activity was improved by released of Cu^{2+} ions from the membrane surface into solution. The hydrophilicity of modified membrane and the negative charge density of membrane surface were also increased by adsorption of $Cu(OH)_2$ particles. Antiadhesion properties towards bacteria were improved by an increase in hydrophilicity and electrostatic repulsion between bacteria and negative surface charge. Thus, the antibiofouling performance of a commercial RO membrane was greatly improved by the enhancement

of antibacterial and antiadhesion effects. Moreover, it was experimentally confirmed that the surface modification with $Cu(OH)_2$ did not strongly affect the membrane performance. However, the stability of modified membrane was not acceptable for long term applications. To use $Cu(OH)_2$-modified membrane for long term application, a further modification should be applied to increase its stability.

6.3. *Use of a polydopamine coating to improve antibiofouling properties of RO membranes*

The improvement of antiadhesion properties is one of two main strategies to improve the antibiofouling potential. The antibiofouling properties can be improved by increasing in hydrophilicity. In this chapter, I attempt to modify the commercial RO membrane surface with polydopamine (PDA) as a well known super-hydrophilic material to improve the hydrophilicity of RO membrane. The membrane was modified with PDA using various dopamine concentrations and modification times under alkaline conditions.

Contrary any expectation, the hydrophilicity and surface charge were not appreciably changed by surface modification with PDA. However, dynamic bacterial filtration showed that membrane modification with PDA clearly enhanced the biofouling resistance of RO membranes. Also, a static adhesion test showed an improvement in the bacterial adhesion resistance. The result of shake flask test demonstrated that the PDA coating layer had good antibacterial properties. The pH dependence of the antibacterial property proved that the bactericidal property was due to protonated amine groups in PDA layer. The salt rejection of PDA-modified membranes

was not also affected by modification with PDA. However, the pure water permeability was decreased, presumably because the PDA coating layer increased the resistance to water transport through the modified membrane.

According to the results described above, modification with a 0.5 kg/m^3 dopamine solution at pH 8.8 for 180 minutes was sufficient to impart a high antibiofouling property to an RO membrane by surface modification with PDA.

6.4. *Enhanced antibiofouling property of RO membranes via polydopamine coating and polyzwitterion immobilization*

It was reported in chapter 4 that PDA coating can improve the antibiofouling properties of a commercial RO membrane. The optimal condition for surface modification of PDA was 0.5 kg/m^3 dopamine solution at pH 8.8 for 180 minutes. In this chapter, I attempted to use a PDA coating with above condition as precursor layer to immobilize PZ layer; because the PDA coating containing reactive groups endows a versatile platform for further surface functionalization and immobilization.

The result showed that the hydrophilicity was not appreciably changed by surface modification with PDA and/or PZ. The surface charge density was become neutral by PZ immobilization even with a PDA coating as precursor layer. Dynamic bacterial filtration showed that membrane modification with PZ clearly enhanced the biofouling resistance of RO membranes. Moreover, the SEM images confirmed that a numerous of the bacteria attached on the unmodified membrane while few bacteria attached to the membrane modified with PDA and/or PZ.

Moreover, it was found that the salt rejection of modified membranes was not affected by modification with PDA and/or PZ. The water permeability was not also changed by PZ immobilization. However, the water permeability was decreased by PDA modification, presumably because the PDA coating layer increased the resistance to water transport through the modified membrane. The bacterial suspension filtration through the modified membranes that immersed in 2M NaCl aqueous solution for one month revealed that the PZ layer on the PDA-modified membrane were more stable than that immobilized on the membrane without PDA coating as precursor layer. The higher stability was attributed to the covalent bonding between PZ and PDA coating.

Doctoral Dissertation, Kobe University

“Enhanced Antibiofouling of Reverse Osmosis Membranes by Surface Modifications, 180 pages

Submitted on January, 22, 2014

The date of publication is printed in cover of repository version in Kobe University Repository Kernel.